File 1.8.2

DOE/ET/20417-4

THERMAL STABILITY TESTS OF HEAT TRANSFER FLUIDS FOR TRANSFER AND STORAGE OF THERMAL ENERGY

23.6

By
G. R. Schneider
G. R. Morgan

December 1980

Work Performed Under Contract No. AC03-76ET20417

McDonnell Douglas Astronautics Company
Huntington Beach, California

U.S. Department of Energy

Solar Energy

DISCLAIMER

Available from the National Technical Information Service, U. S. Department of Commerce, Springfield, Virginia 22161.

Price: Printed Copy A07
Microfiche A01

MDC G9331

DOE/ET/20417-4
Distribution Category UC-62

THERMAL STABILITY TESTS OF HEAT TRANSFER FLUIDS FOR TRANSFER AND STORAGE OF THERMAL ENERGY

By
G. R. SCHNEIDER AND G. R. MORGAN

DECEMBER, 1980

PREPARED FOR THE
U.S. DEPARTMENT OF ENERGY
SOLAR ENERGY
UNDER CONTRACT (E4-76-C-03-1108)

MCDONNELL DOUGLAS ASTRONAUTICS COMPANY

MCDONNELL DOUGLAS CORPORATION

Rockwell International
Rocketdyne Division

ACKNOWLEDGEMENT

The authors wish to acknowledge the effort of their many colleagues who participated in the work reported herein. These include Dr. Rex Mitchell, Dr. Walter Unterberg, John Vrolyk, George Smith, Dick Kistner, Dean Woolery, and Marilyn Levak of Rocketdyne. Project Monitors included Vic Burolla and Lee Radosevich of Sandia Laboratories. McDonnell Douglas Corporation provided direct contract supervision through the efforts of Jerry Coleman and Rusty Lobell.

CONTENTS

CONTENTS

ILLUSTRATIONS

TABLES

ABSTRACT

Laboratory tests were conducted to evaluate the high temperature (288 to 343 C (550 to 650 F)) thermal stability, material compatibility, and surface fouling of selected commercial heat transfer fluids for a sensible heat thermal energy storage system to be used with a solar thermal electrical power generation plant. The tests have provided information on the rate of fluid replenishment required, the change of viscosity, the composition of lost products, and the rate of fouling of heat transfer surfaces as a function of temperature and time. Determinations have been made of the effect of the presence of materials likely to be used in the energy storage subsystem, (rocks, stainless steel, and carbon steel) on these properties.

INTRODUCTION

Solar thermal power plants will be a significant future element of the world's energy supply system. A thermal storage subsystem (TSS) will have a vital role in the effective operation of each of those solar power plants. As a buffer between the solar portion of the plant and the electrical generating portion, the TSS protects the turbine from rapid variations in steam inlet conditions due to rapid and short term changes in insolation from clouds passing over the collector field. In addition, the TSS extends the solar plant's generating capacity into periods with little or no insolation. Providing generating capacity for this period allows the solar plant to displace additional fossil fueled capacity.

Another significant function of the TSS is to assist in matching annual insolation fluctuations to the sizing of the electrical generating portions of the plant. If the electrical subsystem is sized for peak summer noon insolation, its full capacity is unused for most of the year. If it is sized much smaller, a great deal of solar energy is lost unless it can be stored. Trade studies show that six hours of storage provide approximately the optimum capacity in a commercial plant in the southwestern United States.

Energy storage concepts that first require electric generation, e.g., pumped water, compressed air, flywheel or battery storage, do not fulfill the basic requirement of buffering the turbine from solar insolation variations. Thermal storage has an additional advantage by directly providing efficient turbine seal heating during periods of turbine inactivity. Therefore, thermal energy storage is preferable for this solar energy application.

Thermal storage concepts can be classified into three categories; sensible-heat, latent-heat (phase change), and thermochemical (reversible chemical reactions). Of these, sensible-heat systems are clearly within the current state of the art and present the least technical risk and thus the least cost and development risk. Both latent-heat and thermochemical storage systems will require considerable additional development before they can be evaluated in detail and considered for implementation on a large scale.

For these reasons sensible-heat thermal storage was selected for this application. The thermal storage concept devised and selected uses a low-cost stationary solid bed to store most of the energy, with a suitable liquid to transfer energy into and out of the bed (and store a small portion of the energy). This dual-medium type of system (patent pending to Rocketdyne and MDAC) combines the advantages of a low-cost solid with the flexibility, low pumping power, and moderate heat-exchanger requirements of a liquid energy storage system.

Conceptually, in its simplest form, the system uses a bed (shown in the center of Figure 1) of an inexpensive solid (e.g., rock, ore, metal scraps, etc.). An appropriate high-temperature liquid fills the voids in the bed and circulates through the bed to deposit or withdraw energy.

In cyclical operation, heating of the bed (charging) is achieved by removing lower temperature fluid from the bottom of the bed, heating it in a heat exchanger with steam from the receiver, and returning the fluid to the top of the tank. A fairly sharp temperature transition (a thermocline) is maintained naturally between hot and cold fluid because of the lower

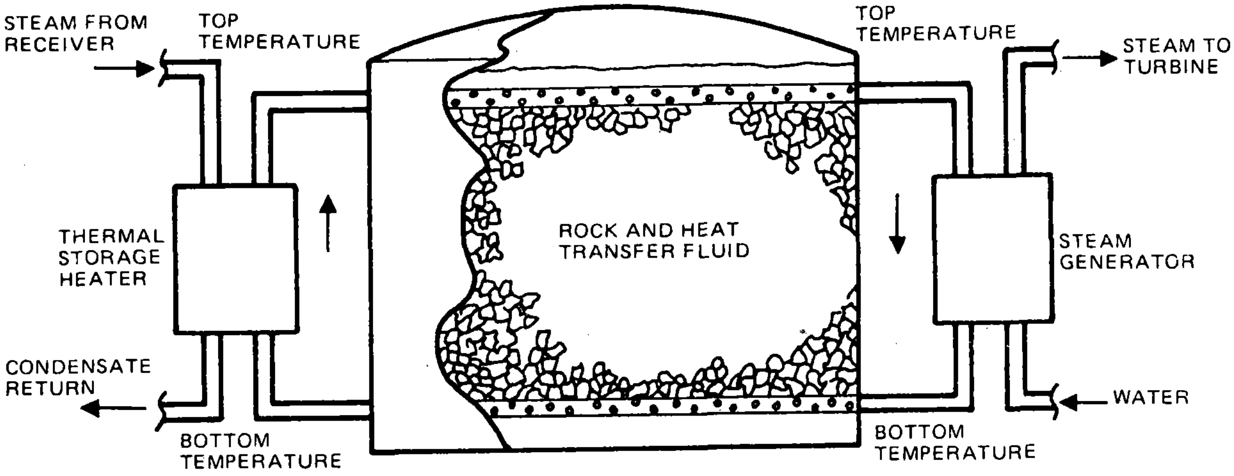

Figure 1. Dual-Medium Thermal Storage Concept

density of hot fluid. This thermocline moves downward through the bed during charging and upward during extraction. When the storage unit is completely charged, all of the bed and the fluid are at the maximum temperature and the thermocline does not exist. The extraction loop uses the fluid to remove energy from the storage unit and produces steam for power plant operation or other plant functions such as equipment heating.

The large cost savings for this type of thermal storage results principally from two factors: (1) replacement of about 75% of the expensive storage liquid with inexpensive rock, and (2) use of the thermocline principle to significantly decrease the tankage volume, thereby substantially reducing thermal losses compared to a system with separate tanks for hot and cold storage.

There are many variations and improvements on the basic concept outlined above. These include: (1) choice of solid material (e.g., various types of rocks, ore, metal scraps, blocks, bricks, ceramics, etc.), (2) size distributions and consequent void fractions of solid bed, (3) method of bed placement, (4) choice of liquid (e.g., water, various petroleum products, heat-transfer fluids, molten salts, liquid metals), (5) single or multiple thermal storage unit (TSU) tanks, (6) combinations of various liquids and solids in series tanks to achieve maximum high-temperature performance at minimum cost, and (7) use of immiscible liquids. These types of variations and design choices were considered at various stages of the design and development work on the thermal storage subsystem, Ref. 20.

Commercially available organic heat-transfer fluids which are liquid at ambient temperature have maximum operating temperatures of about 316C to 344C (600F to 650F). Storage temperatures above this region require alternatives which introduce some negative features. The principal alternatives are: (1) organic fluids which are solid at ambient temperatures (with higher costs and the problems of initial start-up and avoiding solidification during operation*, (2) fluids with higher vapor pressures, e.g., Dowtherm A (with higher fluid costs and much higher container costs), (3) inorganic

---

*Commercial firms are presently developing low cost liquid high temperature fluids that may eliminate this problem.

salts and salt mixtures (with problems of initial start-up and avoiding solidification during operations, plus ususally higher medium costs).

In a review of commercial heat transfer fluids at the beginning of the program it was apparent that very little data were available as to effects from long-term exposure of the fluids to their operating environment. Records of make-up requirements are seldom kept by users. When records are kept, they are generally unavailable (for proprietary reasons) to the manufacturer. Also, in actual use the fluids are heated without measurement of heater hot wall surface temperatures. Other factors affecting the lack of information on commercial heat transfer fluids are:

1) The avoidance of fluid at elevated temperatures in contact with air is only casually adhered to by many users although the requirement is well known.
2) The rapidly changing nature of many industries precludes the use of one specific fluid for more than a very limited number of years.

It is this particular lack of information about basic properties of the fluids, as used, that prompted this program.

Once built, a solar electrical power generation plant must operate reliably and without high maintenance costs for many years (30 typically) in order to produce electricity economically. For maximum performance and economy the heat transfer fluids have to be worked near their operating limits where fluid degradation is not negligible.

Recognizing these problems Rocketdyne initiated a test program to investigate the thermal stability of heat transfer fluids in 1975 as a member of the McDonnell Douglas Central Receiver Solar Thermal Power System design team.

This report summarizes the objectives, hardware description, test results, and discussion of fluid properties, loss rates, degradation mechanism, and recommended fluid monitoring procedures.

SUMMARY

A three year program has been completed determining the suitability of commercial heat transfer fluids (liquids) for use as a heat transfer and sensible heat storage medium for solar thermal electrical power generation plants. As a subcontract to the McDonnell Douglas Astronautics Company (under contract to the Department of Energy) the program provided characterization of those fluids considered desirable for operation in the 302C (575F) to 316C (600F) range. The five fluids tested included Exxon's Caloria HT43, Monsanto's Therminol 55 and 66, Sun Oil 21, and Mobiltherm XMTL 123.

The program had 3 principal objectives: (1) to examine the suitability of the dual medium* concept for thermal energy storage; (2) to select a suitable fluid for the Barstow Pilot Plant thermal storage system; and (3) to establish the loss rate of candidate fluids for the Pilot and Commercial Solar Thermal electric power generation facilities.

The test program consisted of (1) weight loss measurements in constant temperature baths; (2) fouling on simulated heat exchanger tube surfaces; and (3) a model subsystem flow loop.

The results of the program indicate that Exxon's Caloria HT43 is the most cost effective choice of a heat transfer fluid at projected pilot plant conditions(1). When used in combination with low cost river gravel the loss rate is estimated to be approximately 7 percent of the initial fluid volume per operating year†. A summary of the economics of the 5 fluids is given below.

---

*Patent applied for.

†Comparable rates have been observed in tests conducted at Sandia/Livermore Laboratories.

(1) Pilot Plant storage conditions, 218C to 302C (425F to 575F).

	Cost at Barstow $ /gal	Estimated[1] fluid yearly loss rate, % of initial charge	Yearly makeup[1] cost, % of initial plant total capital cost
Caloria HT43	1.05	7	.0138
Mobil 123	1.90	4	.0143
Sun 21	1.00	10	.0186
Therminol 66	7.15	3	.043
Therminol 55	1.85	35	.122

The weight loss value for Caloria is estimated based upon tests in constant temperature baths for durations up to 11,000 hours.

Heat exchanger hot surface exposure indicates little or no fouling with Caloria for durations up to 14,000 hours.

In addition to the constant temperature environment of the material compatibility and surface fouling tests a laboratory flow loop was assembled and operated for approximately 2000 hours using Caloria HT43. The model subsystem flow loop contained the principal elements and operated at the conditions established for the Barstow Pilot Plant thermal storage subsystem. Components duplicated or simulated include the Thermal Storage Unit (TSU) (containing Barstow gravel for heat storage), the ullage maintenance unit (to retain an inert low pressure atmosphere in the TSU), the fluid maintenance unit (to filter particulates), and the fluid heater heat exchanger hot surface (to test for fouling). No evidence of bed or manifold fouling was experienced during the operation of the flow loop.

Various analytical procedures have been used on the aged fluids which will be of value when monitoring full scale plant operation. Fluid viscosity seems to be a sensitive parameter that directly affects fluid performance and can be readily measured on site with modest equipment.

---

(1) Pilot Plant storage conditions, 218C to 302C (425F to 575F)

The test program has demonstrated the economic attractiveness and suitability of using low cost rock in conjunction with commercial heat transfer fluids as a low cost thermal storage medium. However, the program has covered less than a fourth of the 30 year operating life required for commercial solar power plants. Although the limited time data clearly shows the Caloria HT43 and Barstow rock/sand combination satisfactory for the Pilot Plant, it is recommended that tests be continued to verify operational characteristics for durations much closer to commercial plant design requirement.

OBJECTIVES

The objective of the program was to characterize and document the suitability of commercial heat transfer fluids for use in a central receiver solar thermal electrical power generation station. A central theme to the application is the use of a low cost solid to replace a major portion of the relatively expensive heat transfer fluid inventory for storage of thermal energy.

The program was planned to provide data on a laboratory scale to demonstrate the suitability and economics of one or more commercial fluids. By providing an environment in the laboratory duplicating the operational conditions with neat fluids as well as with materials common to the thermal storage system (metals, sand and gravel) a data base is provided that will be applicable to all-liquid storage systems as well as the dual medium concept.

By periodically removing small samples of fluid and capturing the outgassed products of decomposition the loss mechanism may be hypothesized which will provide an approach for fluid refurbishment and maintenance.

Determining the characteristics of aged fluids will enable monitoring procedures and specifications to be established for operating solar thermal power plants in a predictable and economic manner.

BACKGROUND

FLUID DEGRADATION CONSIDERATIONS

Degradation of a hydrocarbon heat transfer fluid can occur over time by two principal processes: pyrolysis (including thermal cracking and polymerization) and oxidation (primarily from contact with air). The rate of pyrolysis depends upon the structure of the hydrocarbon; for an acceptable heat transfer fluid, these reactions must be very slow in the desired temperature range. Catalysts for pyrolysis reactions, which include a variety of compounds, especially copper alloys, must be avoided completely in the system design. The air oxidation reaction rate of the hydrocarbons increases sharply with temperature; the rate is so rapid at 316C (600F) that a fluid in extensive contact with air would be useless after only a few days. One of the types of products of air oxidation, peroxides, are effective polymerization catalysts. Some heat transfer fluids contain antioxidant additives to inhibit the action of dissolved oxygen when the fluid is initially heated.

These pyrolysis and oxidation mechanisms are illustrated in Figure 2. Very low molecular weight compounds, either formed through cracking or initially present in a fluid, present no problems in moderate quantities. They merely cause a moderate increase in vapor pressure (which is normally only 25.5 KPa (3.7 psia) at 316C (600F) for "weathered" Caloria HT43 and 77.9 KPa (11.3 psia) for fresh fluid) and a decrease in velocity. However, if the amount of volatile material becomes excessive, it would be necessary to withdraw some of it through the normal operation of the ullage maintenance unit.

The other products of thermal cracking are olefins, which can polymerize. Normally, the amount of thermal polymerization would be very small at the temperatures involved; however, contact with air and formation of even small amounts of polymerization catalysts could result in significant polymerization, which is potentially harmful. As the fluid degrades, the polymers may increase both in molecular weight and quantity. Unless the

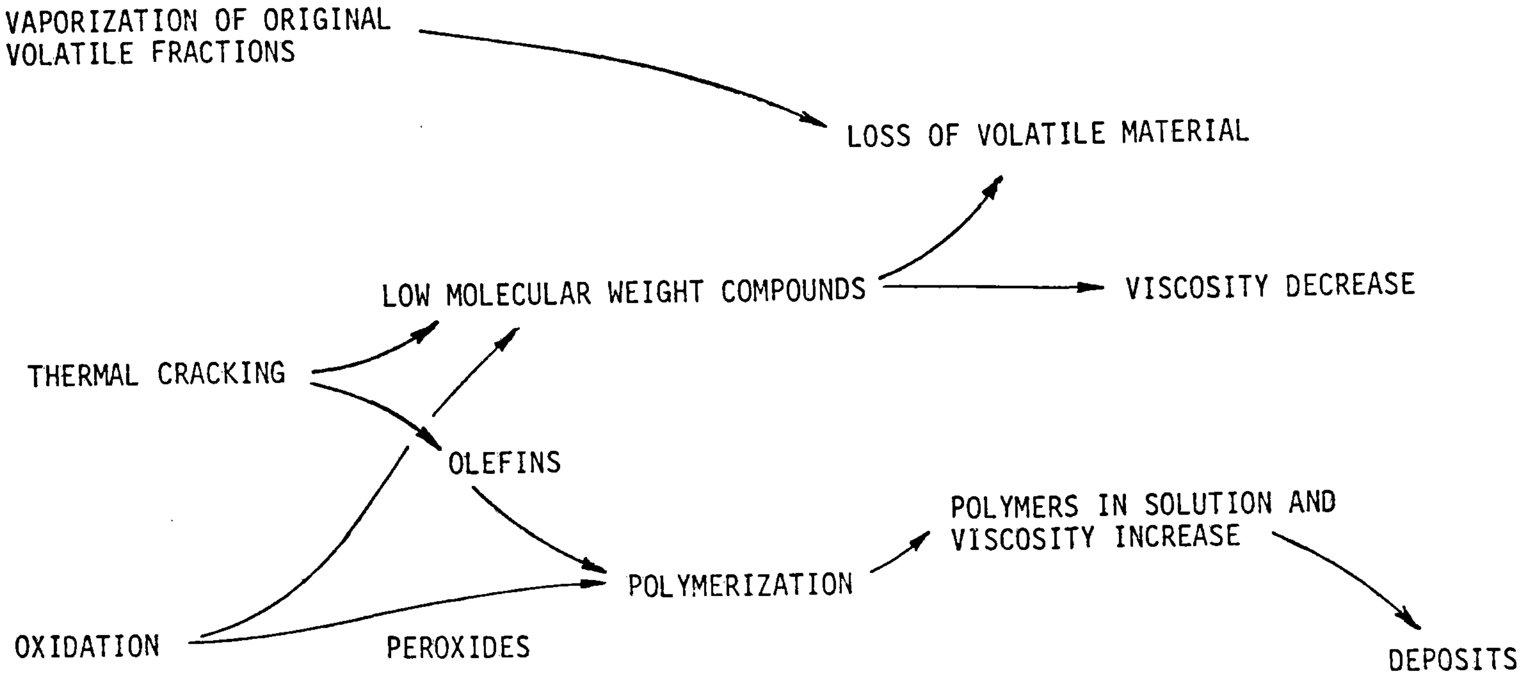

Figure 2. Fluid Degradation Mechanisms

fluid is severely degraded, the polymers remain in solution and cause moderate increases in viscosity. Experience with Therminol 66 indicates that polymers remain in solution up to about 40 wt. percent and systems are operated routinely with about 30 wt. percent polymers (Reference 1). However, the polymers are considered to be the precursors of fouling of the heat exchanger tubes by carbonaceous deposits (coking). Coking tendency in the heat exchanger is not accelerated until the fluid begins to degrade considerably. Severe fluid degradation could result in high-molecular-weight insoluble polymers that separate from the fluid as resins or deposits on heat exchanger tubes.

The Atomic Energy of Canada Limited (AECL) made a distinction between coking and fouling in their work on Therminol 66. Coking is defined as a formation of massive carbonaceous deposits and is caused by decomposition of the fluid and precipitation of the high molecular weight insoluble decomposition products (high boilers) in regions of stagnant or low-flow velocity and high temperature. Fouling is the formation of thermally resistive films on heat transfer surfaces and is dependent upon the nature and concentration of impurities in the coolant.

The two main types of fouling identified by the AECL (References 1 and 11 to 14) are: (1) mass transfer fouling, which involved inorganic deposits, and (2) particulate fouling, which involved carbonaceous deposits. Particulate fouling rates increase with a decrease in velocity while an increase in velocity reportedly increases the rate of mass transfer (or inorganic deposit) fouling (References 1 and 13).

Inorganic deposits occurring in mass transfer fouling are believed by the AECL to be caused by the reaction of soluble impurities with iron from the piping system to produce an iron complex which decomposes at the heat transfer surface to form Fe_3O_4, αFe or Fe_3C. The most important impurity in this process was chlorine (References 1 and 11 to 14). An abbreviated mechanism is cited for the iron-chlorine (Reference 1). The presence of small amounts of water will reduce fouling. Some theories on the role of water are reviewed by Smee, et al (Reference 1). It is surmised that water hydrolyzes a Lewis acid catalyst that can cause polymerization of benzene, biphenyl, and terphenyl.

Methods of fouling detection are discussed and reviewed by the AECL in References 1 and 11. Several methods are discussed such as pressure drop measurements, thermocouple measurements in a standard reactor fuel element with mounted thermocouples (References 1 and 12), measurements of the particulate content, electrical conductivity measurements, and concentration of collodial species measurements (membrane stain test and tetrahydrofuran test), but the most successful technique for determining the fouling potential of an organic coolant was the small probe fouling test (SPFT) (References 1, 6, and 11).

In the SPFT, a small flow of the heat transfer fluid was passed over an electrically heated stainless steel probe for approximately 24 hours after which time the weight of film deposit per unit area was measured. A relationship was developed empirically between the deposited weight per unit area on the SPFT and the fouling potential of the fluid.

CALORIA HT43

Some physical property data are available on Caloria HT43 from Reference 3, Only limited information has been available on thermal stability properties of Caloria. Nothing is available on its fouling or coking properties. It is known that copper compounds can behave as cracking catalysts for Caloria HT43 and cause a rapid degradation in fluid properties. Fluid life prediction information related to polymer formation in Caloria HT43 has been given (References 3 and 4) under its previous name, Humbletherm 500. However, Caloria HT43 contains an antioxidiation additive which was not present in Humbletherm 500, so the thermal decomposition rate and polymerization rate of Humbletherm 500 could have been substantially higher than for Caloria HT43.

A number of heat transfer loops have been operating with Caloria HT43 for extended periods of time. One application in Louisiana containing about 760,000 liters (200,000 gal), has been operating at 305C (580F) for over 6 years without fluid treatment of any kind (Reference 5).*

---

*Physical and chemical characteristics of this fluid are unknown but it is still considered "useable" by the user.

MOBILTHERM XMTL 123

Mobiltherm XMTL 123 is a petroleum base heat transfer fluid produced by Mobil Oil Co. The fluid is in pilot plant production and is not yet available in commercial quantities. Several years ago the Mobil Oil Co. stopped producing Mobiltherm 600 (a highly regarded heat transfer fluid) because one or more steps in the process were deemed to be polluting. Mobiltherm XMTL 123 is very similar to Mobiltherm 600 in most of its physical properties and its high temperature properties are reported to be as good as or better than the high temperature properties of Mobiltherm 600.

A technical bulletin on the physical properties of the new fluid, Mobiltherm XMTL 123, is not yet available and until one is, the reader is referred to the bulletin on Mobiltherm 600.[†] The composition of Mobiltherm XMTL 123 is given as 41% saturates, 2% resins, and 57% aromatics. The maximum recommended bulk temperature for the fluid is 316C (600F) and the maximum film temperature is 329C (625F). No information has been available on its thermal stability at 316C (600F) or on its fouling or coking properties.

SUN OIL 21

Sun Oil 21 is a highly refined paraffinic oil sold by the Sun Oil Co. The fluid has a maximum recommended bulk temperature of 316C (600F). Physical properties data as a function of temperature are available from the Sun Oil Co. The fluid is believed to be similar in its properties to Caloria HT43. Sun Oil 21, however, does not contain antioxidants whereas Caloria HT43 does.

THERMINOL 55

Some data on the stability of Monsanto's Therminol 55 are available in the literature (References 3 and 4). The experimental work (Reference 3) deals primarily with the time required to accumulate 10 percent high boilers at temperatures ranging from 300 to 357C (625 to 675F).

[†] "Heating With Mobiltherm", Technical Bulletin, CRI, RGM, 1-93-006, 1971

THERMINOL 66

Data on polymerization of Monsanto's Therminol 66 are also available in References 3 and 4. A great amount of test data has been accumulated on Therminol 66 as a result of an experimental program conducted by the Atomic Energy of Canada Limited (AECL) to develop an organic cooled and moderated reactor. Therminol 66 was designated HB-40 and OS-84 for the AECL work. The test data made available by contact with the AECL includes: (1) information on physical properties (Reference 6); (2) methods of analysis of the chemical and physical properties (References 7 and 8); (3) impurities and coolant quality tests (References 7 and 8); (4) analyses of thermal decomposition rates (References 9, 10, and 11); and (5) fouling of heat transfer surfaces (References 1 and 12 to 15).

Since the decomposition rate data taken by the AECL were obtained in an irradiated environment, both pyrolysis and radiolysis occurred together. The claim is made, however, (References 9 and 10) that the pyrolytic and radiolytic contributions can be separated out and their interdependence is insignificant until high temperatures are reached. Pyrolytic decomposition was assumed to be a first order reaction dependent only upon temperature and the fraction of low boilers. The data were obtained on a fluid containing 25 percent high boilers. The rate constant giving the best fit of data between 300 and 400C is:

$$K = 1.60 \text{ X } 10^{11} \exp [-43255/RT] \qquad \text{(Reference 9)} \qquad (1)^{*}$$

and the rate of decomposition of a fluid with a higher boiler concentration (HB) is given by:

$$K = 1.60 \text{ X } 10^{13} \exp [-43255/RT] \quad (100-HB)/75 \qquad (2)$$

where K is the fractional rate hr^{-1} in equation (1) and the percent rate (%/hr) in equation (2). T is in degrees Kelvin.

---

*Mathematical equations are numbered on the right to differentiate from chemical ractions which are numbered on the left.

Information is also given for determining the distribution of decomposition products as high boilers, volatiles (generally C_6 and C_{12} hydrocarbons) and gases (generally H_2 and C_1 to C_5 hydrocarbons) (Reference 9).

Specifications to reduce fouling from Therminol 66 (i.e., HB-40, OS-84) are reproduced from Reference 1:

1. Low concentration of particulate material at operating conditions.
2. Low chlorine content.
3. Exclusion of oxygen.
4. Maintenance of adequate water concentration (approximately 150 to 200 ppm).
5. Elimination of dissolved and particulate iron.

FLUID CHARACTERIZATION AND MATERIALS COMPATIBILITY TESTS

Thermal stability and compatibility tests were conducted on five commercially available fluids which were candidates for meeting the requirements of the thermal storage system: Exxon Caloria HT43, Monsanto Therminol 55, Monsanto Therminol 66, Mobiltherm XMTL 123 and Sun Oil 21. The objectives of the tests were: (1) to determine the ability of the heat transfer fluids to function at 288 to 316C (550 to 600F) for extended periods of time, and (2) to assess the high temperature, long-term compatibility of these heat transfer fluids with rock and materials of construction (stainless steel, carbon steel) which will be in contact with fluid in the thermal storage unit.

TEST EQUIPMENT AND PROCEDURES

The tests conducted on the heat transfer fluids are designed to obtain data under conditions which simulate those that will be encountered in both the Pilot Plant and commercial plants.

The Pilot Plant Thermal Storage System will be operated over long periods of time with the heat transfer fluid cycling between 218 and 302C (425 and 575F). In the Pilot Plant and commercial plants, the pressure over the fluid in the thermal storage unit will be slightly over atmospheric, to prevent air leakage into the tank. Some volatile components resulting from thermal decomposition of the fluid will be removed from the ullage space through the ullage maintenance unit.

Operating experience indicates that high boiling viscous polymers can be expected to form from long term service at temperatures either through inadvertent exposure to oxygen and/or a slow but continual polymerization of the base molecules.

These heavy "high boilers" can be removed by conventional vacuum distillation procedures. Commercial equipment is available and can be built in or brought in periodically when needed to refurbish the heat transfer fluid.

The long-term thermal stability tests of the candidate thermal storage fluids were performed using constant temperature molten-salt baths.* The molten salt mixture used was DuPont HITEC (a eutectic consisting of 53% KNO_3, 7% $NaNO_3$, and 40% $NaNO_2$). Five constant temperature baths were used; one was maintained at 288C (550F) and two each were controlled at 302C (575F) and 316C (600F). All baths were 30 cm high by 30 cm wide by 35 cm deep and were heated electrically. Two of the baths were controlled by Halikainen "Thermotrol" units and three others by Bailey Instrument controllers. In addition, the bath temperatures were normally checked in the morning of each work day with a thermocouple and potentiometer. All of the baths were equipped with a base heater that was always on, and a trimming heater that was regulated in power by the temperature controller. Wherever possible the two heaters were placed on separate circuits. In case of heater or controller malfunctions, the redundancy avoided having the salt temperature fall below the freezing point. In addition, two of the baths were supplied with emergency temperature regulators that were set to switch on an auxiliary heater if the bath temperature approached the salt freezing point. Three of the molten salt bath apparatuses are shown in Figure 3.

All of the long-term material compatibility tests were conducted in round-bottom Pyrex flasks with 20/40 standard taper ground glass joints. Each flask was fitted with an air-cooled condenser. The top of the condenser was vented to the atmosphere. A nitrogen atmosphere was maintained over the fluid and oxygen was prevented from entering the flask from the open top of the condenser by a very low flow nitrogen bleed at the top of the condenser. Aluminum foil was lightly wrapped around the top of the condenser and the nitrogen bleedline to prevent any foreign matter from falling into the flask. A schematic of the flasks is shown in Figure 4.

The rocks, coarse sand, metal samples, and fluid placed in the flasks were individually weighed. The sand ranged in size from 0.131 to 0.045 inches and the rocks from 1/2 to 3/4 inches. Rock used in these thermal stability and material compatibility tests was from two different sources in California and were semi-rounded from river bed alluvium. Initially the rocks used came

---

*The samples of Caloria HT43 at 288, 302, and 316C (550, 575, and 600F) and a Therminol 66 sample at 316C (600F) were initially heated using electric heating mantles. After approximately 2000 hours they were transferred to the molten salt baths.

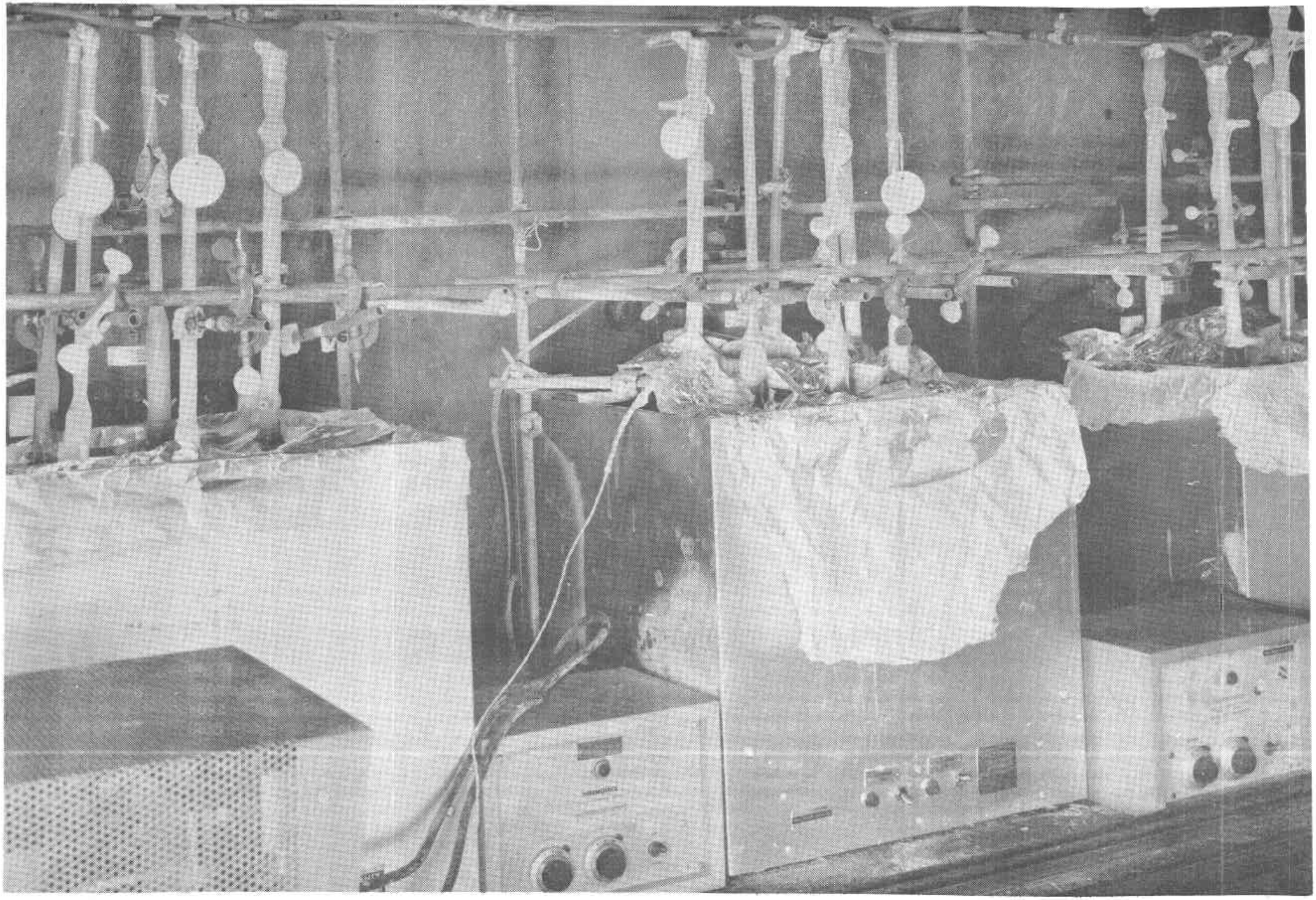

4ES29-12/18/75-C1B*

Figure 3. Fluids/Solids Materials Compatibility Constant Temperature Baths

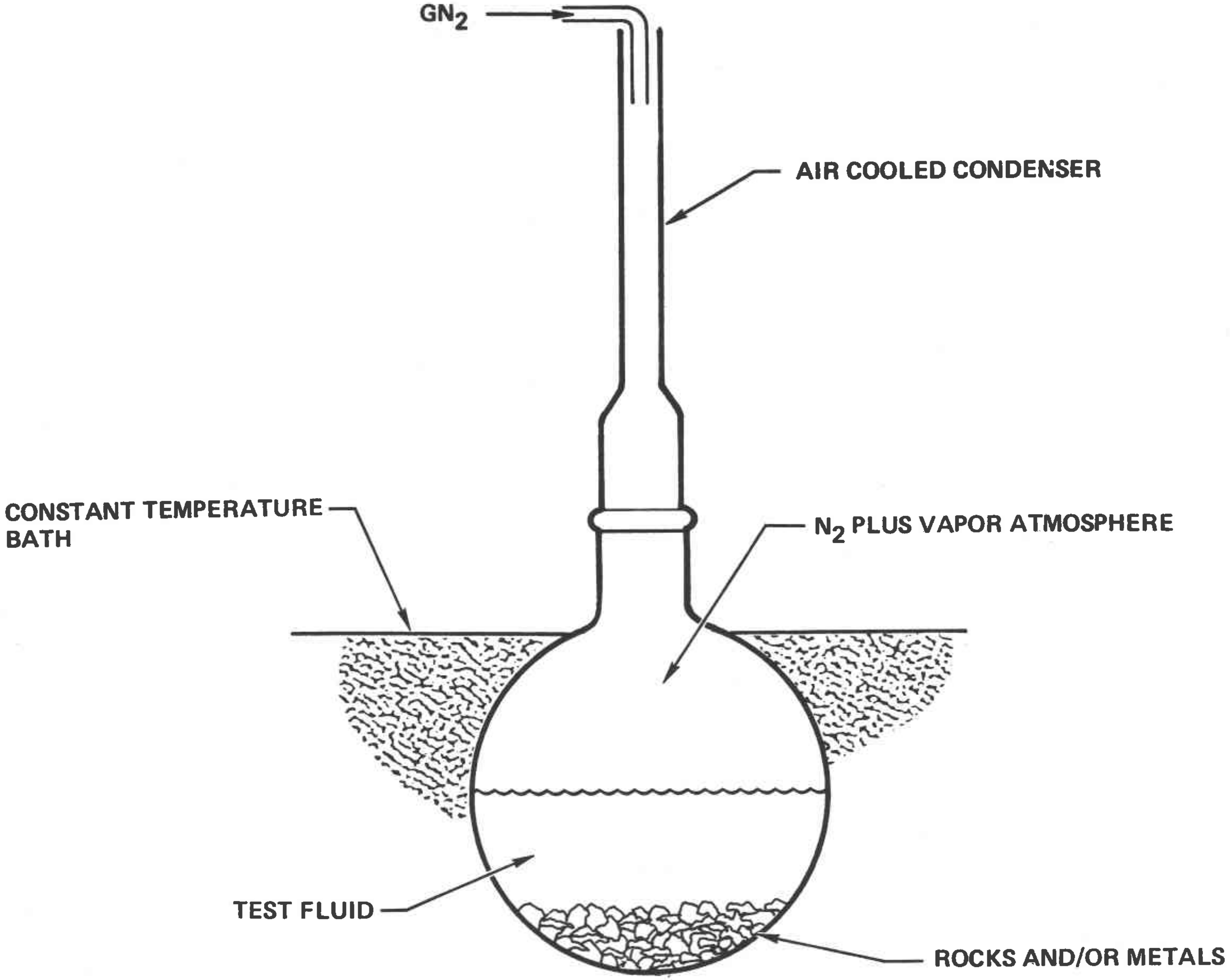

Figure 4. Fluids/Solids Materials Compatibility Setup

from an Irwindale (San Gabriel River) quarry. When the decision was made to locate the solar energy pilot plant in Barstow, samples of rock and sand obtained from the Barstow area (Mojave River quarry) were used in the tests. Prior to being used in these fluid tests the rocks and sand were thoroughly washed in water and rinsed with distilled water. The 321 stainless steel samples were short pieces of 0.6 cm tubing that had been washed in an oxalic acid solution. Carbon steel samples consisted of lathe turnings that had been degreased and rinsed in acetone, methanol and then dried in a stream of N_2. All of the materials were oven dried before being added to the fluid. After the weighed amounts of fluid and solids had been added to a flask. the flask was placed in an ultrasonic cleaner to help in removing small air bubbles entrapped in the rock-sand-metal layer at the bottom of the flask. About every 15 or 20 minutes the flask was removed from the ultrasonic device and given a slight shake or swirl to remove the air bubbles. This was done for about an hour before the flask was placed in the constant temperature bath.

At the beginning of the program consideration was given to the size and proportion of the rock and metal samples to be used. The liquid volume could be filled with rock and sand or the solids volume could be a much smaller portion of the liquid. Since it was known that the liquid volume would shrink through losses it was decided to reduce the solids volume and observe the results.

After the first few 1000 hour evaluation periods, Caloria HT43 began to appear as the most economic choice. The Caloria samples with rock and sand had smaller fluid losses than the neat fluid samples, indicating that the rock acted somewhat as an inhibiter to Caloria degradation. These results indicated that the most conservative results would be obtained with existing samples without changing the rock volume. More rock would possibly reduce decomposition even further. These test set ups effectively set the pattern for other samples to follow.

The rock and sand volume was arbitrarily selected to be approximately one fourth that of the fluid volume in the test set ups. Based on rock and sand size, a typical value of rock and sand surface to liquid volume (S/V) was approximately 8 cm^{-1}. Allowing for the fact that larger size rock and sand will be used, a full scale thermal storage unit would have a surface to volume ratio of approximately 25cm^{-1}.

Near the end of the program, there was some evidence by Burolla of Sandia Laboratories that the rock surface to fluid volume was a critical parameter. A fluid sample was put on test using Caloria HT43 at 575F. Test results are discussed in the appropriate section.

Glass containers for the fluid samples were selected as being the least likely to react with the heat transfer fluids. Certain metals and metal oxides were known to catalyze the decomposition reactions. Experience has shown that complete immersion of the flasks in a stirred liquid bath held at the desired temperature was a satisfactory method of providing a uniform temperature environment. Although it was recognized that there was a risk of losing the sample through breakage, it was determined that this was offset by the advantage of a single wall container which would minimize thermal gradients and provide a uniform temperature throughout the sample. Test set ups that involved double wall construction would likely result in a thermal gradient through the sample which were considered undesirable since it would result in varying degradation rates throughout the sample. Since the fluids were to be tested at a temperature where fluid degradation rate would be quite sensitive to temperature, it was considered important to check for the existence of a gradient. This was done by using a single thermocouple and moving it through the sample. This test performed at the beginning of the program verified that set ups did have a uniform temperature profile.

Later in the program the existence of thermal gradients was questioned and these measurements when repeated showed the existence of a thermal gradient on the order of 5C (9F) in some samples. Close examination revealed that the flasks with the temperature gradient were protruding somewhat from the bath. When these flasks were submerged the gradients disappeared. An examination of the records indicated that this condition could have existed for 1 to 2 months out of the total 3 year test period.

At intervals of approximately 1,000 hours, the flasks of fluid were removed from the constant temperature environment for weight loss and viscosity measurements. The flasks with contents were weighed to determine weight loss. Kinematic viscosity of the fluid was determined at 37.8C (100F) with a Cannon-Ubbelohde viscosimeter. In addition, a fluid sample of approximately 10 ml was withdrawn at each 1,000 hour interval for further fluid testing. These fluid samples were forwarded to Sandia/Livermore (as required by the contract) for analysis. Sandia/Livermore performed gel permeation chromatographic (GPC) and infrared IR spectroscopic analyses of the samples (Reference 16). The GPC tests are used to reveal the distribution of molecular size in the sample fluids. The distribution of molecular weights can be obtained after calibration of the GPC columns by chromatographing pure components of known molecular weight and size. The IR data indicate the presence of functional groups, i.e., double or triple bonds, OH, -COOH, ring compounds, etc. In addition, some GC - distillation curves were determined. Results are discussed under Analysis of Liquid-Phase Thermal Degradation.

RESULTS

Data on mass loss and kinematic viscosity change for the tests are summarized in Table 1. The loss of fluid from each of the flasks over the heating time was determined from weighings before and after each heating interval. The percent weight loss was calculated based on the original weight of fluid and corrected for the amount of sample material removed after each heating interval. Kinematic viscosity of all fluid samples was measured at 37.8C (100F) with a Cannon-Ubbelohde viscosimeter to further assess the effect of heating on the fluid. Experimental data on weight loss and kinematic viscosity changes with time are plotted in Figures 5 through 26.

Caloria HT43

Weight Loss. Flasks of Caloria HT43 with and without solids (rock, coarse sand carbon steel, and stainless steel) were prepared and tested at three temperatures, 288C (550F), 302C (575F), and 316C (600F). The percent weight loss vs time data are given in Figures 5, 6, and 7. A number of experiments were terminated, as noted in the figures, by mishaps occurring over the months of testing. In some cases a failure of a bath heater, a temperature controller or an accidental power interruption, might have caused the salt

TABLE 1. THERMAL STABILITY TESTS

Material Compatibility as of 8/21/78

Fluid	Initial Sample Weight, Grams	Sample I.D.	Temp °C (°F)	Rock and Metal	Time (Hrs)	Wt. Loss (Percent)	Kinematic Viscosity (Centistokes)	Kinematic Viscosity* Change (Percent)
Caloria HT43 (Figure 7)	Fluid 224		316 (600)	No	500	4.9		-34.4
					1189	19.4		-36.0
					1890	28.4		-42.2
Caloria HT43 (Figure 7)	Fluid 170		316 (600)	No	1171	9.3		-33.0
					2178	33.0		-22.5
Caloria HT43 (Figures 7, 10)	Fluid 179	7	316 (600)	No	1008	6.33	22.0	-29.4
					2027	11.8	17.9	-42.5
					3564	16.6	15.8	-49.3
				†	5265	27.1	16.0	-48.7
					6373	3.23	17.2	-44.9
					7791	5.83	15.8	-49.4
					8917	6.95	15.6	-50.0
					10213	10.34	14.2	-54.5
Caloria HT43 (Figure 10)	Fluid 338		316 (600)	Yes (Irwindale)	230	1.4		--
	Rock 181				500	2.8		-27
	Sand 101				1299	13.5		-34.3
	Metal 56				2000	31.9		-35.3
Caloria HT43 (Figure 7)	Fluid 157		316 (600)	Yes (Irwindale)	1020	4.4		-35.7
	Rock 41				2027	38.2		-12.0
	Sand 76							
	Metal 17							
Caloria HT43 (Figures 7, 10)	Fluid 150	5	316 (600)	Yes (Irwindale)	1008	4.6	20.4	-34.6
	Rock 28				2027	10.8	17.8	-42.9
	Sand 52				3564	15.8	15.8	-49.3
	Metal 22			†	5265	20.8	14.4	-54.0
					6373	3.54	14.6	-53.2
					7791	6.10	14.6	-53.3
					8917	7.42	14.5	-53.5
					10213	10.6	13.1	-58.0

---

*See last page of table

†Fresh oil added after measurements

TABLE 1. (Continued)

Fluid	Initial Sample Weight, Grams	Sample I.D.	Temp °C (°F)	Rock and Metal	Time (Hrs)	Wt. Loss (Percent)	Kinematic Viscosity (Centistokes)	Kinematic Viscosity* Change (Percent)
Caloria HT43 (Figure 7)	Fluid 438	6	316 (600)	Yes	1018	3.73	21.3	-31.8
	Rock 239		Gas Sampling		2076	5.82	18.4	-40.9
	Sand 348		(Irwindale)		3588	8.0	20.7	-33.6
	Metal 44							
Caloria HT43 (Figures 7, 10)	Fluid 225	15	316 (600)	Yes (Barstow)	1498	4.49	24.4	-21.8
	Rock 129				2604	6.75	22.1	-29.2
	Sand 112				4022	9.05	20.2	-35.2
	Metal 27				5296	10.81	19.9	-36.2
Caloria HT43 (Figures 6, 9)	Fluid 170		302 (575)	No	1241	8.8		-8.2
					2248	20.6		-9.2
Caloria HT43 (Figures 6, 9)	Fluid 354		302 (575)	Yes (Irwindale)	512	1.3		-6.4
	Rock 159				1299	2.1		-13.8
	Sand 110				2000	3.0		-17.1
	Metal 50				3028	6.3		-24.1
					4035	22.3		-11.3
					5159	26.5		-20.0
Caloria HT43 (Figures 6, 9)	Fluid 156	9	302 (575)	Yes (Irwindale)	1024	1.6	26.1	-16.2
	Rock 41				2024	6.4	24.0	-23.1
	Sand 72				3148	8.7	22.0	-29.5
	Metal 16				4157	11.4	16.5	-47.2
					5151	13.1	17.4	-44.1
					6923	19.3	19.9	-36.3
					8029	21.4	19.6	-37.2
					9447	25.1	20.5	-34.2
				†	10573	27.30	20.7	-33.6
					11850	4.50	35.5	+13.8

---

*See last page of table

†Fresh oil added after measurements

TABLE 1. (Continued)

Fluid	Initial Sample Weight, Grams	Sample I.D.	Temp °C (°F)	Rock and Metal	Time (Hrs)	Wt. Loss (Percent)	Kinematic Viscosity (Centistokes)	Kinematic Viscosity* Change (Percent)
Caloria HT43 (Figures 6, 9)	Fluid 238	16	302 (575)	Yes (Barstow)	1498	2.43	29.3	-6.01
	Rock 98				2604	6.60	29.7	-4.8
	Sand 120				4022	12.65	31.4	+0.74
	Metal 25				5148	14.37	31.7	+1.6
					6444	16.18	30.1	-3.5
Caloria HT43 (Not Shown)	Fluid 210	25	302 (575)	Yes (Barstow) Extra Rock	1254	11.24	29.4	-5.8
	Rock 469				6300	33 (1)		
	Sand 153							
	Metal 14							
Caloria HT43 (Figures 5, 8)	Fluid 173		288 (550)	No	1196	2.8		-3.5
					2203	9.8		+2.1
					3327	--		+0.3
					4361	13.6		-24.0
Caloria HT43 (Figures 5, 8)	Fluid 347		288 (550)	Yes (Irwindale)	512	1.1		-5.8
	Rock 155				1287	1.4		-6.1
	Sand 163				1987	1.6		-7.1
	Metal 59				2971	11.8		+14.7
					3978	12.3		+14.7
					5102	12.3		+11.0
					6136	15.0		-17.9
Caloria HT43 (Figures 5, 8)	Fluid 164		288 (550)	Yes (Irwindale)	976	2.3		-4.8
	Rock 41				1983	5.9		-1.8
	Sand 73				3107	--		-4.6
	Metal 16				4141	9.8		-27.9
Caloria HT43 (Figures 5, 8)	Fluid 230	17	288 (550)	Yes (Barstow)	1498	1.47	30.4	-2.45
	Rock 84				2604	2.17	30.1	-3.5
	Sand 91				4022	3.82	30.3	-2.76
	Metal 24				5148	4.60	30.8	-1.3
					6444	5.11	30.2	-3.2

---

*See last page of table

(1) Heavy oxidation, not consistent with basic test procedures

TABLE 1. (Continued)

Fluid	Initial Sample Weight, Grams	Sample I.D.	Temp °C (°F)	Rock and Metal	Time (Hrs)	Wt. Loss (Percent)	Kinematic Viscosity (Centistokes)	Kinematic Viscosity* Change (Percent)
Therminol 66 (Figure 14)	Fluid 168		343 (650)	No	1004	3.12		-13
					1988	12.7		-17.1
					3020	17.6		-23.2
					4068	25.1		-20.6
					5760	30.3		-26.1
					6942	31.7		--
Therminol 66 (Not Shown)	Fluid 167 Rock 41 Sand 78 Metal 20		343 (650)	Yes (Irwindale)	1004	55.3		+91.0
					1984	66.1		--
Therminol 66 (Figure 14)			329 (625)	Yes (Irwindale)	1013	3.2		-16.1
					2061	5.2		-20.6
					3753	7.3		-24.5
					4935	9.0		--
Therminol 66 (Figures 13, 17)	Fluid 158	8	316 (600)	No	1195	0.50	25.0	-0.6
					2202	2.26	25.2	0
					3210	2.85	25.0	-0.7
					4229	4.08	25.6	+1.18
					5747	4.75	25.4	+0.8
					7467	5.70	25.4	+1.0
					8573	6.18	25.6	+1.67
					9991	6.69	25.7	+1.95
					11117	7.21	26.0	+3.3
					12413	7.95	26.1	+3.6
Therminol 66 (Figures 13, 17)	Fluid 363 Rock 98 Sand 130 Metal 47		316 (600)	Yes (Irwindale)	405	1.7		--
					842	2.8		-13.3
					1303	3.9		-15.0
					2010	12.1		-3.2
					3017	24.7		+31.3

---

*See last page of table

TABLE 1. (Continued)

Fluid	Initial Sample Weight, Grams	Sample I.D.	Temp °C (°F)	Rock and Metal	Time (Hrs)	Wt. Loss (Percent)	Kinematic Viscosity (Centistokes)	Kinematic Viscosity* Change (Percent)
Therminol 66 (Figures 13, 17)	Fluid 169 Rock 45 Sand 61 Metal 21		316 (600)	Yes (Barstow)	1498	2.5		-6.0
					2604	3.0		-5.5
Therminol 66 (Not Shown)	Fluid 245 Rock 99 Sand 105 Metal 17	27	316 (600)	Yes (Barstow)	965	3.28	22.6	-10.3
Therminol 66 (Figures 12, 16)	Fluid 154	11	302 (575)	No	1266	4.2	31.0	+23
					2273	25.3	27.4	+8.9
					3397	25.4	27.2	+7.8
					4406	26.0	--	--
					5400	26.9	28.4	+12.6
				Terminated	7172	27.4	28.7	+13.8
Therminol 66 (Figure 12)	Fluid 158 Rock 42 Sand 73 Metal 16	10	302 (575)	Yes (Irwindale)	1024	6.74	30.4	+20.8
					2031	43.5	55.2	+119
					3155	45.5	55.4	+120
					4164	49.9	56.7	+125
					5160	51.2	60.7	+141
				Terminated	6932	51.8	--	--
Therminol 66 (Figures 12, 16)	Fluid 178 Rock 56 Sand 56 Metal 19	19	302 (575)	Yes (Barstow)	1475	1.84	24.6	-2.43
					2581	2.74	25.0	-0.7
					4000	5.67	27.8	+10.5
					5125	7.14	29.3	+16.3
					6421	8.92	31.9	+26.6
Therminol 66 (Figures 11, 15)	Fluid 159 Rock 42 Sand 80 Metal 17		288 (550)	Yes (Irwindale)	956	3.1		-7.2
					1963	18.8		+47
					3087	18.8		+46
					4121	19.8		+58.8

---

*See last page of table

TABLE 1. (Continued)

Fluid	Initial Sample Weight, Grams	Sample I.D.	Temp °C (°F)	Rock and Metal	Time (Hrs)	Wt. Loss (Percent)	Kinematic Viscosity (Centistokes)	Kinematic Viscosity* Change (Percent)
Therminol 66 (Figures 11, 15)	Fluid 179	20	288 (550)	Yes (Barstow)	1475	1.60	24.9	-1.13
	Rock 60				2581	1.95	25.2	0
	Sand 58				4000	2.46	25.3	+0.48
	Metal 21				5125	2.74	25.6	+1.6
					6421	3.48	27.2	+8.1
Therminol 55 (Not Shown)	Fluid 181		316 (600)	No	1100	13.4		-55.3
					2107	52.8		-38.6
Therminol 55 (Not Shown)	Fluid 287		316 (600)	Yes (Irwindale)	500	19.0		-54.7
	Rock 149				1189	38.6		-52.2
	Sand 133				1076	38.9		-56.8
	Metal 65				2083	68.2		--
Therminol 55 (Not Shown)	Fluid 161		302 (575)	Yes (Irwindale)	1146	17.1		-45
	Rock 51				2153	68.1		--
	Sand 76							
	Metal 19							
Therminol 55 (Not Shown)	Fluid 153		288 (550)	Yes (Irwindale)	976	10.4		-56.0
	Rock 51				1983	34.9		-24.2
	Sand 74							
	Metal 18							
Mobiltherm 123 (Figures 20, 23)	Fluid 302	2	316 (600)	No	1077	4.23	31.9	-38.2
					2778	11.45	29.0	-43.8
					3884	14.37	26.4	-48.8
					5302	18.02	27.6	-46.4
					6428	20.58	31.4	-39.1
					7724	22.87	30.4	-41.1

---

*See last page of table

TABLE 1. (Continued)

Fluid	Initial Sample Weight, Grams	Sample I.D.	Temp °C (°F)	Rock and Metal	Time (Hrs)	Wt. Loss (Percent)	Kinematic Viscosity (Centistokes)	Kinematic Viscosity* Change (Percent)
Mobiltherm 123 (Figures 20, 23)	Fluid 237	1	316 (600)	Yes (Irwindale)	1077	4.06	35.3	-31.6
	Rock 44				2778	15.34	39.2	-24.1
	Sand 64				3884	19.12	37.4	-27.5
	Metal 22				5302	22.22	39.4	-23.7
				†	6428	24.86	54.4	+5.2
					1296	4.07	43.7	-15.3
Mobiltherm 123 (Figures 20, 23)	Fluid 267	12	316 (600)	Yes (Barstow)	1498	5.10	37.2	-27.8
	Rock 81				2604	8.26	32.6	-36.8
	Sand 45				4022	28.44	69.4	+34.5
	Metal 23				5496	34.46	59.0	+14.3
Mobiltherm 123 (Figures 19, 22)	Fluid 298	4	302 (575)	No	1077	1.49	44.5	-13.8
					2849	3.92	39.9	-22.7
					3955	5.38	38.1	-26.2
					5373	6.93	36.6	-29.0
					6499	8.52	37.0	-28.3
					7795	12.06	41.4	-19.8
Mobiltherm 123 (Figures 19, 22)	Fluid 253	3	302 (575)	Yes (Irwindale)	1077	1.79	44.5	-13.7
	Rock 56				2849	4.96	42.3	-18.1
	Sand 62				3955	6.68	40.3	-21.9
	Metal 22				5373	8.53	38.9	-24.6
					6499	10.77	40.7	-21.1
					7795	12.45	41.9	-18.8
Mobiltherm 123 (Figures 19,22)	Fluid 224 Rock 103 Sand 106 Metal 20	26	302 (575)	Yes (Barstow)	1254	1.75	47.5	-7.9

---

*See last page of table

†Fresh oil added after measurements

TABLE 1. (Continued)

Fluid	Initial Sample Weight, Grams	Sample I.D.	Temp °C (°F)	Rock and Metal	Time (Hrs)	Wt. Loss (Percent)	Kinematic Viscosity (Centistokes)	Kinematic Viscosity* Change (Percent)
Mobiltherm 123 (Figures 19, 22)	Fluid 155 Rock 52 Sand 61 Metal 23		302 (575)	Yes (Barstow)	1498 2604	1.9 4.2		-11 -13
Mobiltherm 123 (Figures 18, 21)	Fluid 275 Rock 94 Sand 112 Metal 20	14	288 (550)	Yes (Barstow)	1498 2604 4022 5148 6444	1.02 1.64 2.69 3.46 3.93	48.5 48.2 47.7 47.3 48.4	-6.03 -6.59 -7.48 -8.3 -6.2
Sun Oil 21 (Figures 24, 25)	Fluid 208	29	316 (600)	No	965	4.95	24.4	-44.2
Sun Oil 21 (Figures 24, 25)	Fluid 221 Rock 98 Sand 102 Metal 25	28	316 (600)	Yes (Barstow)	965	8.70	22.2	-49.2
Sun Oil 21 (Figures 24, 25)	Fluid 215	22	302 (575)	No	1097 2393	2.06 4.64	43.0 37.7	-1.6 -13.7
Sun Oil 21 (Figures 24, 25)	Fluid 223 Rock 96 Sand 104 Metal 25	21	302 (575)	Yes (Barstow)	1097 2393	1.61 8.93	38.2 37.1	-12.6 -15.1
Sun Oil 21 (Figures 24, 25)	Fluid 210	24	288 (550)	No	1097 2393	0.34 0.94	40.9 40.1	-6.4 -8.2

---

*See last page of table

TABLE 1. (Concluded)

Fluid	Initial Sample Weight, Grams	Sample I.D.	Temp °C (°F)	Rock and Metal	Time (Hrs)	Wt. Loss (Percent)	Kinematic Viscosity (Centistokes)	Kinematic Viscosity* Change (Percent)
Sun Oil 21 (Figures 24, 25)	Fluid 214 Rock 102 Sand 102 Metal 25	23	288 (550)	Yes (Barstow)	1097 2393	0.18 22.12	41.8 41.5	-4.3 -5.0

---

*Initial viscosity, 37.8C (100F)

Caloria HT43	31.2 Centistokes
Therminol 66	25.2 Centistokes
Therminol 55	28.9 Centistokes
Mobiltherm 123	51.6 Centistokes
Sun Oil 21	43.7 Centistokes

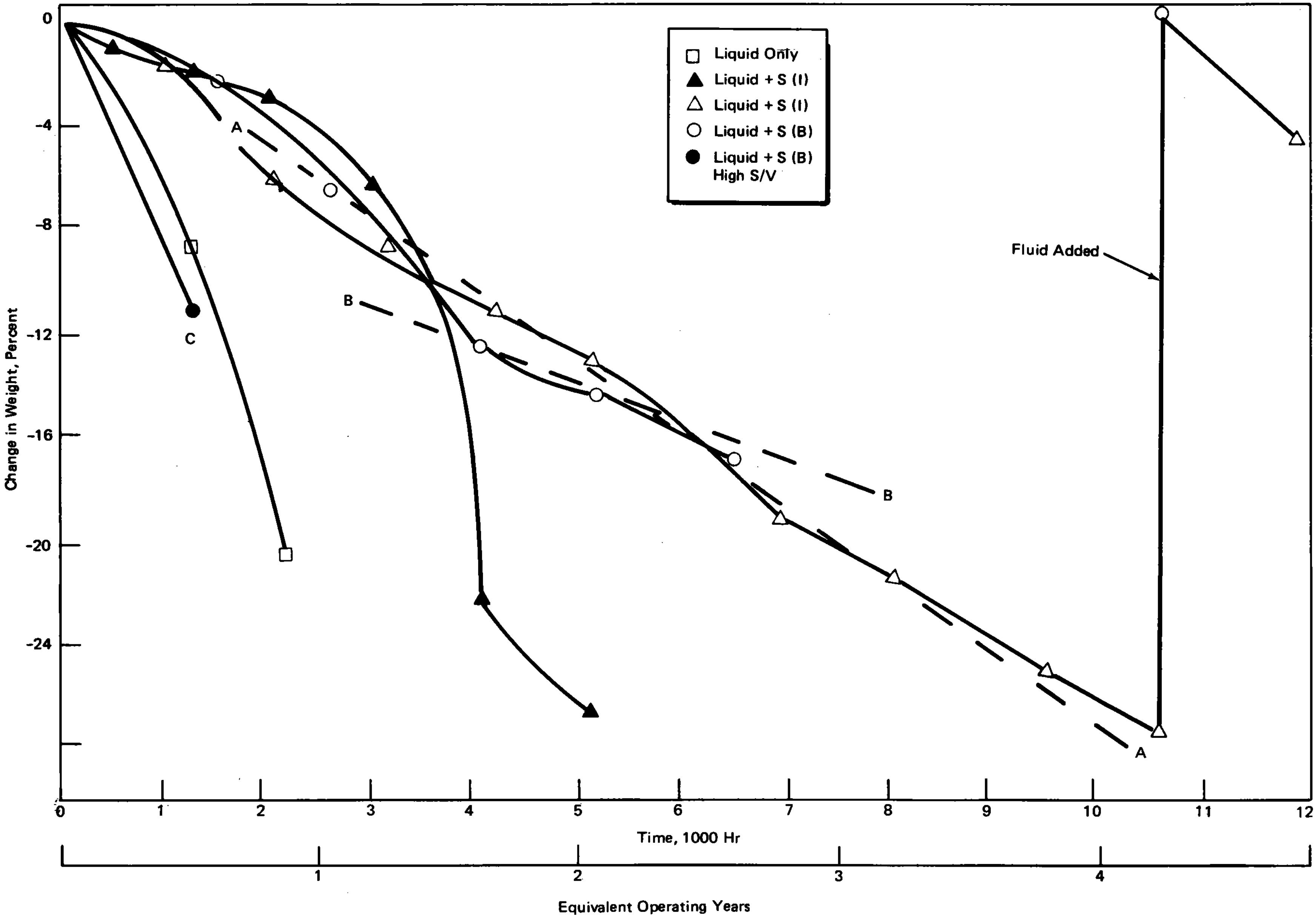

Figure 6. Caloria HT43 Change in Weight 302 C (575 F)

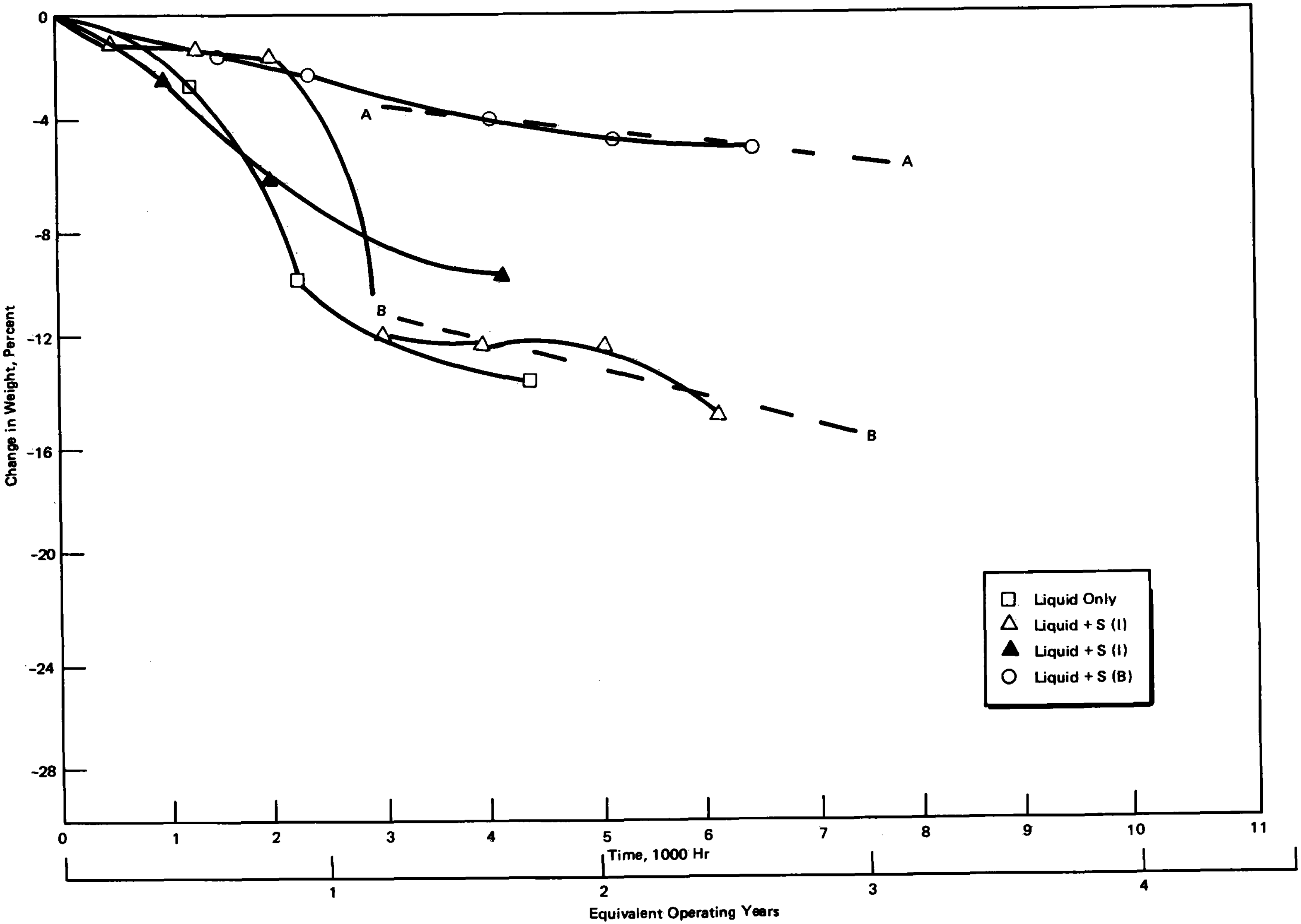

Figure 5. Caloria HT43 Change in Weight 288 C (550 F)

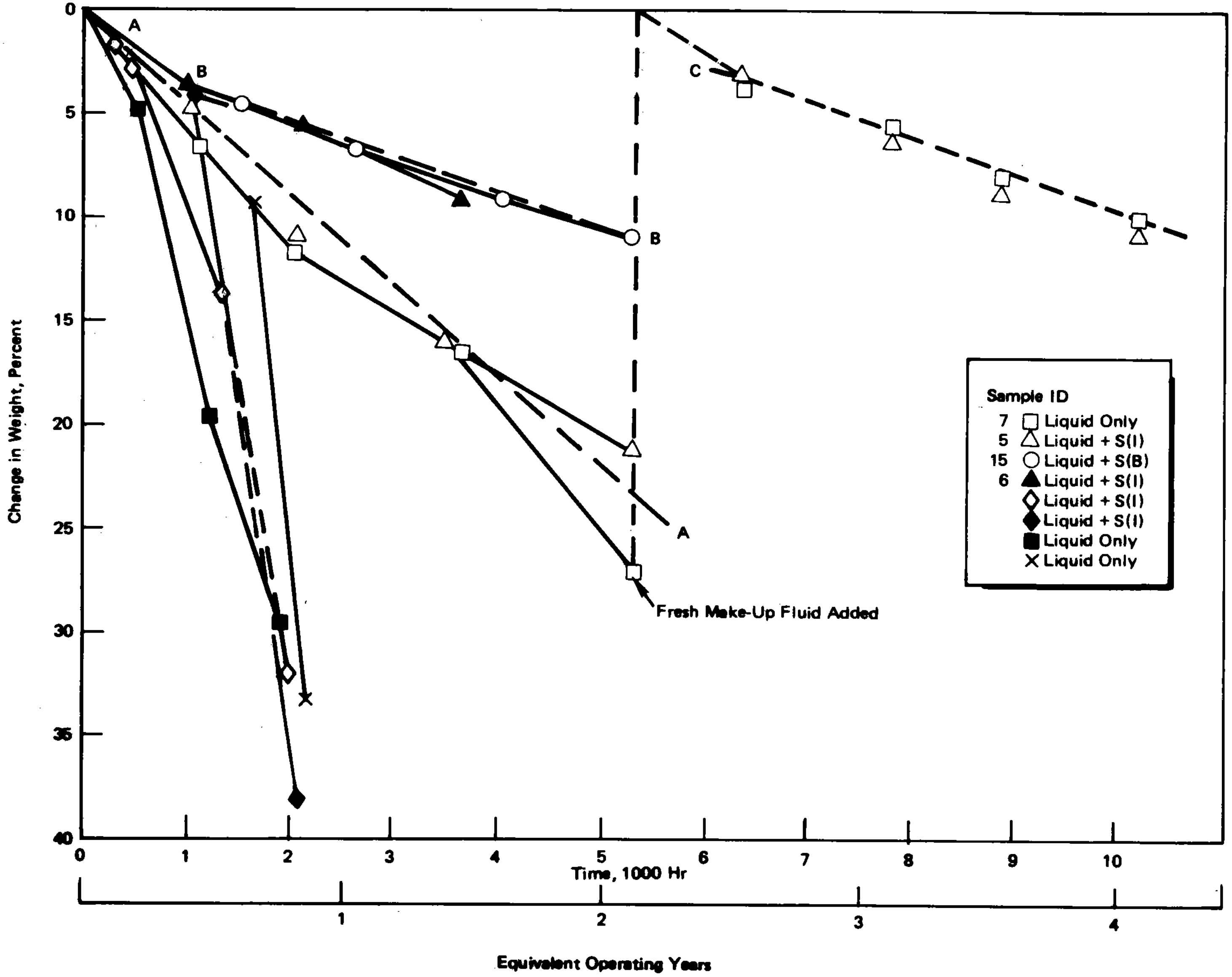

Figure 7. Caloria HT43 Change in Weight 316 C (600 F)

bath to solidify. Stresses accompanying the freezing and melting of the salt could crack a glass flask. Later improvements eliminated bath freezing.

At 288C (550F) only one flask of Caloria HT43 reached the end of the program. This flask containing metal, plus Barstow rock and sand indicated a loss rate* of 0.48 10^{-3}%/hour for the last 300 hours, line A-A**, Figure 5. The three terminated tests displayed large weight loss after 1000 to 3000 hours of heating while the sample with Barstow rock had no such loss after 6400 hours of heating. It would appear that, initially, the Irwindale rock behaves as a catalyst with the fluid, and that the Barstow rock behaves as a stabilizer.

It should be noted, however, that after the comparatively large weight loss, the weight loss rate decreased. Between 3000 and 6000 hours the loss rate is roughly equal to that found for the sample containing the Barstow solids, $1.06 \cdot 10^{-3}$%/hr, line B-B, Figure 5. Slopes A-A and B-B were chosen as the most likely straight line paths through the data points in the section of the curves showing a trend toward linear degradation.

Data taken on fluids, with and without solids, heated to 302C (575F) are given in Figure 6. The two tests not terminated early, one with Irwindale rocks and the other with Barstow rocks, both displayed similar slopes. Both terminated tests experienced very large weight losses. The terminated tests with Irwindale rock appears to be leveling off to a slope (or weight loss rate) that is quite close to that exhibited by the two ongoing tests.

The slope of the last portion of this curve was used in the Phase I Thermal Storage Subsystem Report to obtain the rate of weight loss reported for 302C (575F). A line A-A has been drawn in Figure 6 with a slope corresponding to a weight loss rate of $2.81 \cdot 10^{-3}$%/hr*** for comparison with the data. Line B-B in Figure 6 has been drawn through the last three data points of the ongoing sample with Barstow rock; the slope of this curve is $1.76 \cdot 10^{-3}$%/hr.

---

*Loss rate per year for particular plant depends upon the duty cycle. This is explained in Figure 27.

**Lines A-A, B-B, etc. are straight line loss rates representing an average of a group of data points.

***7% per year for a 2500 hr. equivalent year. Also, see Figure 27.

Near the end of the program a test was initiated using a larger volume of rock with respect to the fluid volume. This sample (ID 25, Table 1) contained a volume of rock with a rock surface to fluid volume ratio of 15 cm^{-1} compared to the typical test sample of 8 cm^{-1}. Only a single weight loss was determined (at 1254 hours) before the termination of the program. This is shown as point C on Figure 6. Based on this single point, the yearly loss rate would be approximately 22 percent.

It should be noted that because of the nature of the tests, there were considerable variations in fluid loss rate. Many samples settled down to consistent and relatively low loss rates after exhibiting large initial values.

After termination of the prescribed tests the gaseous nitrogen supply was shut off. In approximately 1 day all samples became very dark and viscous. This served to show the need for the exclusion of oxygen as well as verifying the absence of oxygen in the samples during the 3 year program.

In Figure 7, data are given that have been obtained with Caloria HT43, with and without solids, at 316C (600F). The lowest weight loss rate was found for fluid test samples containing Barstow rock and sand. Two other tests, one with fluid only and the other with Irwindale rock and sand, display greater fluid loss rates up at 5265 hours when fresh make-up fluid was added to the flasks. The line labeled A-A represents a weight loss rate of 4.31×10^{-3}%/hr reported in the Phase I Thermal Storage Subsystem Report for Caloria HT43 at 316C. The line B-B was drawn through data from two different (and more recent) tests of the fluid with Barstow rock. A third line, C-C, has been drawn through the weight loss data points of the Irwindale rock and the neat fluid sample. The slope of line C-C is somewhat greater than line B-B and less than half the slope of line A-A used to correlate the weight loss data before fresh fluid was added to the flasks.

Test samples with neat fluid and with rocks indicated a higher loss rate than those tested at a later time which were used to establish the estimated loss rates. The later data were more consistent and were used for comparison of the various temperature levels, fluid types, and conditions.

Viscosity Change. The kinematic viscosity data obtained for Caloria HT43 are plotted as a function of time in Figures 8, 9, and 10. Initially, the kinematic viscosity of the fluid was observed to decrease with thermal exposure time; the higher the temperature to which the fluid was subjected, the faster the kinematic viscosity decreased. Time intervals where the fluid sample had undergone a large weight loss are seen to correspond to those time intervals where the fluid also increased in kinematic viscosity. This increase, coming after several time intervals during which the fluid kinematic viscosity steadily decreased, is probably due to the vaporization of accumulated lower molecular weight compounds. Why this should occur with relative suddenness after 2000 or 3000 hours in some of the samples and not with others is unknown at present.

Gaseous Decomposition Products. The decomposition products vaporized from a sample of Caloria HT43 in contact with Barstow rocks, sand, stainless steel, and carbon steel were collected and analyzed in a set of three experiments. The usual simple thermal stability and material compatibility test apparatus was slightly modified for collection of the volatilized products by sealing a ball joint to the end of the air cooled condenser. This ball joint permitted the heated flask to be linked, via a 1/4 inch stainless steel line, to a simple gas collection system. Initially the gases were collected in a teflon sampling bag. The bags were required very little attention as they slowly filled with gas over a period of several weeks. A disadvantage in the use of plastic sampling bags is their permeability. Gases like H_2 will rapidly diffuse through any plastic sheet. When the collection time is long, even gases with low rates of diffusion through the polymer wall of the sampling bag can undergo large concentration changes. In order to establish some basis for correcting the gas concentrations in the sampling bag for the effects of diffusion losses, a teflon sampling bag was filled with a gas mixture of known composition (the control) at the same time another bag was connected to the flask of Caloria HT43. The contents of the control bag were analyzed along with the bag of decomposition products to ascertain the effect of diffusion.

The gas sampling bag was removed from the flask of Caloria HT43 with solids after 460 hours. The flask had been heated to 316C (600F). The

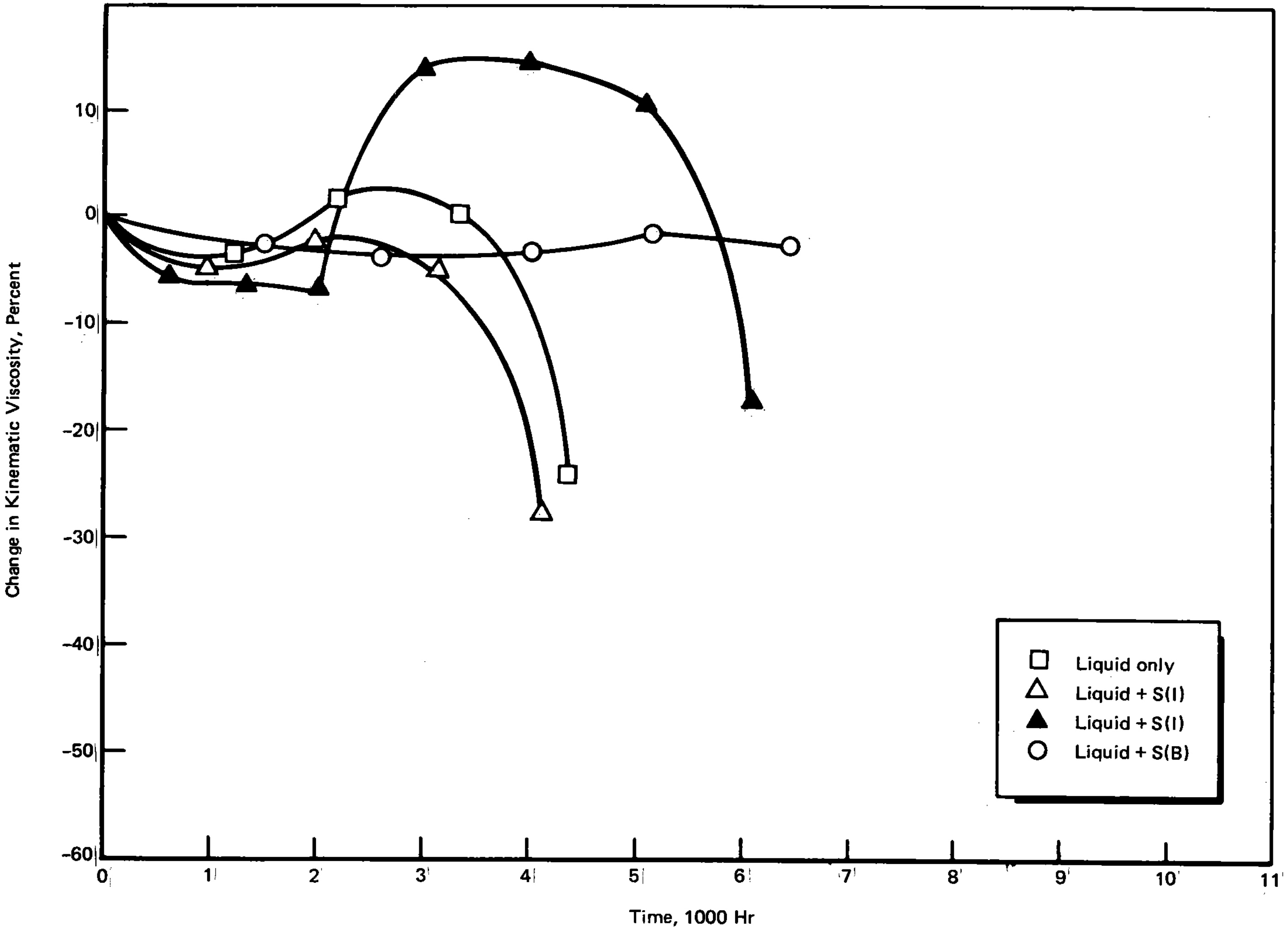

Figure 8. Caloria HT43 Change in Kinematic Viscosity 288 C (550 F)

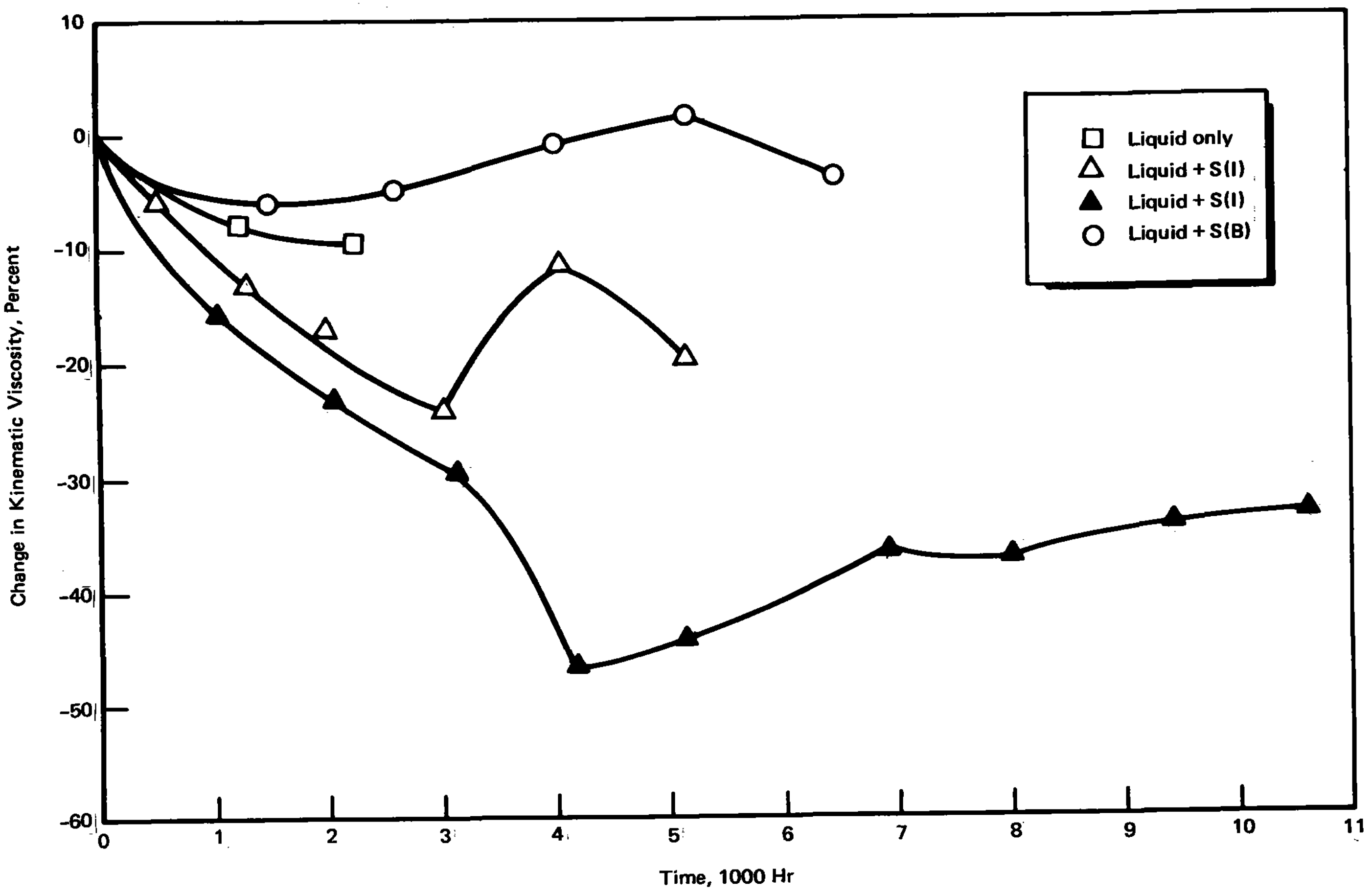

Figure 9. Caloria HT43 Change in Kinematic Viscosity 302 C (575 F)

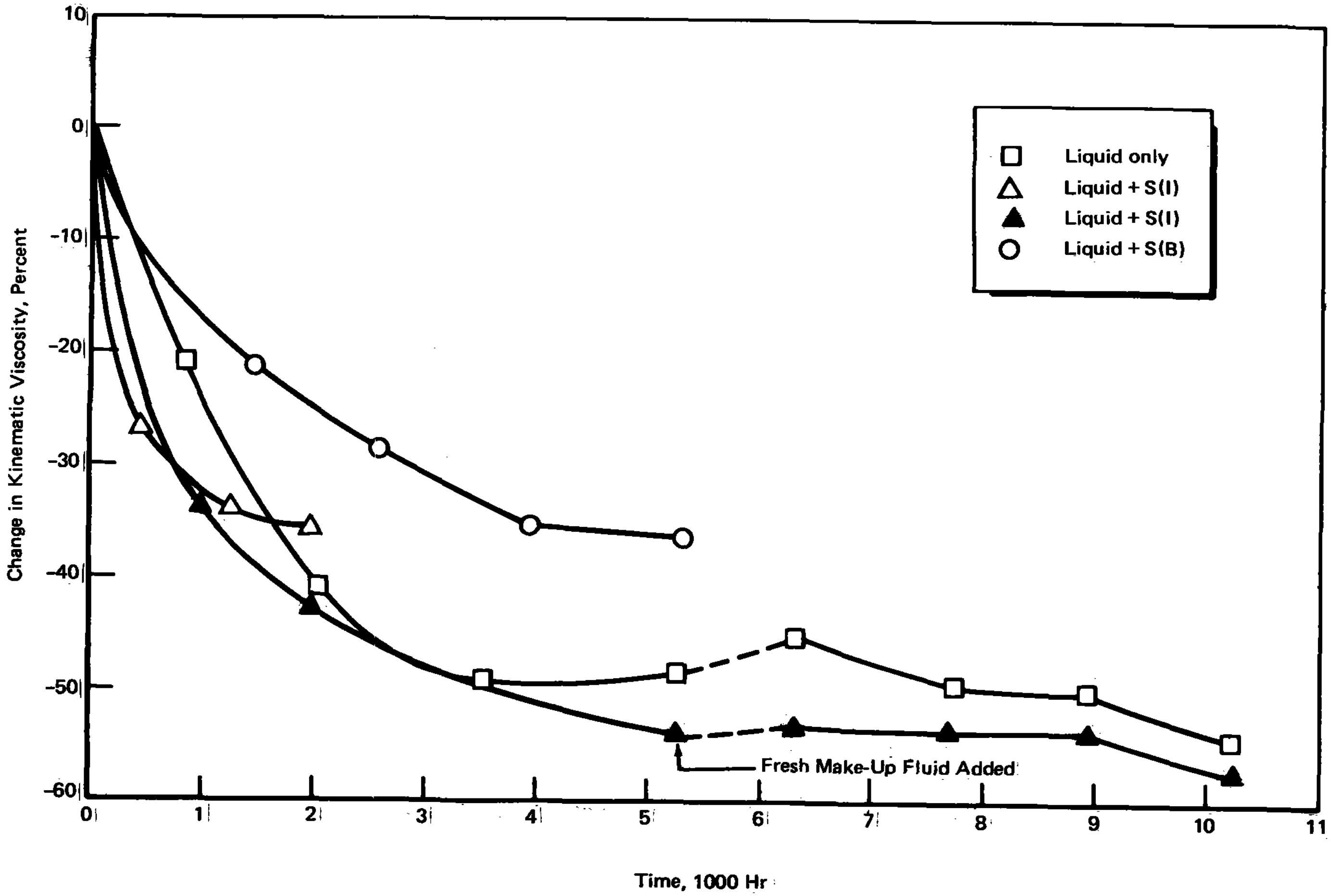

Figure 10. Caloria HT43 Change in Kinematic Viscosity 316 C (600 F)

accumulated gaseous decomposition products and the control sample were analyzed by gas chromatography (GC). Hydrocarbon compounds from methane up to pentane were identified and their concentrations determined. Adjustments in the measured concentrations were made from the control bag by assuming the ethane, propane, and butane did not diffuse through the bag and that the percent of each compound retained in the control would be the same in the decomposition products. The results of the analysis are summarized in Table 2. It was not possible to estimate the initial H_2 concentration in the gas since no residual H_2 remained in the gas sampling bag.

TABLE 2. ANALYSIS OF GASEOUS DECOMPOSITION PRODUCTS OF CALORIA HT43 WITH SOLIDS AT 316 C (600 F) (Volume Percent)

Compound	Calibration Gas	Calib. Control Gas Bag	Caloria HT43 Decomp. Gas	Corr. Decomp. Gas Anal.
CH_4	8.32	15.4	2.4	2.77
C_2H_6	1.96	4.04	2.4	2.4
C_3H_8	2.05	4.59	3.9	3.9
$n\text{-}C_4H_{10}$	1.99	4.29	3.0	3.0
N_2	7.54	48.0	49.1	19.0
CO	1.87	2.7	--	--
CO_2	2.15	0.15	0.03	0.92
H_2O	--	--	--	--
H_2	74.1	1.4	?	?
O_2	--	19.4	18.4	--
C_2H_4	--	--	0.2	0.2
C_3H_6	--	--	1.2	1.2
$i\cdot C_4H_{10}$	--	--	5.7	5.7
$n\text{-}C_5H_{12}$	--	--	8.0	8.0

Because of diffusion of various gases through the teflon bags (both out of and into the bag) and a desire to obtain the H_2 concentration, their use was discontinued. In a later experiment, the decomposition gases were collected over mercury in a gas-tight 250 ml pyrex sampling bottle connected to a mercury leveling bulb. Periodically the mercury level was adjusted as the gas accumulated in the sample bottle. The results of a GC analysis of the gases collected from the same Caloria HT43 sample about 1500 hours later is given in Table 3. The gases were collected from fluid that had accumulated between 2076 and 2623 hours at 316C (600F).

The large percentage of H_2 in the gas strongly indicates a residual fluid that is becoming increasingly unsaturated. A comparison of the gas composition as given in Tables 2 and 3, that is, between gas collected in the first 500 hours of heating and gas collected after 2000 hours of heating, is difficult without knowledge of the amount of H_2 in the sample so that the composition could be normalized to 100%. Then, too, the corrected analysis of gas from the teflon bag includes more N_2 than was likely to have been present (N_2 and O_2 diffuse from the atmosphere into the bag).

Therminol 66

Weight Loss. No tests were conducted with fluid only at 288C (550F). Since Therminol 66 was rated by the manufacturer, Monsanto, for use at bulk temperatures up to 343.3C (650F) it was felt that 288C (550F) would present no problem for a neat fluid sample. In Figure 11, tests of the fluid with Barstow rock and sand and with Irwindale rock and sand are presented. After a rapid weight loss in the first 2000 hours, the Irwindale sample weight losses are quite small and, in fact, exhibit a weight loss rate not too different from that shown by the fluid sample containing the Barstow rock and sand. As shown in Figure 11, the sample with the Barstow solids did not display a rapid weight loss after over 6420 hours of testing at 288C (550F).

The data plotted in Figure 12 indicate, as in Figure 11, that some flasks of Therminol 66 will undergo large weight losses over one or two thousand hour intervals and then level off. In this case one of the flasks contained only Therminol 66 while the other contained Irwindale rocks and metal. The more recently prepared fluid test containing Barstow rocks and sand produced a more well-behaved curve. The straight line A-A drawn through the data points for the fluid containing Barstow rocks and sand, represents a weight loss rate of 1.38 X 10^{-3}%/hr. The value reported previously for Therminol

TABLE 3. ANALYSIS OF GASEOUS DECOMPOSITION PRODUCTS OF CALORIA HT43 WITH SOLIDS AT 316C (600F)

Compound	Volume Percent		
CH_4	20.5	Calibrated	
C_2H_6	11.6	↓	
C_3H_8	12.3	↓	
$n\text{-}C_4H_{10}$	8.1	↓	
N_2	2.0	↓	
CO	2.4	↓	
CO_2	2.0	↓	
H_2O	1.0	↓	
H_2	20.8	↓	
O_2	0.2	Using calibration for	N_2
C_2H_4	0.5	↓	C_2H_6
C_3H_6	2.0	↓	C_3H_8
iC_4H_{10}	2.4	↓	nC_4H_{10}
nC_5H_{12}	6.0	↓	nC_4H_{10}
TOTAL	91.8%		

Unknowns on molecular sieve column

eluted between CH_4 and C_2H_6 (not C_2H_4) = 5.9% using CH_4 calibration

eluted after C_2H_6 = 1.8% using CH_4 calibration

Unknowns on PORAPAK Q column

eluted between $n\text{-}C_4H_{10}$ and nC_5H_{12}, three compounds = 0.1%, 0.1% and 3.2% using nC_4H_{10} calibration

eluted after nC_5H_{12} = 0.4% using nC_4H_{10} calibration

---

*Fluid testing time: 2076 to 2623 hours.

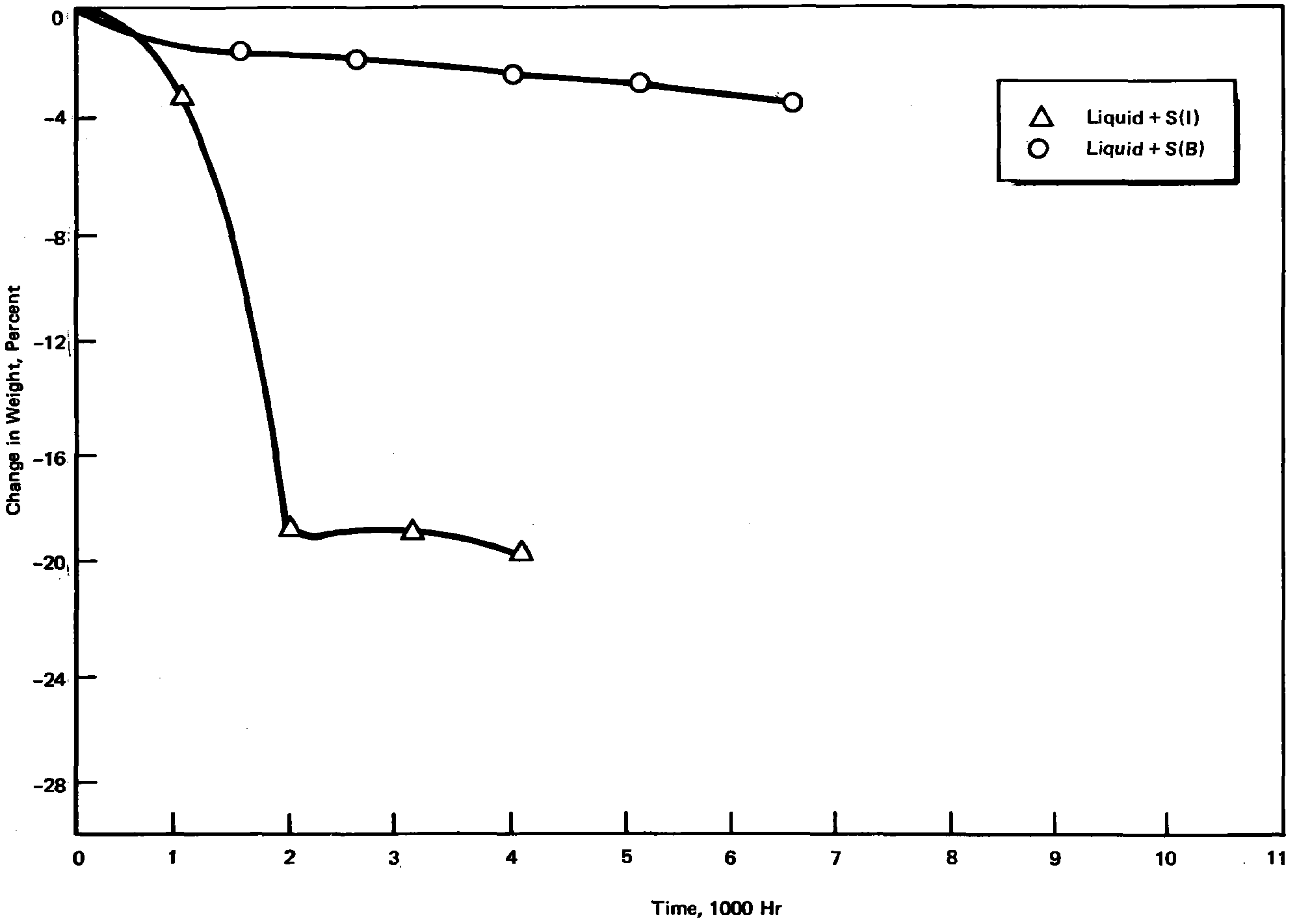

Figure 11. Therminol 66 Change in Weight 288 C (550 F)

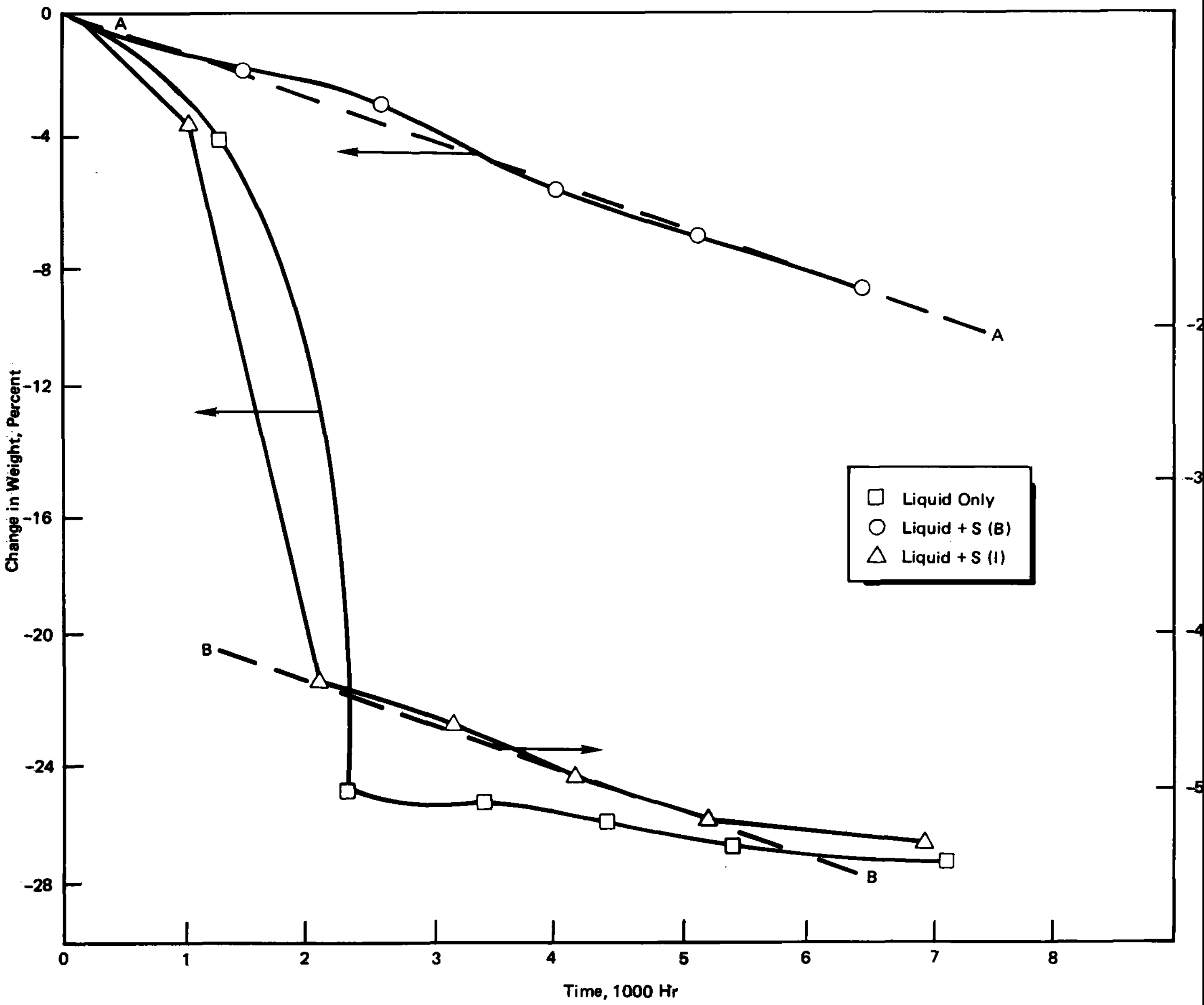

Figure 12. Therminol 66 Change in Weight 302 C (575 F)

66 (Reference 20), 2.74 X 10^{-3}%/hr, was obtained from a test containing Irwindale rocks and is shown as line B-B in Figure 12.

Data on Therminol 66 obtained at 316C (600F) are given in Figure 13. The data plots obtained at this temperature are very similar to those found at 288C (550F) and 302C (575F) in that they either show gradual weight losses over long periods of time or rapid weight losses over a 1000 or 2000 hour period. The weight loss rate of the neat Therminol 66 sample, indicated

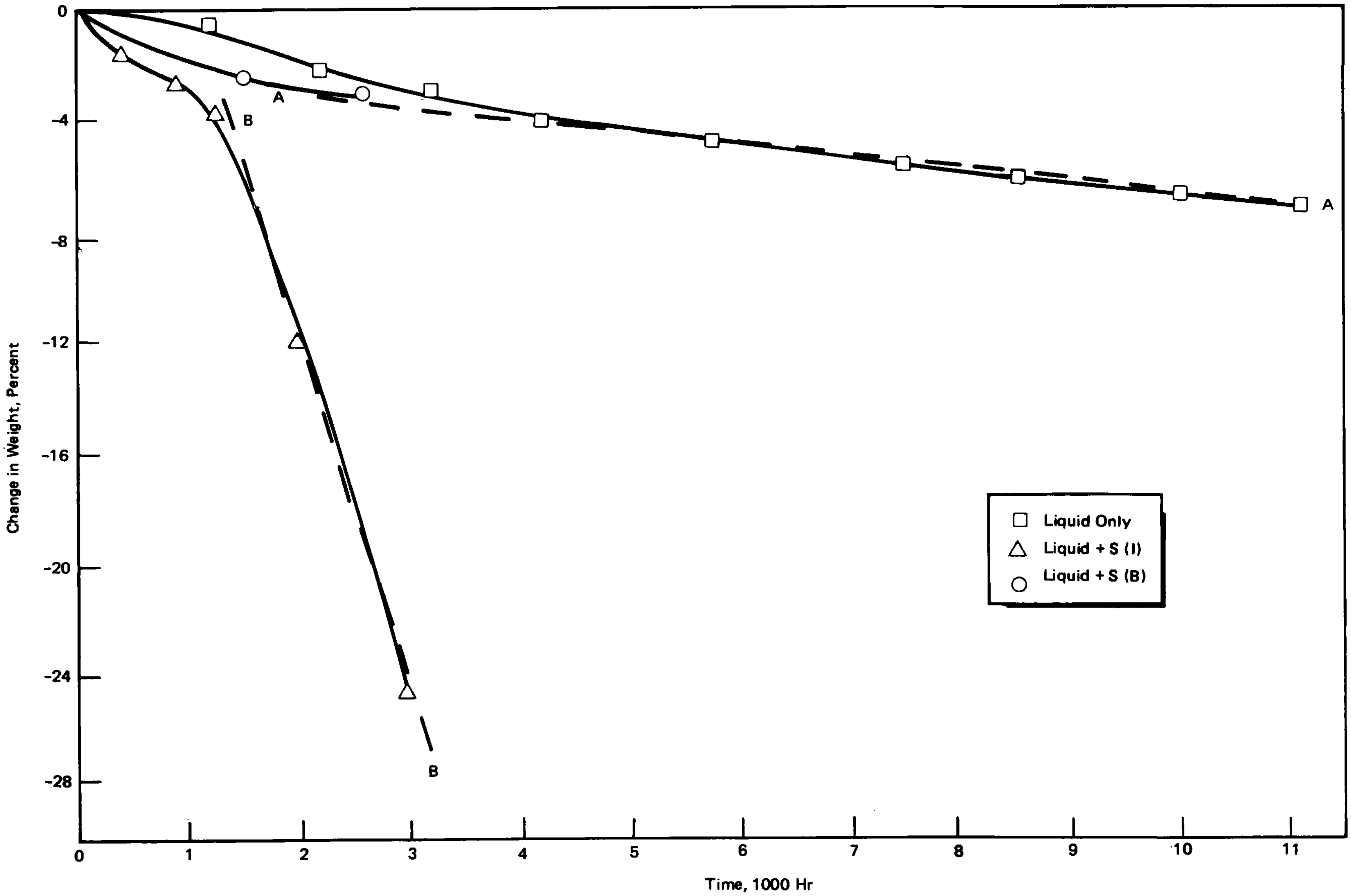

Figure 13. Therminol 66 Change in Weight 316 C (600 F)

by line A-A, is 0.43 X 10^{-3}%/hr which is substantially less than the 1.38 X 10^{-3}%/hr measured at 302C (575F) for a test sample that contained Barstow rocks. The weight loss rate previously reported for 316C (600F) (Reference 20) was 12.6 X 10^{-3}%/hr for a sample with Irwindale rocks; the line B-B representing this rate is also drawn in Figure 13.

The 30 fold difference in reaction rates indicated by the slopes of lines A-A and B-B drawn through the data in Figure 13 may have been caused by several things. First, the low value (line A-A) is less than the rates measured at 302C (575F) and is almost identical with the rate measured at 288C (550F) for Barstow rock. There is therefore reason to believe that the rate represented by line A-A at 316C (600F) is anomalously low. Second, for the most part, the line A-A in Figure 13 has been drawn through data points taken on a sample of Therminol 66 liquid with no rock or metal. The data points near line A-A plotted in Figure 13 for fluid containing Barstow rock and sand extend only to 2500 hours. At 302C (575F) a sample of Therminol 66 with Barstow rock and sand experienced a severe weight loss over a 1000 hour span after which the data points indicated a lesser rate of weight loss (line B-B in Figure 12). These sudden losses of Therminol 66 measured over one or two thousand hour intervals have been noted before and have not been explained. It is always possible that air may have leaked in but fluid samples subsequently examined by IR have not given any indication of the presence of partially oxidized species in the fluid (although it is possible that oxygen may initiate a chain reaction and be volatilized as CO, CO_2, or H_2O). Longer reaction times for the Therminol 66 with Barstow rock and sand at 316C (600F) might also have resulted in a rapid loss of 15% or more of its weight and a subsequent greater weight loss rate, i.e., the rate might have been closer to 4.3 X 10^{-3}%/hr obtained by extrapolating to 316C (600F) the rate data obtained for Therminol 66 at 288C (550F) and 302C (575).

Although the possibility exists that fluid could escape from a cracked vessel it is extremely unlikely. First, a crack can be readily observed in a glass vessel and secondly, the higher density molten salts would leak into the flask instead of the fluid leaking out.

Tests of Therminol 66 were also conducted at 329C (625F) and 335C (635F) using electric heating mantles manually controlled with Variacs. The flask with neat fluid was restricted to 335C (635F) since the Therminol was boiling at this point. The data obtained at these higher temperatures (Figure 14) indicate percent weight losses that are quite low when compared to test results obtained with Therminol 66 with solids at lower temperatures. In general, fluid samples heated in salt baths show greater weight losses and changes in kinematic viscosity than those heated with electric heating mantles. This could be due to the differences in the surface area of the flask that is heated.

Flasks placed in the salt bath were usually immersed to a depth sufficient to cover the entire round portion of the flask. In heating mantles, however, only the bottom half of the flask is heated; the top of the flask is wrapped with fiberglass insulation. It is suspected that the unheated top of a flask results in larger heat losses from the flask and the setting up of thermal gradients in the contents of the flask.

Viscosity Change. Determination of the kinematic viscosity changes occurring in Therminol 66 subjected to long term exposure to various solids and heat, has indicated that while some decrease may occur in the first 1000 at 2000 hours, eventually the kinematic viscosity will increase. The measurements of the kinematic viscosity of Therminol 66 are given in Figures 15, 16, and 17. Decreases in kinematic viscosity noted early in the tests were not as great as those encountered with Caloria HT43. Evidently the products of thermal degradation that remain in the liquid phase of Therminol 66 at the test temperatures do not have a substantial effect on the kinematic viscosity of the fluid. There also may be a tendency towards polymerization since the fluid kinematic viscosity would increase. Without other information on the fluid it is difficult to relate viscosity changes to cracking or polymerization processes in any definite manner since both may be occurring simultaneously. As with the Caloria HT43 data, rapid increases in kinematic viscosity accompanied periods of high weight loss.

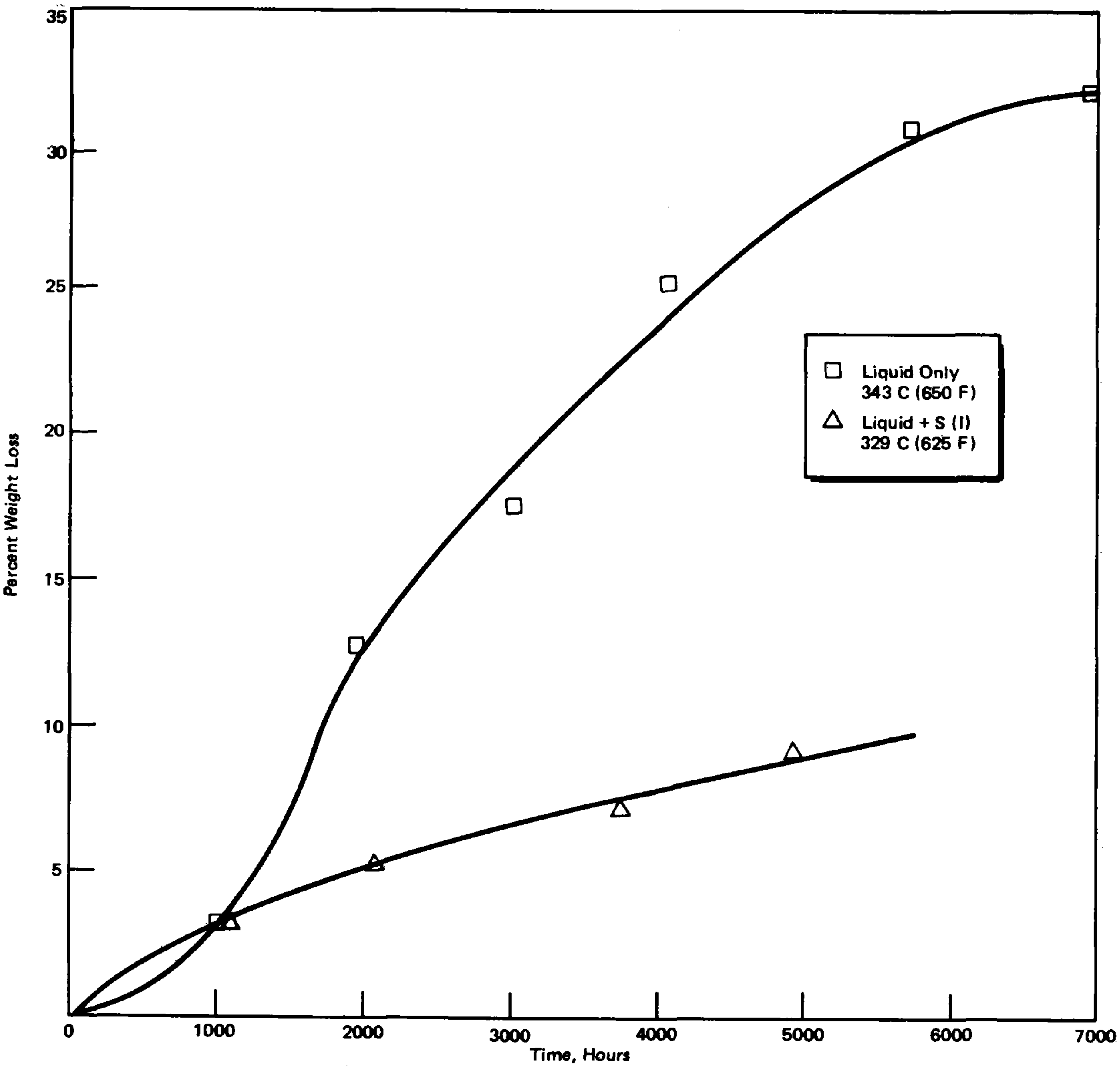

Figure 14. Therminol 66 Change in Weight 329 C (625 F), 343 C (650 F)

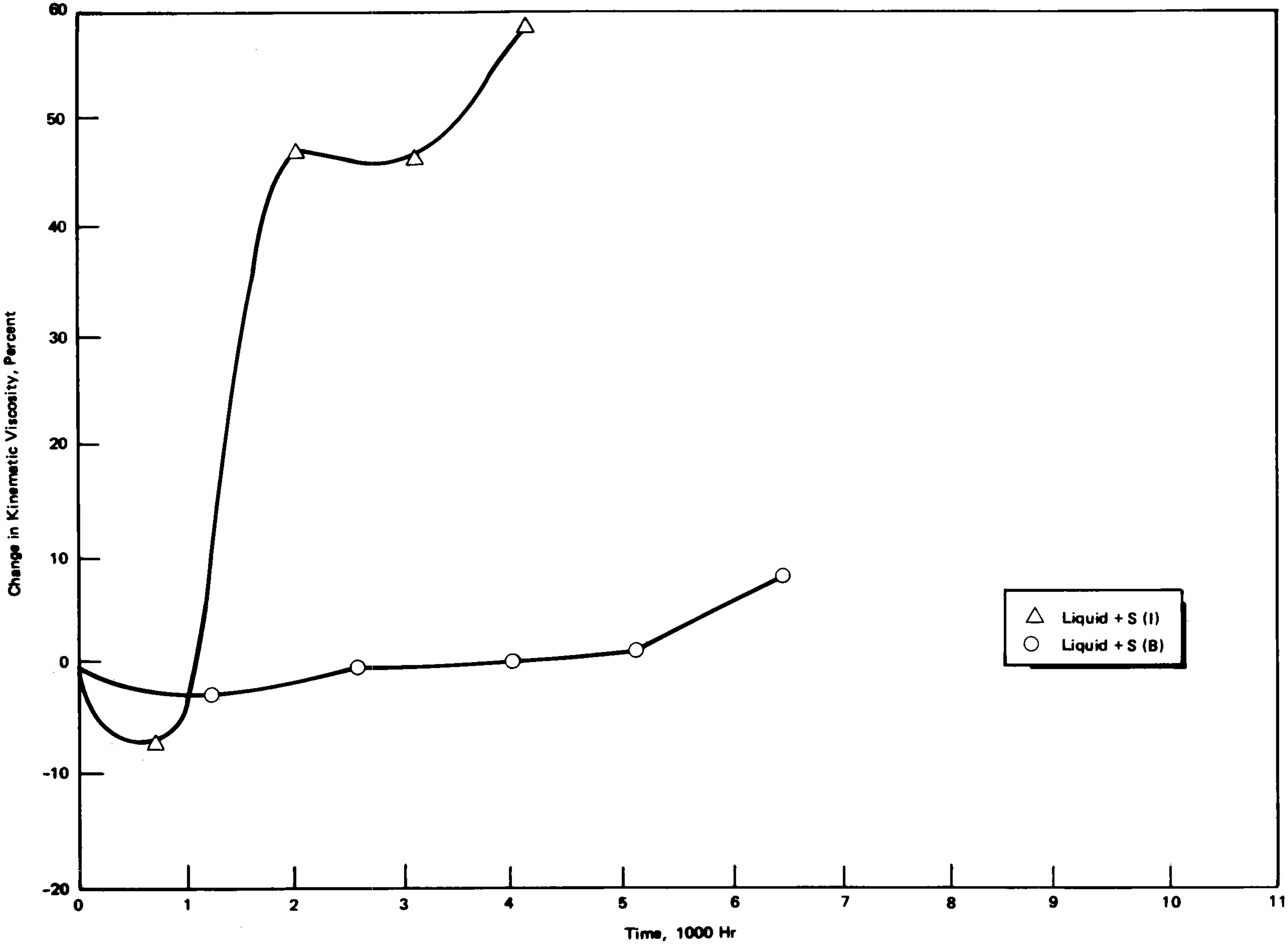

Figure 15. Therminol 66 Change in Kinematic Viscosity 288 C (550 F)

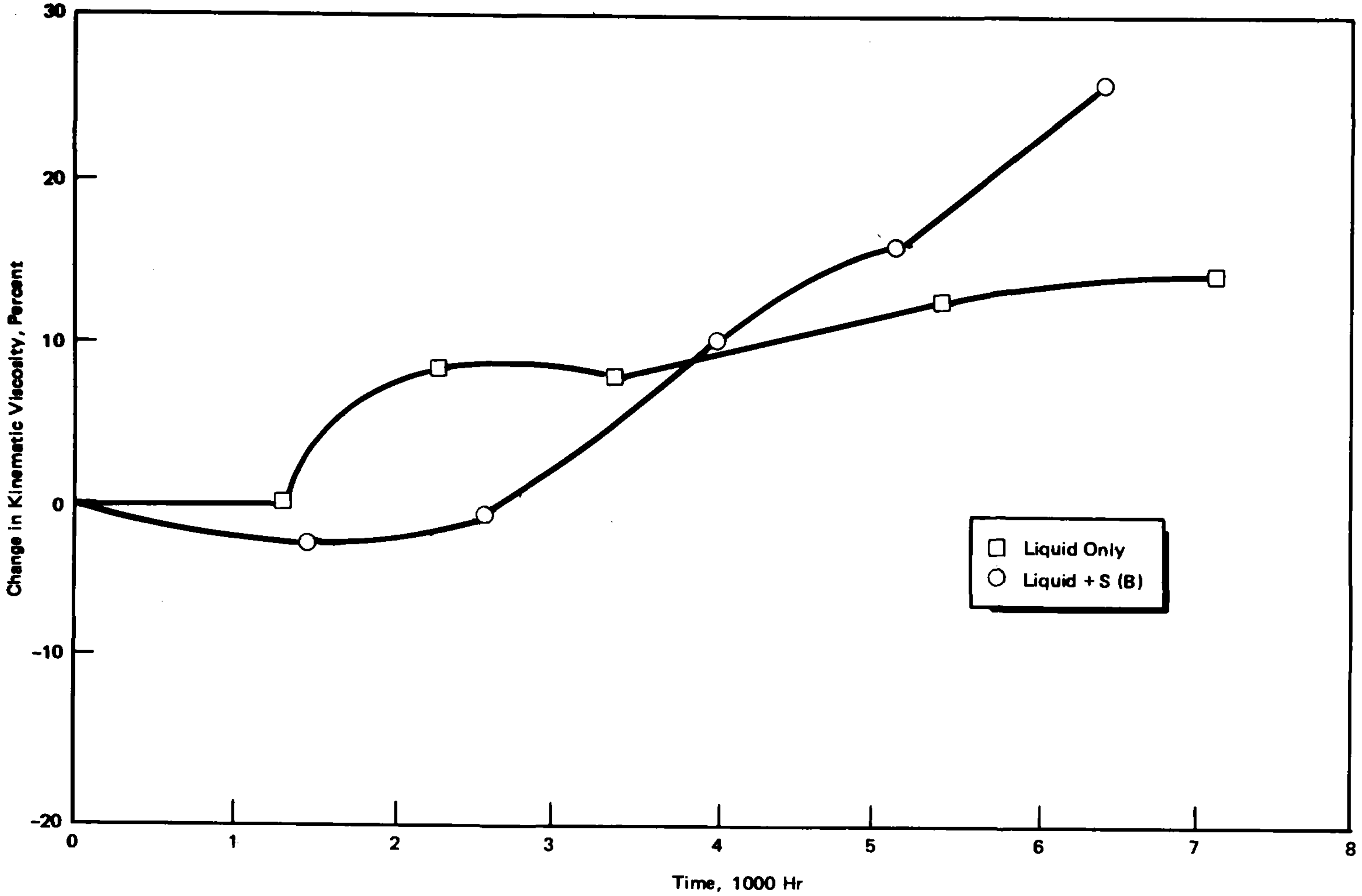

Figure 16. Therminol 66 Change in Kinematic Viscosity 302 C (575 F)

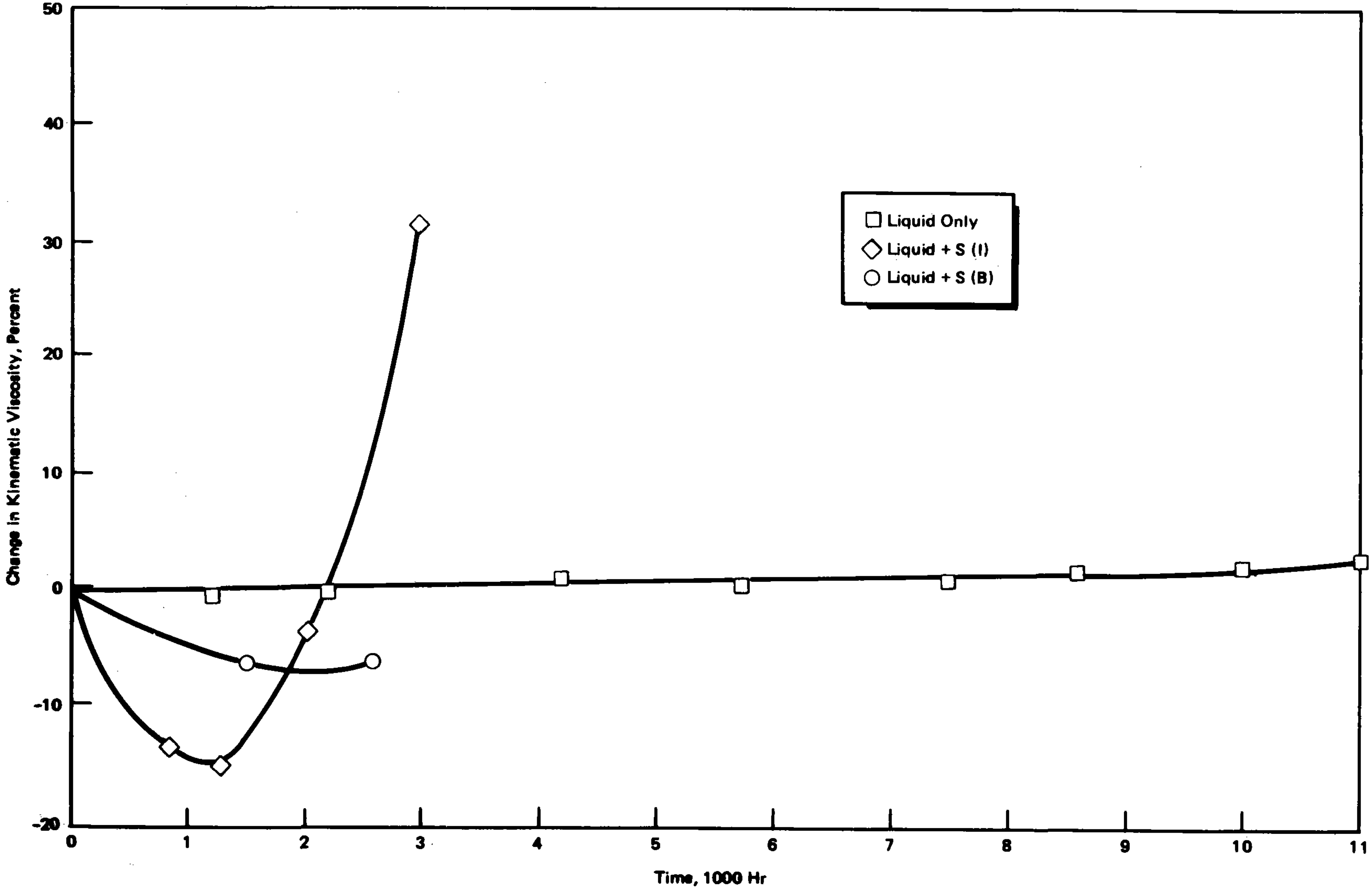

Figure 17. Therminol 66 Change in Kinematic Viscosity 316 C (600 F)

Therminol 55

Samples of Therminol 55 were subjected to temperatures of 288, 302 and 316C (550, 575 and 600F) (Table 1). The earliest test, conducted using a heating mantle, resulted in an excessive weight loss (38.6 wt. percent after 1189 hours). This test was discontinued. Duplicate tests were performed using Therminol 55 from another batch of the fluid (to eliminate the possibility that the original Therminol 55 sample had some unusual defect). As shown in Table 1, tests conducted with the second batch of therminol 55 corroborate the earlier results. All testing of Therminol 55 was discontinued after about 2100 hours, when large weight losses and changes in kinematic viscosity indicated this fluid could not be used economically in the desired temperature range.

Mobiltherm XMTL 123.*

Weight Loss. The experimental data gathered on the thermal stability and compatibility tests performed on Mobiltherm XMTL 123 are given in Figures 18, 19, and 20. At the lowest temperature, 288C (550F), only one test was conducted. The weight loss rate measured during the 6444 hours of testing of this sample which contained Barstow rock and sand plus stainless and carbon steel, was found to be 0.62 X 10^{-3}%/hr, line A-A.

At 302C (575F), tests were performed with neat fluid and in the presence of Barstow rock and sand and Irwindale rock and sand. The weight loss data indicate a rate of 1.32 X 10^{-3}%/hr for neat fluid, line A-A, and 1.55 X 10^{-3}%/hr for Irwindale rock, line A-A. The solids do appear to have accelerated the weight loss rate somewhat.

For 316C (600F), tests were again performed for the neat fluid and with the fluid in contact with Barstow rock and sand plus steel and Irwindale rock and sand plus steel (Figure 20). One of the three tests (with Barstow rock) is seen to have experienced a large weight loss in one of the time intervals.

---

*Near the end of the tests, the manufacturer stated that based on the original fluid color, the sample used here may not have been a valid representation of XMTL 123.

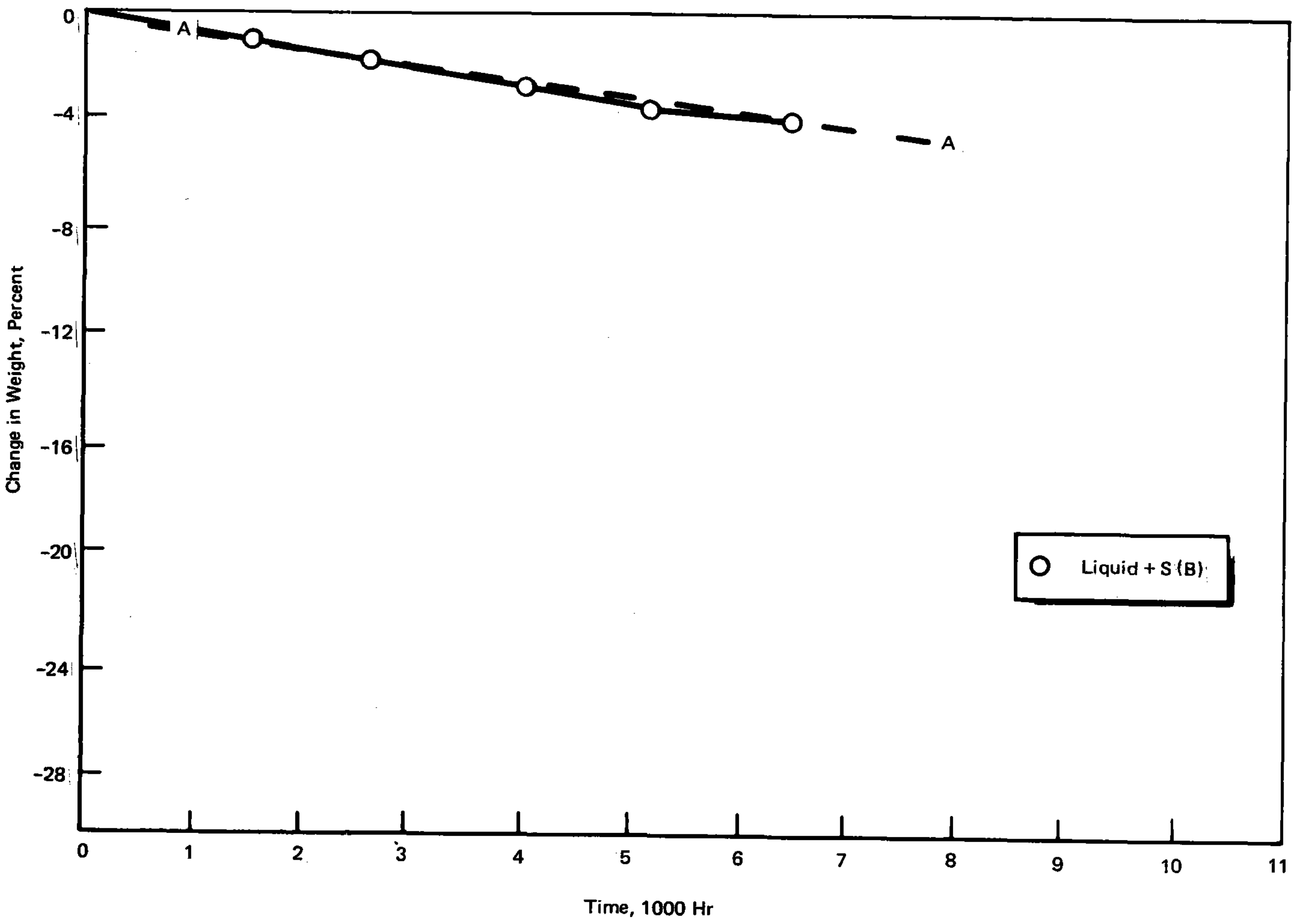

Figure 18. Mobiltherm 123 Change in Weight 288 C (550 F)

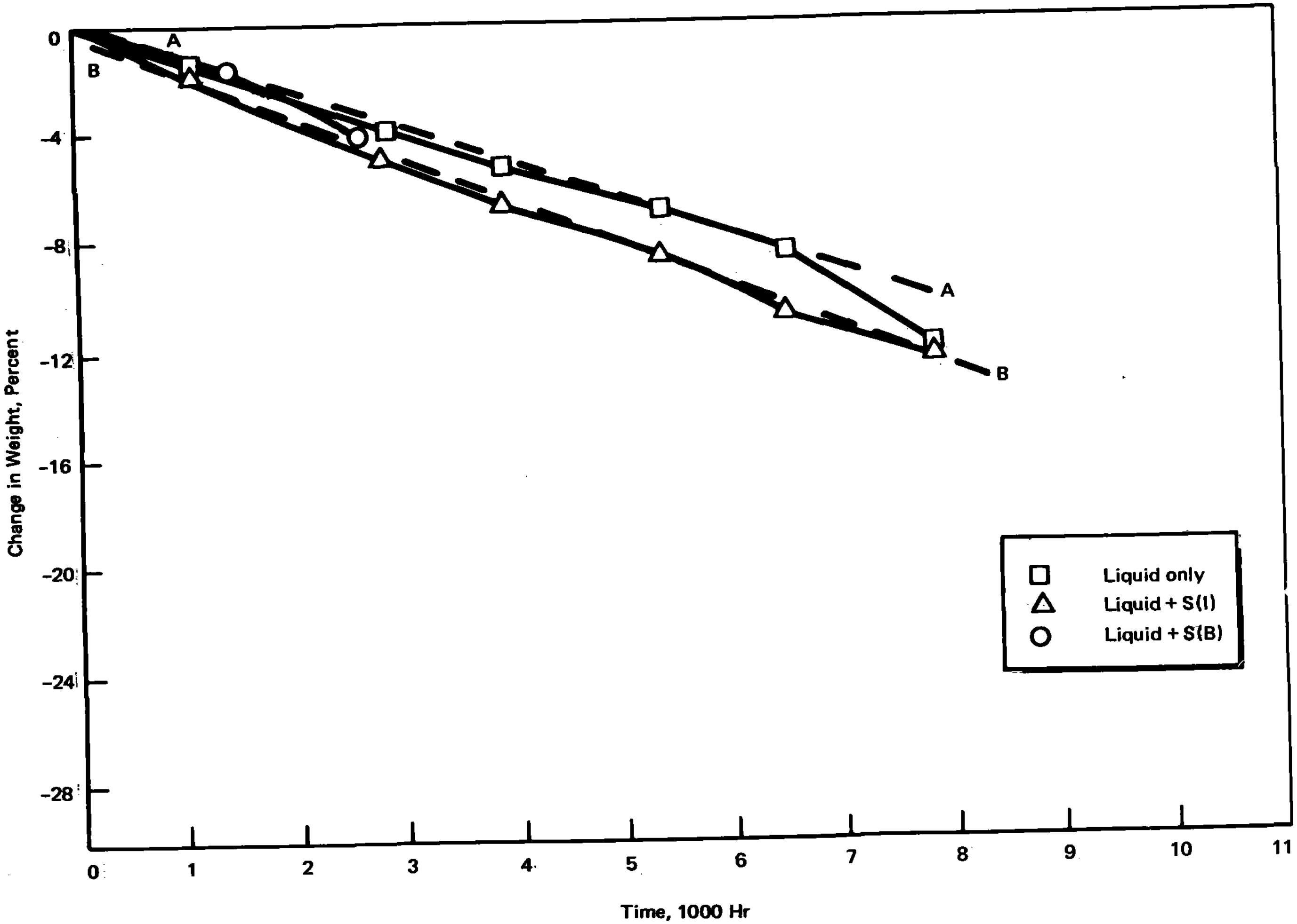

Figure 19. Mobiltherm 123 Change in Weight 302 C (575 F)

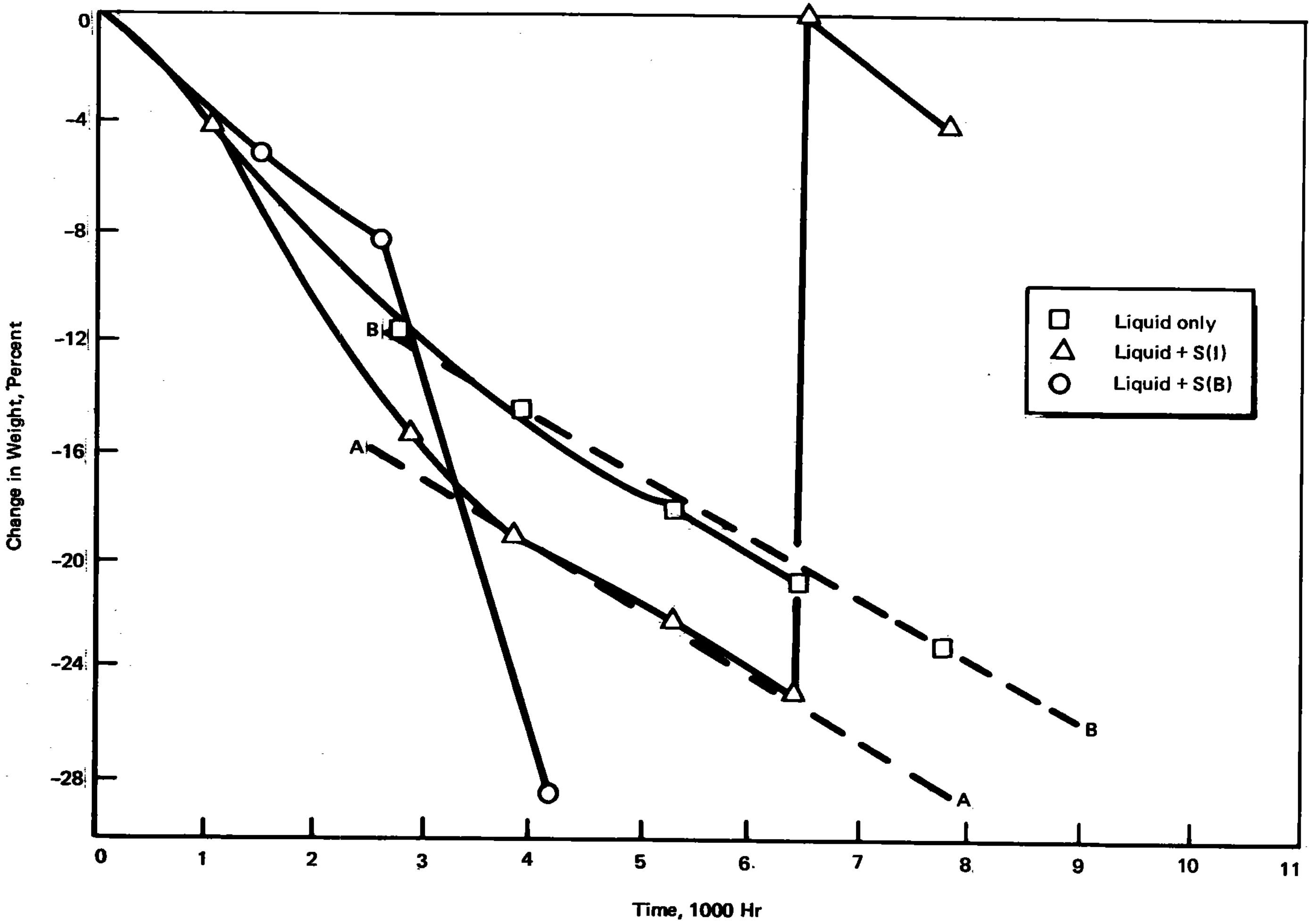

Figure 20. Mobiltherm 123 Change in Weight 316 C (600 F)

Loss rate for Irwindale rock was 2.36 X 10^{-3}%/hr, line A-A, and 2.2 X 10^{-3}%/hr for the heat sample, line B-B. Over this same time interval the kinematic viscosity more than doubled indicating that some distillation of more volatile and less viscous components had occurred.

After 6428 hours of testing at 316C (600F) and the loss of 23.7% of the original fluid weight, fresh Mobiltherm XMTL 123 was added to replenish the amount lost. Only one data point has been recorded since the addition of fresh fluid and it is thus too early to definitely predict any trend in the weight loss rate.

Viscosity Change. The change in kinematic viscosity of Mobiltherm XMTL 123 with temperature and time is fairly similar to that found for Caloria HT43, i.e., all of the tests show an initial decrease in kinematic viscosity and higher fluid temperatures resulted in greater initial reductions in kinematic viscosity (Figures 21, 22, and 23).

Sun Oil 21

Testing of Sun Oil 21 began late in the course of the program as replacements for several Therminol 66 tests that were terminated. Thus, for each sample only two data points (2393 hours) have been recorded at 288C (550F) and 302C (575F) and one data point recorded for the Sun Oil 21 samples at 316C (600F), Figures 24 and 25. To date, the data indicate that the presence of Barstow rocks (no tests were initiated with Irwindale rocks) and metal will increase the weight loss rate. It is worth noting that at 288C (550F), during the second time interval, the fluid apparently lost almost 22% of its initial weight. During this same time interval, however, the kinematic viscosity of the fluid (Figure 25) barely changed at all. The apparent incongruity of the changes in these values may indicate an error in one of the measurements. Further testing is required to indicate long term trends.

Analysis of Liquid-Phase Thermal Degradation

When the flasks were weighed and the kinematic viscosity of the fluid determined, a small (5 ml to 10 ml) sample of the candidate thermal storage

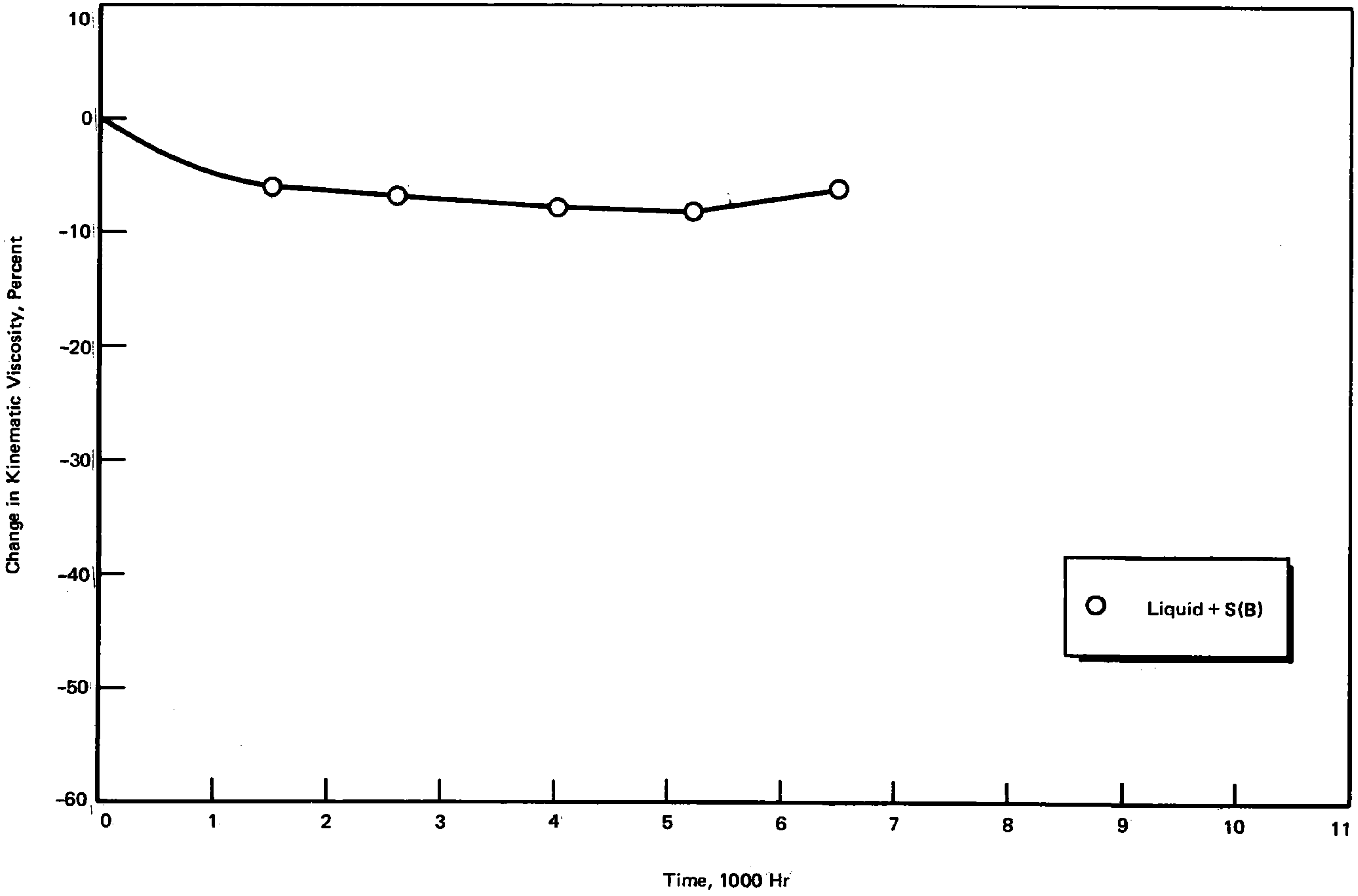

Figure 21. Mobiltherm 123 Change in Kinematic Viscosity 288 C (550 F)

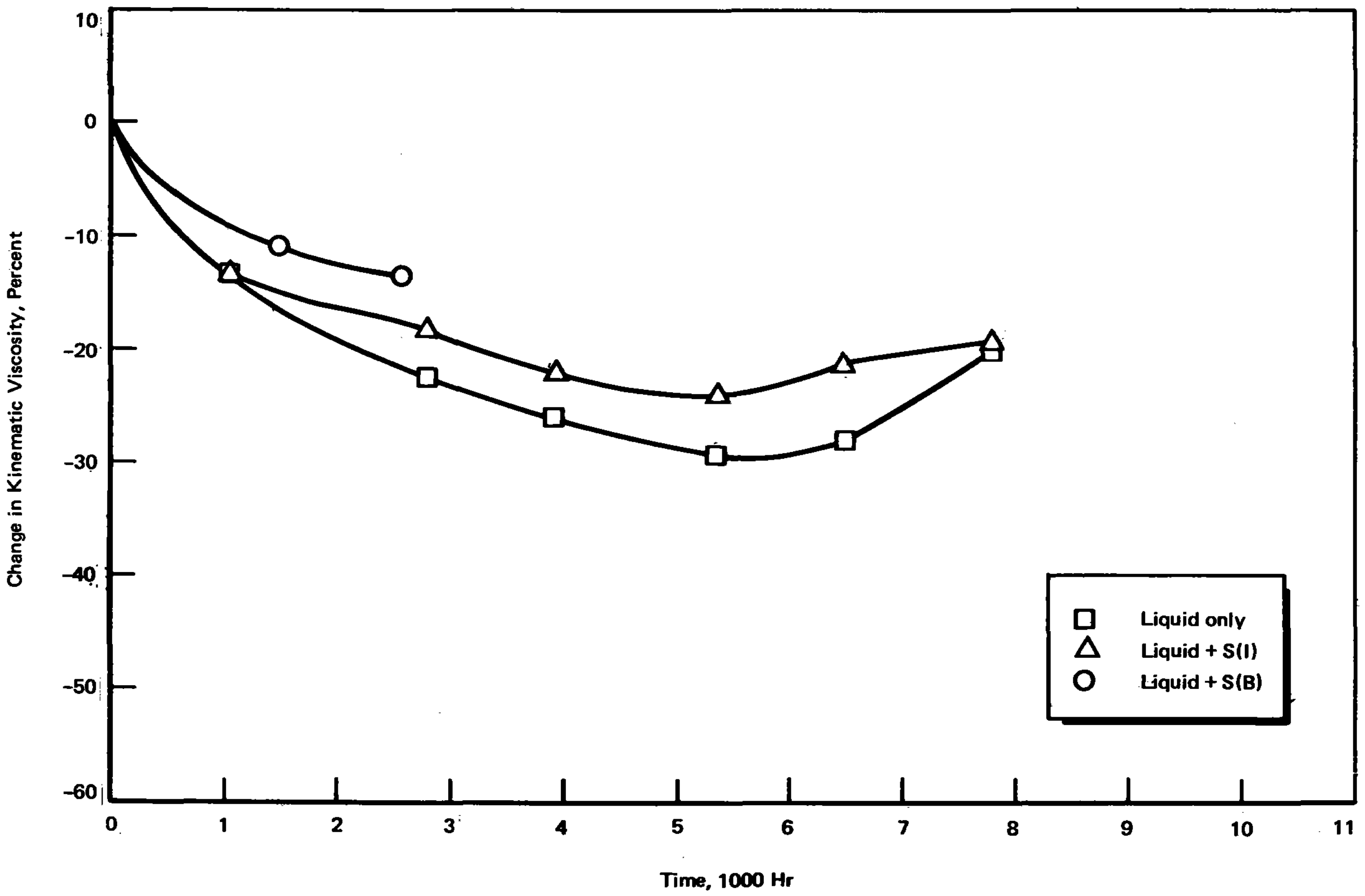

Figure 22. Mobiltherm 123 Change in Kinematic Viscosity 302 C (575 F)

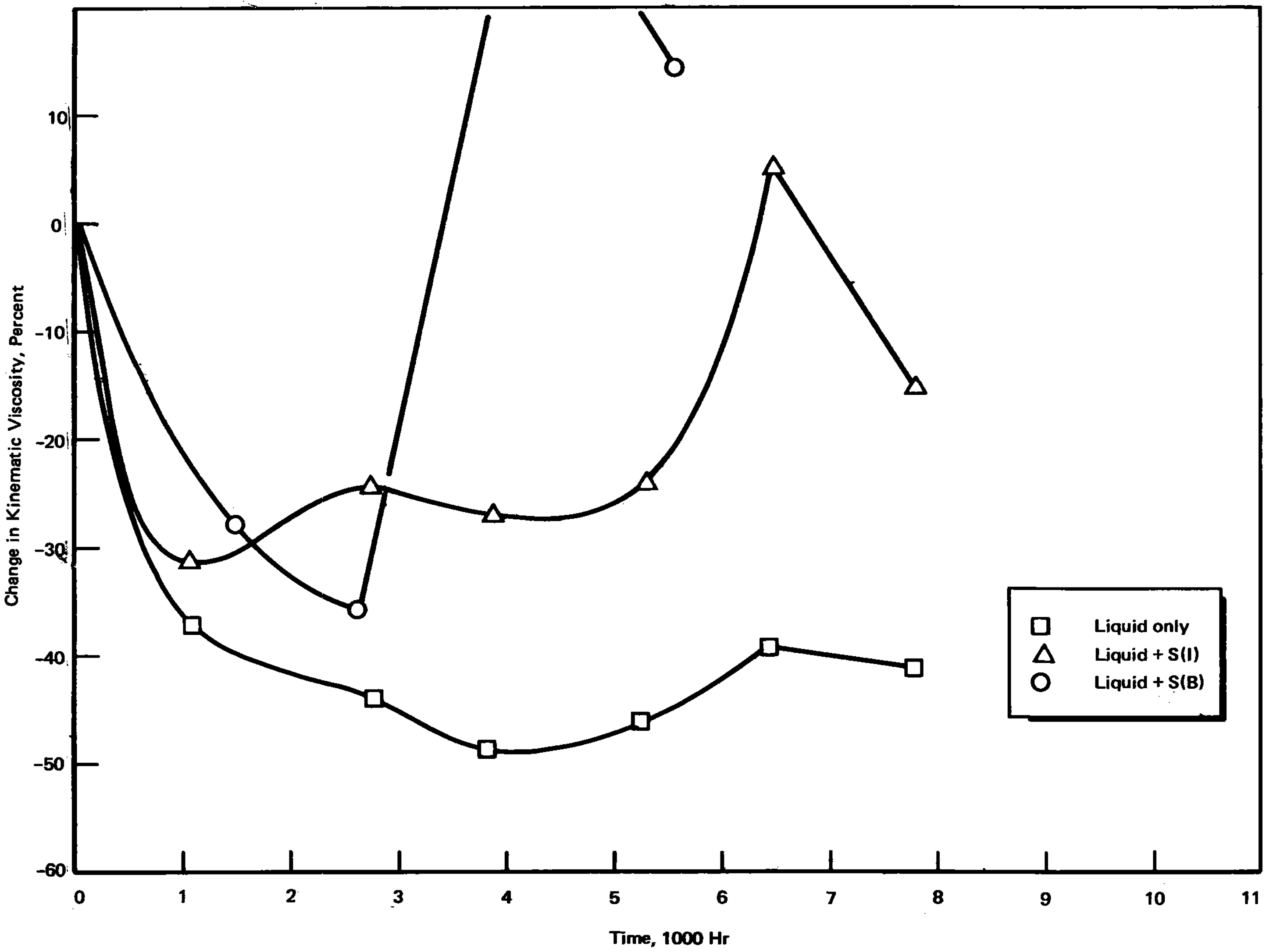

Figure 23. Mobiltherm 123 Change in Kinematic Viscosity 316 C (600 F)

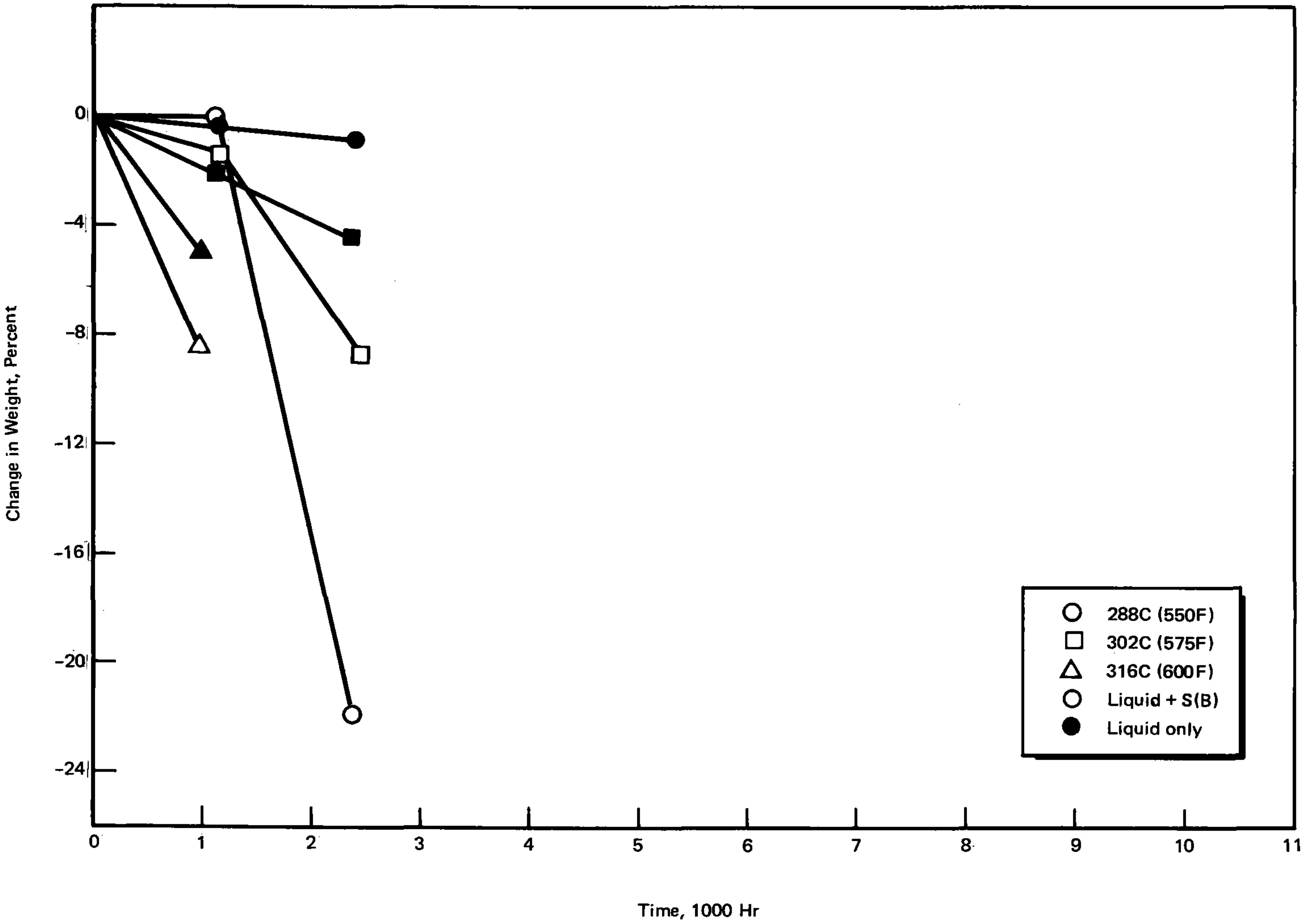

Figure 24. Sun Oil Change in Weight 288 C (550 F), 302 C (575 F), 316 C (600 F)

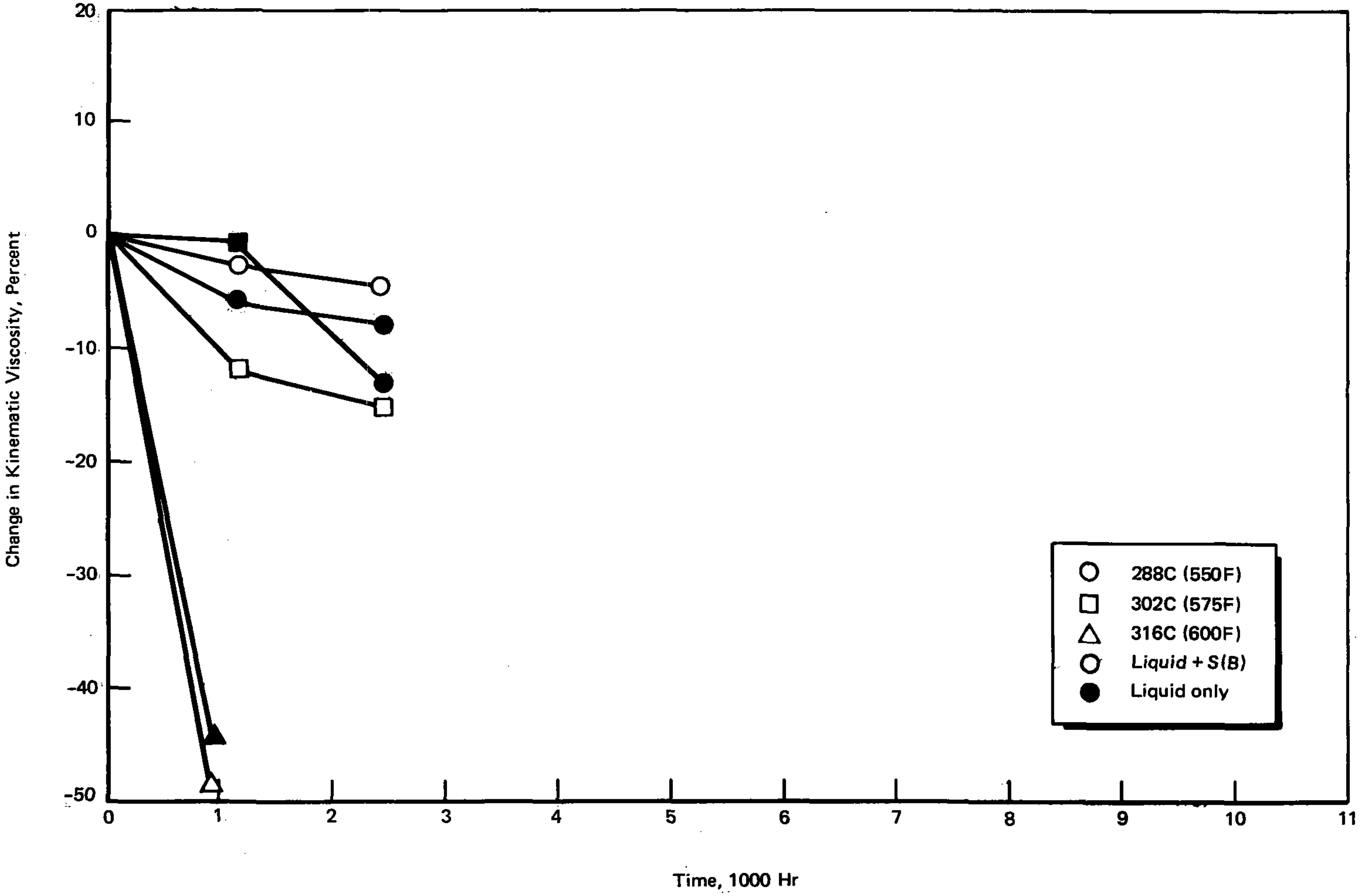

Figure 25. Sun Oil Change in Kinematic Viscosity 288 C (550 F), 302 C (575 F), 316 C (600 F)

fluid was removed for later possible analysis. These samples were forwarded to Sandia/Livermore for gel-permeation chromatography (GPC) and infrared (IR) spectroscopic analyses. Initial long term fluid tests were set up to study Caloria HT43 and Therminol 66. A number of samples of these fluids shipped to Sandia/Livermore have been analyzed. Later, the fluid study program was broadened to include further testing of Caloria HT43 and Therminol 66 and the addition of Mobiltherm XMTL 123 and Sun Oil 21. Samples of fluid from these recent tests have not yet been analyzed.

The results of the GPC and IR tests conducted on Caloria HT43 and Therminol 66 have been reported elsewhere (Reference 16) and need not be repeated here except for some general conclusions. The results of these tests indicate that Caloria HT43 experienced a great deal of thermal cracking and dehydrogenation. No conclusive evidence of polymerization was found, though some samples did show an indication of polymerization. In the worst case examined, the degree of polymerization was estimated to be less than 1%. Only one of the samples analyzed by IR was found to yield evidence of oxidation. The evidence for dehydrogenation of Caloria HT43 via the GPC analyses is in agreement with the results of the GC analysis of the collected gaseous decomposition products from Caloria HT43; hydrogen accounted for 20.8% of the product gas.

Evaluation of Weight Loss Rates

The fluid replacement rates for Caloria HT43, Mobiltherm XMTL 123, Sun Oil 21 and Therminol 66 were measured from the slope of the correlating curves drawn through the plots of percent weight loss vs time given in Figures 5, 6, 7, 11, 12, 13, 14, 18, 19, 20, and 24 for three different temperatures and for rocks and sand of two different types. A number of these thermal stability tests exhibit unusually large weight losses over a 1000 or 2000 hour period that are preceded and followed by intervals of lower steady weight loss that can be correlated with lines of similar slope. The cause of the anomalous rapid weight loss has not been established but it may be due to accidental contact of the hot fluid with oxygen. With the constant flow of N_2 into the top of the condenser, however, it is difficult to see how this could occur. With the exception of sample 11, no measurements were made of the composition of gases in these flasks. In a later test in which O_2 was known to have entered the flask via the condenser, there was evidence of charring (carbon deposits) on the walls of the condenser.

There was no evidence that oxygen had entered the flasks of Therminol 66 other than a weight loss rate. Therminol 66, a light yellow color when fresh, darkened gradually through the course of the experiment. Rapid discoloration of the fluid or the formation of a carbon char on the inside of the air-cooled condensers, clues which would indicate oxygen intrusion, were not observed. Samples of Therminol 66 fluid, withdrawn from the flasks at each weighing interval, were forwarded to Sandia-Livermore for examination by IR spectroscopy. The results as reported gave no indication of partially oxidized products.

The lower reaction rates indicated by the AECL data may have been caused by use of a fluid with much higher concentrations of high boilers than were present in the fluid used in this study, or possibly the higher decomposition rate was caused by the presence of the rock and sand.

Efforts were made to repeat Therminol 66 experiments with and without solids. The effort had to be limited in scope by the availability of space in constant temperature baths and commitments to study four other fluids (Caloria HT43, Mobiltherm XMTL 123, Sun Oil 21 and Therminol 55).

The weight loss rates recorded here were determined from portions of the correlation curves that were perceived as normal. In many cases the regions of the curves used to obtain the weight loss rate are indicated in the figures. The fluid weight loss rates measured are given in Table 4.

These rates have been plotted vs 1/T on semilog coordinates in Figure 26. The reactions rate equations (with W in wt %/hr and T in K*) obtained from Figure 26 are

$$W = 5.38 \times 10^{10} \exp(-35100/RT) \quad \text{(For Caloria HT43, Irwindale rock)} \quad (3)$$

$$W = 1.63 \times 10^{9} \exp(-31980/RT) \quad \text{(For Caloria HT43, Barstow rock)} \quad (4)$$

---

*R = 1.98 Cal/K

TABLE 4. WEIGHT LOSS RATE MEASUREMENTS

°C(°F)	Caloria HT43 Rate, %/hr	Therminol 66 Rate, %/hr	Mobiltherm XMTL 123 Rate, %/hr	Sun Oil 21 Rate, %/hr
288(550)	1.06×10^{-3} (I)	4.85×10^{-4}(I)	--	--
	0.48×10^{-3} (B)	4.0×10^{-4} (B)	6.2×10^{-4} (B)	--
	--	--	--	3.93×10^{-4} (F)
302(575)	2.81×10^{-3} (I)	2.74×10^{-3} (I)	1.55×10^{-3} (I)	--
	1.46×10^{-3} (B)	1.38×10^{-3} (B)	--	--
	--	--	1.32×10^{-3} (F)	1.94×10^{-3} (F)
316(600)	4.3×10^{-3} (I)	1.26×10^{-2} (I)	2.36×10^{-3} (I)	--
	1.72×10^{-3} (B)	4.3×10^{-4} (B)	--	9.0×10^{-3} (B)
	1.8×10^{-3} (F,I)	4.3×10^{-4} (F)	2.2×10^{-3} (F)	5.1×10^{-3} (F)

(I) = Irwindale rocks and metal

(B) = Barstow rocks and metal

(F) = Neat fluid - no solids

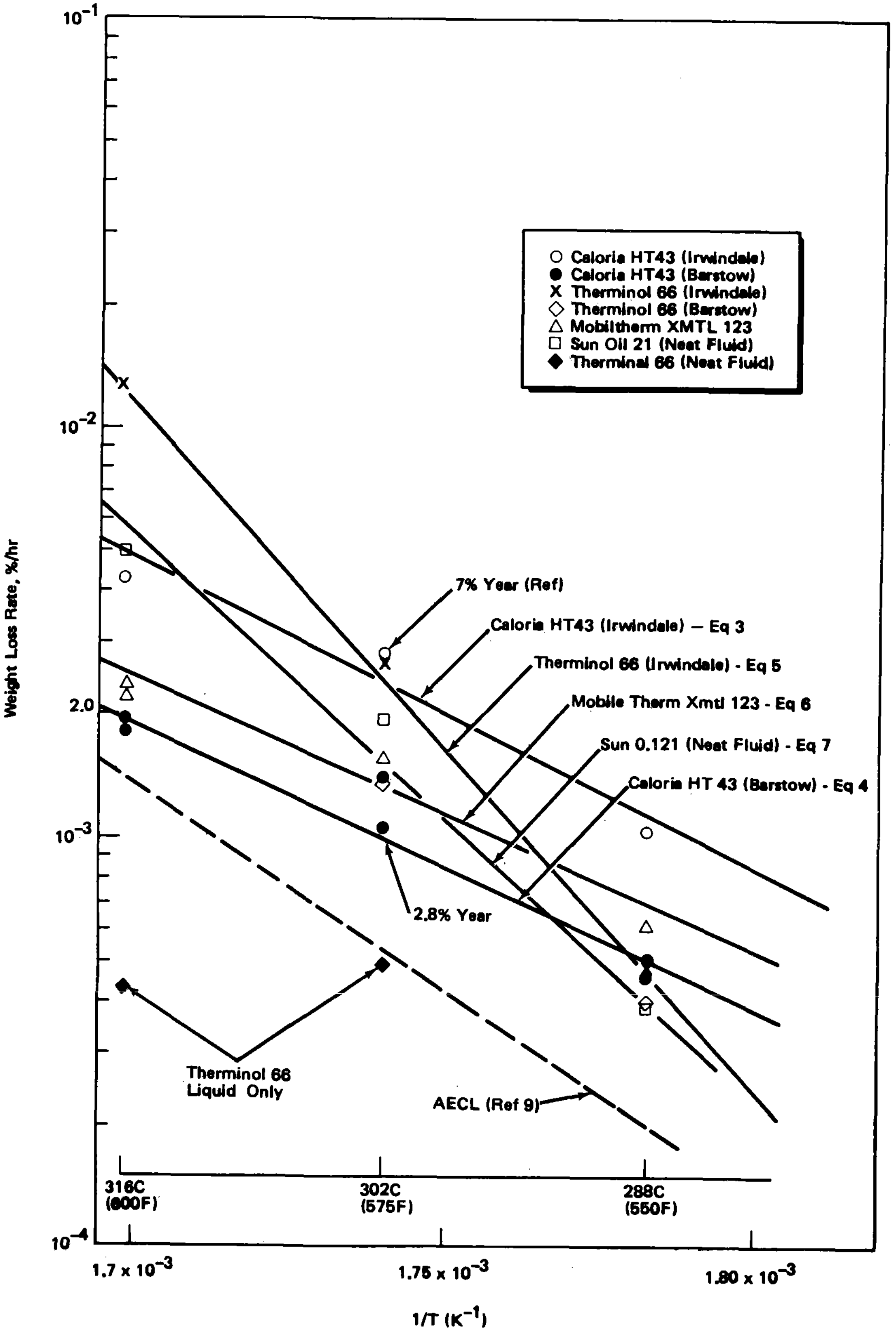

Figure 26. Weight Loss Rate of Fluids as a Function of Temperature

$W = 1.93 \times 10^{27} \exp(-78600/RT)$ (For Therminol 66, Irwindale rock) (5)

$W = 8.84 \times 10^{8} \exp(-31060/RT)$ (For Mobiltherm XMTL 123, rock) (6)

$W = 6.03 \times 10^{21} \exp(-64600/RT)$ (For Sun Oil 21 - neat fluid) (7)

The activation energy of a steady state chain reaction process such as the thermal degradation of the fluids can be shown to be given by $E_p + 1/2\ (E_i - E_b)$ where E_p, E_i, and E_b are the activation energies of the propagation step, the initiation step and chain breaking step, respectively (Reference 21). The high activation energy measured for Therminol 66 could be due to a greater value of E_i, the chain initiation step, and/or to a greater value of E_p and smaller value of E_b. Therminol 66 is a partially hydrogenated biphenyl and consists of ring structures, while Caloria HT43 is primarily an aliphatic compound; therefore it is not unreasonable to expect the activation energies (E_p, E_i and E_b) for the two oils to differ.

The high activation energy measured for Sun Oil 21, an aliphatic fluid similar to Caloria HT43, is puzzling but may be related to the lack of an antioxidant which is present in Caloria HT43.

Thermal rate data when properly interpreted and plotted, as in Figure 26, will yield straight lines. In general, the rate data given in Figure 26 are consistent over the temperature range covered. An exception is the filled diamond point shown in Figure 26 at 316C ($1/T = 1.698 \cdot 10^{-3} K^{-1}$), representing Therminol 66 with Barstow rock and with neat fluid. The weight loss rate for these experiments was 4.3×10^{-4}%/hr. A dashed line has been drawn in Figure 26 to represent the weight loss rate measured by AECL for Therminol 66 containing 25 percent high boilers. The rate measured for Therminol 66 liquid only at 302C (575F) is quite close to the AECL data curve. At 316C (600F) our measured percent weight loss rate for Therminol 66 liquid was about 0.30 of the AECL value. The Rocketdyne Therminol 66 (316C), data point is believed to be anomalous. The weight loss data obtained for Therminol 66 with Irwindale rock and with Barstow rock at 288C (550F) and 302C (575F) range from about 2 to 8.7 times the AECL curve for the liquid only. Catalytic reactions included by the added rock are believed to be responsible for the higher weight loss rates of Therminol 66 measured in this study.

Toward the end of the 3-year test period there was some concern expressed as to the effect of the rock and sand surface area to the volume (S/V) of the liquid. Tests were initiated (sample 25) using Caloria HT43 at 302C (575F) filled with rock and sand to the level of the liquid with a resulting S/V ratio of 15 cm^{-1}. The single data point (C on Figure 7) at 1254 hours showed a weight loss rate of 22 percent per year (approximately three times the rate considered "normal" for equivalent samples with lower surface to volume ratios). This may or may not be representative. Many of the samples exhibited high loss rates in the first 1000 to 2000 hours and then "settled down" to loss rates considered normal.

Rock and sand surface area to liquid volume, S/V, is quite variable and is primarily sensitive to the sand since the sand used has a partical surface area to volume ratio approximately 10 times the rock. The surface to volume ratio, assuming the particles are spheres, is 6/D, where D is the partical mean diameter. This is not precisely accurate but serves as a measure of the relative S/V.

The value of S/V for the 10 MW pilot plant is expected to be on the order of 15 cm^{-1} to 50 cm^{-1} depending upon the sizes to be used. There is very little effect on thermocline performance and tank sizing using solids varying in size by a factor of 3 provided the rocks are not larger than 25 to 50 mm range (approximately).

If it is determined that S/V is a significant parameter, then larger, size solids can be used to reduce S/V. Further testing should be conducted to establish the importance of this parameter.

The data for Mobiltherm XMTL 123 shows that the presence of rocks and metal has very little effect on the decomposition rate. The weight loss rate correlation curve given in Figure 26 indicates the Mobiltherm XMTL 123 loss rate is only 50 to 60% of the loss of Caloria HT43 with Irwindale rock. More recent data on the loss rate of Caloria HT43 in contact with Barstow rocks (the filled circles in Figure 26) indicates that this fluid-rock system is slightly more stable than the Mobiltherm and twice as stable as Caloria HT43 with Irwindale rocks.

Weight loss rate data for Sun Oil 21 are based on very few data points spanning a relatively short time period. Available data, however, reveal a high activation energy for thermal degradation of the neat fluid. Additional experimental time is required to obtain more reliable rate data for Sun Oil 21.

No correlating line was drawn in Figure 26 for the data points on Therminol 66 with Barstow rocks and metal. The data point at 316C (600F) is much too low to correlate well with data taken at the other two temperatures.

FLUID REPLACEMENT RATE FOR PILOT & COMMERCIAL PLANT APPLICATIONS

The fluid loss rate vs time has been established at 288, 302 and 316C (550, 575 and 600F) in batch systems. In the thermal storage unit (TSU) the makeup fluid required to replace losses due to thermal decomposition and subsequent devolatilization or perhaps polymerization and filtration, will be supplied continuously to the fluid inventory. With the passage of time, the fluid inventory attains a constant average age and a constant fluid makeup. If it is assumed that the decomposition rate (or rate of fluid loss by devolatilization) of fluid subjected to high temperatures for a certain time (and hence having a certain age), is unaffected by the age of fluid it is mixed with, i.e., the fluid decomposition rate is a function only of its age and is independent of the ages of other fluid it may be mixed with, the problem can be formulated as follows. If W(y) is the amount of fluid added to the TSU at time y to y + dy, W(t,y) represents the amount of fluid added at y to y + dy remaining at time t, L is the equation relating weight loss of the fluid to residence time at temperature T, and $\frac{dL(t-y)}{dt}$ is the weight loss rate of the fluid after a residence time t-y, then the rate of addition of makeup fluid caused by losses from W(y) at time t is

$$\frac{dW(t,y)}{dt} = W(y) \quad 1-L(t-y) \quad \frac{dL(t-y)}{dt}$$

and the total fluid makeup required at time t, W(t), is

$$W(t) = \int_{y=o}^{y=t} \frac{dW(t,y)}{dt}\, dy = \int_{y=0}^{y=t} W(y) \quad 1-L(t-y) \quad \frac{dL(t-y)}{dt}\, dy \qquad (8)$$

If there is an interaction between fluid of various ages due, for example, to some intermediate present in older fluid that may catalyze or stabilize the decomposition of fresh fluid, then Equation 8 is invalid. The fluid replacement rate would then have to be determined from experiments in which fresh makeup fluid was continually added to the system to replace the volatilized fluid.

Equation 8 has not been solved for W(t) in closed form. The solution, however, would indicate that with the passage of time the fluid would attain a steady state composition and W(t) would therefore approach a constant value. It is believed that this steady state value can be closely approximated by using the fluid weight loss rate equations (3 and 4 for Caloria HT43, Equation 5 for Therminol 66, and Equation 6 for Mobiltherm XMTL 123) determined for the constant weight loss regime of fluid batches.

Application of the fluid weight loss equations for the Pilot and commercial plants is dependent upon (1) TSU cycling time; (2) the percent of the time the fluid spends at each temperature; and (3) the temperature level. Experiments with the TSU subsystem have shown that the thermoclines in the thermal storage tank are very steep. Thus, the percentage of fluid present at temperatures between the high and the low temperatures of the TSU is rather small and can be neglected.

Let Figure 27 represent a typical 24 hour duty cycle. Between zero and 10 hours the TSU is discharged and all of the fluid in the bed is at the lower temperature. The loss rate for all practical purposes is zero. During charging, the percentage of fluid at the upper temperature increases.

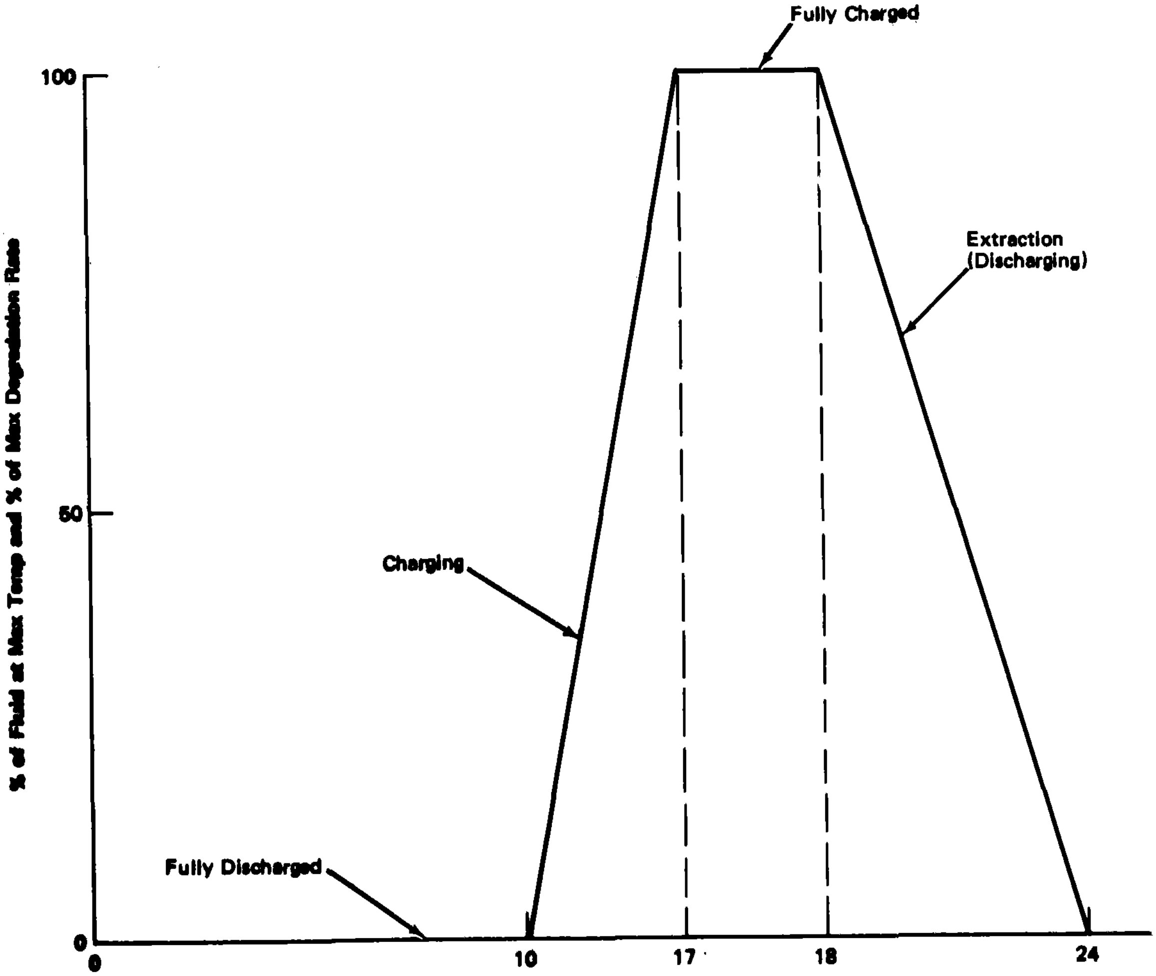

Figure 27. Typical 24 Hour Duty Cycle

For a constant charging rate, the increase in proportion of fluid at the upper temperature as well as the loss rate increases. When fully charged, all of the fluid is at the maximum temperature and the loss rate is also at the maximum value. During extraction, the loss rate as well as the amount of fluid at the maximum temperature decreases, again in the same proportion.

The fluid loss over a 24 hour period is represented by the area under the curve in Figure 27. Thus:

Loss = charging time x 1/2 maximum degradation rate
+ time at upper temperature x maximum degradation rate
+ discharging time x 1/2 maximum degradation rate

Letting the sum of the charging and discharging times be the transient time, the loss becomes:

Loss = 1/2 transient time x 1/2 maximum degradation rate
+ time at upper temperature x maximum degradation rate

The equivalent time at the upper (fully charged condition) becomes:

Time = 1/2 transient time + time at fully charged condition

For the example in Figure 27, which is considered typical for a commercial plant, the equivalent time during a 24 hour period at maximum temperature is 7.5 hours.

Equivalent fully charged time = 1/2 (7 + 6) +1
= 7.5 hours

For the Pilot Plant and Commercial Plant duty cycles, the loss rate per day can be computed based on the amount of time spent at the upper and lower temperatures.

The results are presented in Table 5 as %/day and %/year, calculated using the temperature-time cycle shown in Figure 27, with one year being defined as 330 cycles.

TABLE 5. CALCULATED FLUID REPLENISHMENT RATE*

Plant	Temp °C(°F)	Caloria HT43 (Irwindale)		Caloria HT43 (Barstow)		Therminol 66		Mobiltherm 123	
		%/day	%/yr	%/day	%/yr	%/day	%/yr	%/day	%/yr
Pilot	302(575)	0.0212	7.00	0.0087	2.87	0.0184	6.07	.0105	3.47
	218(425)								
Commercial	316(600)	0.0391	12.9	0.017	5.49	0.0936	30.9	.020	6.57
	232(450)								

---

* Based on faired lines of hourly rates in Figure 26 integrated over 24 hour duty cycle in Figure 27

Figures 28 expands the concept further to cover a range of transient and fully charged durations for Caloria HT43 at Pilot Plant conditions (decomposition rate equals $2.83 \cdot 10^{-3}$%/hr at 302C, 575F). For the case shown in Figure 27, the transient time equals 7 hours, the total time fully charged equals 1 hour and the resultant fluid loss for one year of operation (330 daily cycles) is 7.0 percent.

The family of curves in Figure 28 are based on the relationship that the loss rate in percent per year is equal to the loss rate in %/hr. times the equivalent hours fully charged per cycle times the number of cycles per year. For the specific case where Caloria HT43 with Irwindale rock had an hourly loss of $2.83 \cdot 10^{-3}$%/hr. (at 575°F) for a typical 24 hour duty cycle,

$$2.83 \cdot 10^{-3}\text{\%/hr. x 7.5 hrs at maximum temperature/cycles x}$$
$$\text{330 cycles/yr} = 7\text{\% year}$$

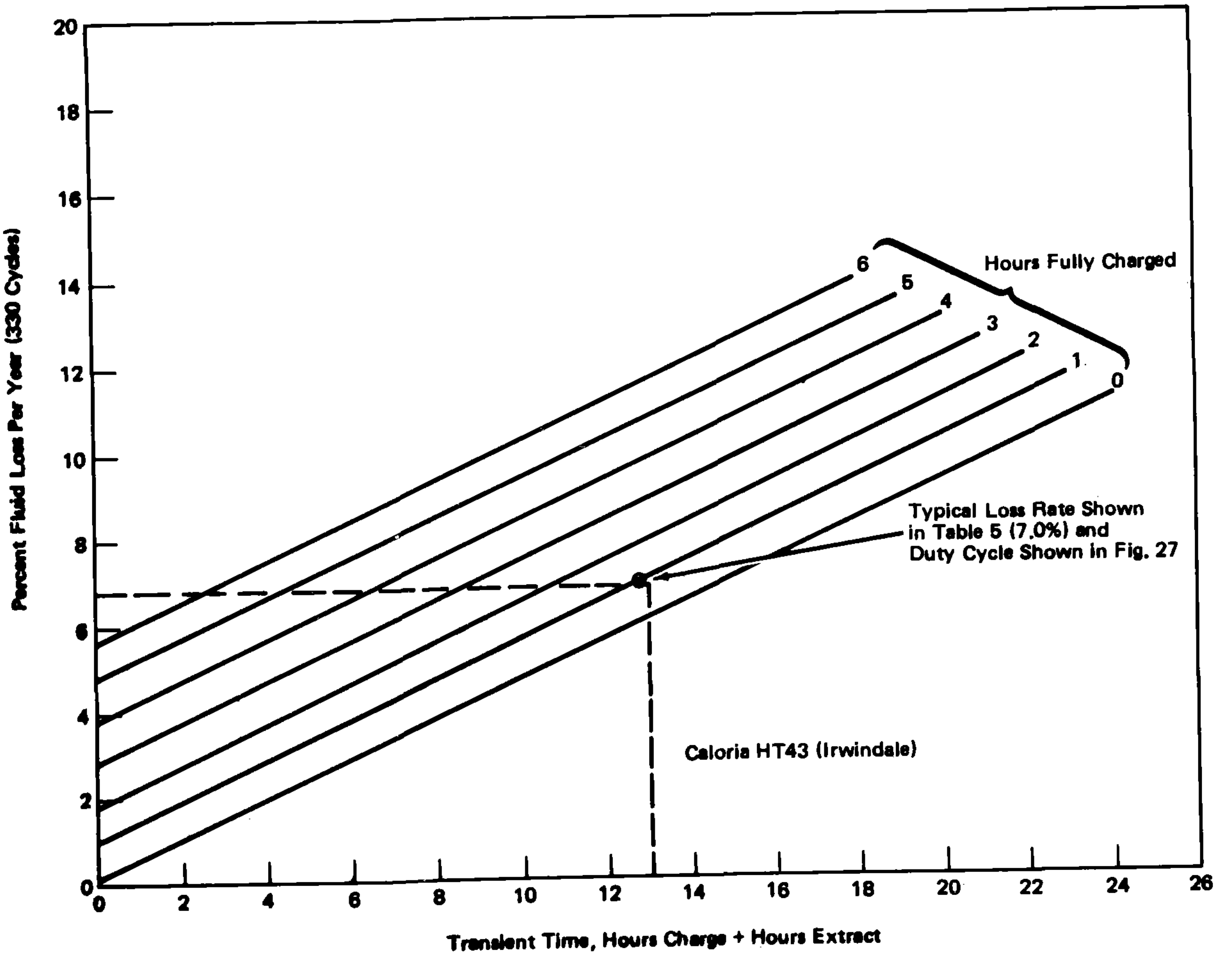

Figure 28. Fluid Loss (Percent Per Year) for the Pilot Plant Operating With Caloria HT43

CHEMICAL REACTIONS IN THERMAL STORAGE FLUIDS

Long term subjection of the candidate thermal storage fluids to temperatures from 288C (550F) to 316C (600F) will produce a variety of chemical reactions in the mixture of compounds that make up the fluids. These reactions may be classified as being part of cracking, polymerization and dehydrogenation processes. In the event oxygen was permitted to contact the fluids, one could add oxidation to this list. The reactions may further be classified as chain initiating, chain propagating or chain terminating steps.

Aliphatic Hydrocarbon Fluids

Thermal Cracking. Several plausible reactions are presented in the discussion that follows. The reaction steps are quite general. In thermal cracking, the initiating reaction is

(1)* $R \longrightarrow R'\cdot + CH_3\cdot$

or

(1A) $R \longrightarrow R'\cdot + R''\cdot$

These reactions involve the breaking of a C-C bond to form various alkyl radicals and requires roughly from 70 to 78 kcal/mol if R is a straight chain saturated hydrocarbon. After this reaction, several possible chain propogating steps can occur such as

(2) $CH_3^{\bullet} + R_1\text{-}CH_2\text{-}CH_2\text{-}R_2 \rightarrow CH_4 + R_1\text{-}\dot{C}H\text{-}CH_2\text{-}R_2 \quad \Delta H \simeq 14 \text{ kcal}$

(3) $R_1\text{-}\dot{C}H\text{-}CH_2\text{-}R_2 \rightarrow R_1\text{-}CH = CH_2 + R_2^{\bullet}$

(4) $R'^{\bullet} + R_3\text{-}CH_2\text{-}CH_2\text{-}R_4 \quad R'H + R_3 - \dot{C}H\text{-}CH_2\text{-}R_4 \quad \Delta H \simeq 5 \text{ kcal}$

---

*Chemical reactions are denoted by numbering on the left to differentiate from mathematical equations which are numbered on the right.

In a mixture of hydrocarbons like Caloria HT43, the number of possible chain carrying reactions involving $\dot{CH_3}$ and various other alkyl radicals (designated with the dot •) is quite large. A second possible initiating reaction for the thermal cracking would involve the breaking of a C-H bond in the hydrocarbon, i.e.,

$$(5) \qquad R'H \rightarrow R'\cdot + H$$

Reaction step 5 will require around 85 to 93 kcal/mol at most for a straight chain, saturated hydrocarbon, depending on whether the H was a primary or secondary hydrogen. For unsaturated hydrocarbons the C-H bond energy would range down to about 75 kcal/mol. This reaction would be followed by chain propagating steps very similar to reactions 2 and 4, such as

$$(6) \qquad H + R_1\text{-}CH_2\text{-}CH_2\text{-}R_2 \rightarrow H_2 + R_1\text{-}\dot{C}H\text{-}CH_2\text{-}R_2 \qquad \Delta H = 16 \text{ kcal}$$

Reaction 6 would lead to chain propagating steps similar to reaction 3 if a hydrogen was removed from a $-CH_3$ group in step 5. The removal of a hydrogen from a CH_2 group would result in a hydrocarbon product similar to that produced in reactions 2, 4 or 6, which would then react as indicated by step 3. Also possible are addition reactions at double bonds, such as

$$(7) \qquad H + R_1\text{-}CH = CH\text{-}R_2 \rightarrow R_1\text{-}CH_2\text{-}\dot{C}H\text{-}R_2$$

which could then decompose as shown in reaction 3.

The major gaseous products of these reactions would be CH_4, H_2 and a number of saturated and unsaturated volatile hydrocarbons formed in reactions similar to reactions 3 and 4.

The chain terminating steps would include reactions that result in the net loss of chain-carrying radicals. Typical terminating reactions might include for example, (a) the combination reactions

(8) 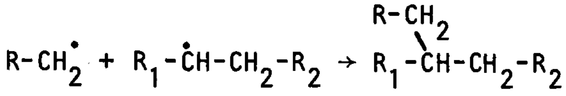

$$R\text{-}CH_2^{\bullet} + R_1\text{-}\dot{C}H\text{-}CH_2\text{-}R_2 \rightarrow R_1\text{-}\overset{R\text{-}CH_2}{\dot{C}H}\text{-}CH_2\text{-}R_2$$

where R on the $CH_2^{\bullet}$ or R_1 on the other radical could be H or any hydrocarbon, and

(9) $H + R^{\bullet} \rightarrow RH$

or, (b) the disproportionation reactions such as

(10) $R\text{-}\dot{C}H_2 + R'\text{-}CH_2\text{-}\dot{C}H_2 \rightarrow R\text{-}CH_3 + R'\text{-}CH = CH_2$

As the pyrolysis reactions proceed, the species remaining in the liquid phase become increasingly unsaturated and more likely to undergo some kind of addition reactions at the double bonds that will increase the average molecular weight. The double bond is highly reactive towards atoms and free radicals. Addition reactions such as step 11, for example

(11) 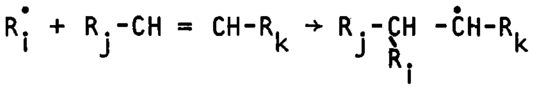

$$R_i^{\bullet} + R_j\text{-}CH = CH\text{-}R_k \rightarrow R_j\text{-}\underset{R_i}{CH}\text{-}\dot{C}H\text{-}R_k$$

will occur.

Decomposition in the Presence of Oxygen. If somehow oxygen was allowed to enter the flask of hot fluid, the reaction of oxygen with hydrocarbons would proceed by the following general mechanism.

(12) $R\,H + O_2 \rightarrow R^{\bullet} + HO_2^{\bullet}$

(13) 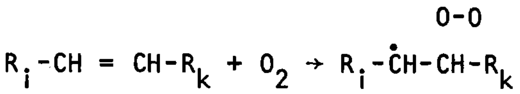

$$R_i\text{-}CH = CH\text{-}R_k + O_2 \rightarrow R_i\text{-}\overset{O\text{-}O}{\dot{C}H\text{-}CH}\text{-}R_k$$

(14) $R^{\bullet} + O_2 \rightarrow R\text{-}O\text{-}O^{\bullet}$

Reaction steps 12 and 13 are plausible initiation mechanisms involving a saturated and unsaturated hydrocarbon. The alkyl radical, $R^\bullet$, could react with O_2 as shown in reaction 14 or undergo a decomposition as shown in reaction 3 to produce an olefin and a smaller alkyl radical. The peroxy radical $RO_2^\bullet$ formed in reaction 14 could react as given by steps 15 or 16.

(15)

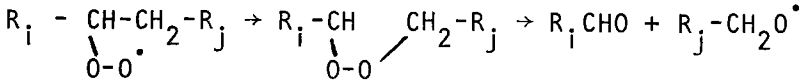

$$R_i - \underset{O-O^\bullet}{CH}-CH_2-R_j \rightarrow R_i-\underset{O-O}{CH}\;CH_2-R_j \rightarrow R_iCHO + R_j-CH_2O^\bullet$$

(16)

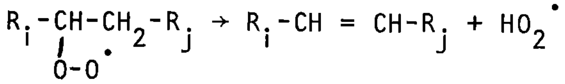

$$R_i-\underset{O-O^\bullet}{CH}-CH_2-R_j \rightarrow R_i-CH = CH-R_j + HO_2^\bullet$$

The $RO_2^\bullet$ could instead react with a hydrocarbon RH as in 17

$$(17) \quad RO_2^\bullet + RH \rightarrow ROOH + R^\bullet$$

to produce the hydroperoxide ROOH. The reaction of this species could lead to chain branching with RH via reaction 18

$$(18) \quad ROOH + R'H \rightarrow RO^\bullet + R'^\bullet + H_2O$$

or with the double bond, via reaction 19.

(19)

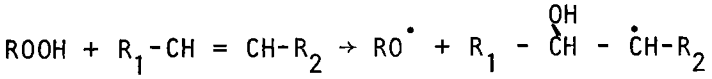

$$ROOH + R_1-CH = CH-R_2 \rightarrow RO^\bullet + R_1 - \overset{OH}{CH} - \dot{C}H-R_2$$

At temperatures around 300C, aldehydes produced in reactions such as step 15 will very likely decompose rapidly to CO, H_2 and olefins. Reaction products such as $RO^\bullet$ produced in steps 15, 18, and 19 will extract a hydrogen from a hydrocarbon, i.e.,

$$(20) \quad RO^\bullet + R'H \rightarrow ROH + R'^\bullet$$

The alcohol ROH may then decompose to H_2O and an alkyl radical $R^\bullet$.

In general, exposure of the heated fluid to small amounts of O_2 will result in a greater amount of cracking and hydrogen stripping. The oxygen will eventually leave the fluid as CO, CO_2, and H_2O, while the fluid will contain more unsaturated (olefinic) compounds and more lower molecular weight hydrocarbons in general.

Polymerization. Polymerization reactions in fluids composed of petroleum fractions such as Caloria HT43, Mobiltherm XMTL 123, and Sun Oil 21, will not occur with great frequency but should become increasingly likely as the fluid becomes more unsaturated, or, more olefinic in character. The addition of a radical $\dot{R}_i$ to a double bond, as shown previously in step 11, results in a larger hydrocarbon radical which could then add to another double bond in another molecule and so forth. Termination of the polymer chain can occur by combination with another radical, i.e.,

(21)

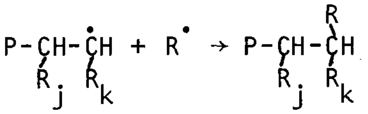

$$P\text{-}\underset{R_j}{CH}\text{-}\underset{R_k}{\dot{C}H} + R^{\bullet} \rightarrow P\text{-}\underset{R_j}{CH}\text{-}\overset{R}{\underset{R_k}{CH}}$$

where P represents the polymer chain. Termination of the polymer chain could also have occurred by reactions similar to step 4 which would quench the polymeric radical and start a new (and presumably lower molecular weight) radical.

Ionic mechanisms of polymerization also exist. These reactions proceed by addition of the ion to one of the carbons in a double bond and result in the formation of an ion which can add to the double bond of another molecule. Metallic halides, such as $CuCl_2$ or $FeCl_2$, may induce polymerization via this mechanism (Reference 17).

Therminol 66 (Aromatics)

Therminol 66 is a mixture of partially hydrogenated terphenyls. The fluid consists primarily of three-ring compounds with cyclohexane and benzene rings. When exposed to temperatures of 288C (550F) to 316C (600F) the fluid undergoes a slow cracking process. The initiation reaction will probably consist of the elimination of a hydrogen atom from a cyclohexyl ring.

$$(22) \qquad \phi^{*} - C_6H_{11} \rightarrow \phi - C_6\dot{H}_{10} + H$$

The hydrogen atom would then extract an H from another cyclohexyl or from a benzene ring.

$$(23) \qquad \phi\text{-}C_6H_{11} + H \rightarrow \phi\text{-}C_6\dot{H}_{10} + H_2$$

$$(24) \qquad \phi\text{-}C_6H_5 + H \rightarrow \phi\text{-}C_6\dot{H}_4 + H_2$$

The cyclohexyl ring radical $(-C_6H_{10})$ may then undergo the following reactions to open up the ring

(25)

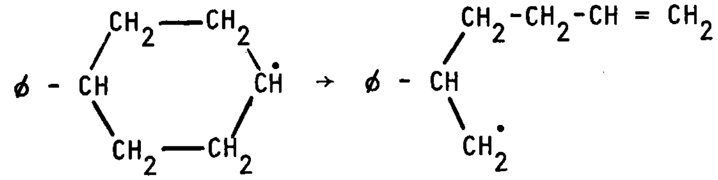

If the hydrogen had been removed from the second or third positions, the ring opening would leave the double bond at the end of a slightly longer or shorter chain. For the case of the phenyl type radical, the most likely reaction would be to remove an H atom from more hydrogenated rings as shown in reaction 26 rather than open the phenyl ring, which would be quite endothermic.

$$(26) \qquad \phi\ \text{-}C_6\dot{H}_4 + \phi'\text{-}C_6H_{11} \rightarrow \phi\text{-}C_6H_5 + \phi'\text{-}C_6\dot{H}_{10}$$

Reaction 25, opening the cyclohexyl ring, leads to a thermal degradation of the side chain, a situation very much like that outlined for the alkanes. The decomposition products vaporized from Therminol 66 should therefore include H_2, CH_4, C_2H_4 and other low molecular weight hydrocarbons. Decom-

---

*The symbol ϕ will designate the rest of the hydrogenated terphenyl molecule.

position products with more than six carbons should not be found. Aside from reaction 25, another possible reaction for the $-C_6H_{10}^{\bullet}$ radical would be to lose an H and form a hexene structure as shown in reaction 27.

(27)

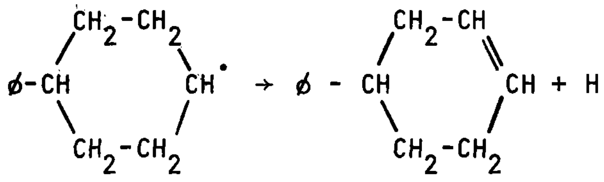

Reaction 27 will be quite endothermic and may not be as likely to occur as reaction 25. If the H atom had been removed from the 2 position on the ring, the ϕ-C bond could break to produce cyclohexene.

Decomposition in the Presence of Oxygen. As previously discussed in connection with straight chain hydrocarbons, the presence of O_2 will tend to accelerate the degradation of Therminol 66. The oxidative mechanism outlined for a cyclohexane ring is based on schemes proposed by Semonov (Reference 18), data on radiation-induced reaction of O_2 with cyclohexane (Reference 19), and information presented on Therminol 66 oxidation by AECL (References 1 and 10). The general process is postulated to proceed via the reactions

$$(28) \quad \phi-C_6H_{11} + O_2 \rightarrow \phi - C_6H_{10}^{\bullet} + HO_2^{\bullet}$$

(29)

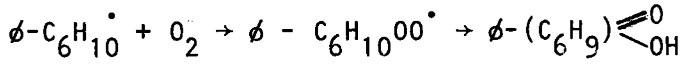

$$\phi-C_6H_{10}^{\bullet} + O_2 \rightarrow \phi - C_6H_{10}OO^{\bullet} \rightarrow \phi-(C_6H_9)\begin{matrix} \nearrow O \\ \searrow OH \end{matrix}$$

The hydroperoxide, $\phi = C_6H_9OOH$, in reaction 29 will eventually result in opening the cyclohexane ring. There is no reason to believe that the partially hydrogenated terphenyls are any more susceptible to oxidative acceleration of cracking than are the straight chain hydrocarbons.

Polymerization. Benzene, diphenyl and terphenyl compounds, when subjected to temperatures of 750C or higher will form condensation compounds. Benzene for example will react to form biphenyl

$$2C_6H_6 \rightarrow (C_6H_5)\text{-}(C_6H_5) + H_2$$

In hot Therminol 66, radicals such as $\phi\text{-}C_6H_{10}^{\bullet}$ may link with similar radicals to produce a larger molecule that may, like the condensation compounds produced by phenyl species, be more stable at higher temperatures.

Estimated Overall Activation Energy

Among the 11 general reaction steps presented to describe the thermal decomposition of straight chain saturated hydrocarbons, two were initiation reactions, six were chain propagating reactions (five bimolecular reactions and one monomolecular) and three were second order chain terminating reactions. The chain carriers were alkyl radicals, R•, and H atoms.

It can be shown that for a steady state reaction one can write the proportionality equation (e.g., Reference 21).

The overall reaction rate is $\propto r_p(r_i/r_b)^{i/w}$, where r_p, r_i, and r_b are the reaction rates of the propagation, initiation and breaking steps, and w is the order of the chain breaking process. If reaction 3 (the sole monomolecular chain propagating step) is neglected then w = 2, and if average activation energies are used to represent the three types of reactions, the overall activation energy can be written as

$$E_a = E_p + \frac{1}{2}(E_i - E_b)$$

The value of E_i will be slightly greater than the endothermicity of the initiating reactions which is 70 to 78 kcal for step 1 and 85 to 93 kcal for step 5. For step 5, the lower value is preferred since most H atoms will come from secondary carbons. The average value of E_p for steps 2, 4, 6, 7 and 11 is estimated to run about 8 kcal. For E_b the estimated average value is 2 kcal since these radical recombination steps will be fairly exothermic. Using a value of 80 kcal for E_i, E_a is calculated to be 47 kcal. The experimental value of E_a for Caloria is 35.1 kcal.

HEAT EXCHANGER SURFACE FOULING TESTS

Surface fouling from degradation of the heat transfer fluid is most likely to occur at locations of highest surface temperatures and lowest fluid velocity within the heat exchangers. Examination of the fluid flow loops shows that the highest temperatures occur in the thermal storage heater. The potential impact of fouling, if it should occur, would be greater for the heater than for many other portions of the system; e.g., fouling of the piping or heat storage media (rocks) would have little impact. Ideally, these tests should provide confirmation that the fouling factor(s) chosen for heat exchanger design are, indeed, correct. However, quantitative verification was not an objective and if no fouling was observed during testing, standard fouling factors will be employed.

Tests have been performed to determine the extent and rate of fouling of electric heaters immersed in the heat transfer fluids as a function of the surface temperature of the heater, for four fluids, Caloria HT43, Therminol 66, Mobiltherm XMTL 123, and Sun Oil 21.

TEST EQUIPMENT AND PROCEDURES

Typical surface fouling test apparatus (see Figure 29) consists of a 180 watt electric heating element, sheathed with 304 stainless steel, that is immersed in a pool of the heat transfer fluid. The fluid is contained in a 10 cm (4 inch) diameter Pyrex glass pipe cap bolted to a stainless steel plate. Heat transfer from the electric heater to the fluid occurs by natural convection and should represent a worst possible situation because of the low fluid velocity over the heater. Thermocouples spot welded to the heater surface are used to monitor the surface temperature, which is maintained constant by manual adjustment of the heater voltage. The surface temperatures were continuously monitored by a multipoint recorder. The ullage space at top of the Pyrex cap contains nitrogen. A 1/4-inch SS tube extends into the ullage space to prevent a pressure buildup when the apparatus is initially brought up to temperature and to vent gaseous decomposition products produced during the course of the experiment. A nitrogen bleed is maintained over the end of the 1/4-inch SS tube that is open to the atmosphere, to prevent air from

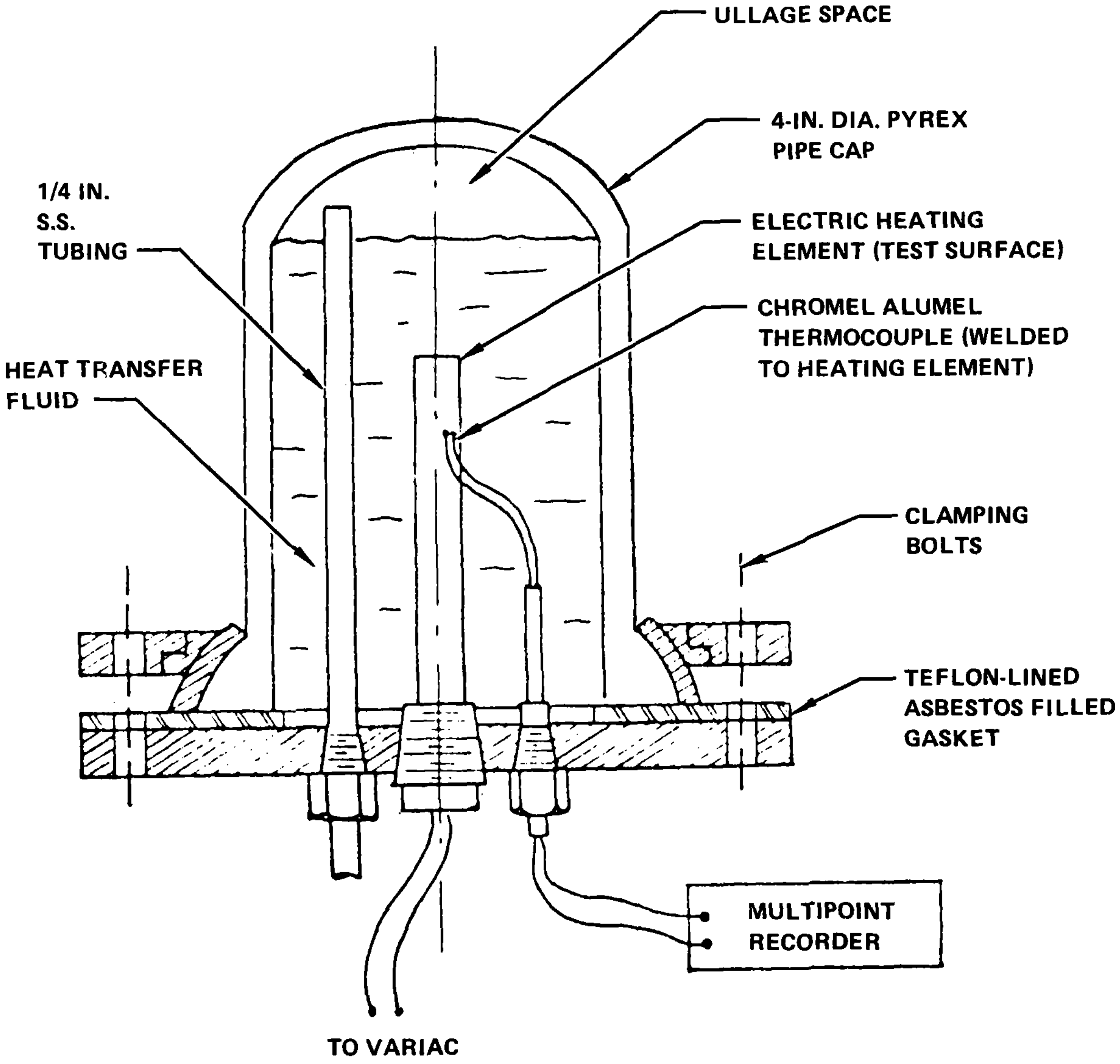

Figure 29. Surface Fouling Test Setup

getting into the ullage space. The Pyrex pipe can was wrapped with fiberglass insulation.

At the start of the fouling tests, six tests were conducted simultaneously. Three of the test setups were filled with Caloria HT43 and three with Therminol 66. Later in the program three more fouling test setups were assembled and filled with Mobiltherm XMTL 123. Still later, one test from each of the three fluids was terminated and the apparatuses were filled with Sun Oil 21. The surface temperatures of the electrical heaters were controlled at 316, 329, and 343C (600, 625, and 650F). The manufacturer's recommended maximum film temperatures are 360C (680F) for Caloria HT43 and 374C (705F) for Therminol 66.

Visual examination, still and motion photography, and measurement of the change with time in power supplied to the heater to maintain the surface temperature at a constant value, were used to detect the presence of a surface film. The weight per unit area of deposits was determined in one case by removing the deposit from a known area and weighing it.

RESULTS AND DISCUSSION

The fouling experiments were run continuously. Several times a day the heater surface temperature was checked and the heater voltage adjusted accordingly. From the outset, bubbles appeared on the heater surface of all three Caloria HT43 tests. Some slow bubbling was also observed at the surface of the heaters in the Therminol 66 tests. Convective flow patterns near the heater surface were quite visible because of the differences in the refractive index of the fluid caused by the temperature gradients in the fluid. At the lowest heater wall temperature, 316C (600F), the flow near the heater wall was laminar as shown in Figure 30, while at 329C (625F) a transition from laminar to turbulent could be seen near the top of the heater (Figure 31). At 343C (650F) the transition zone had moved some distance down to the base of the heater.

The results from fouling tests on Caloria HT43 and Therminol 66 indicate, that no problems would be encountered at Pilot Plant temperatures due to fouling of heating surfaces. There was, however, a temperature abnormality in the lowest temperature test with Caloria HT43. After about 200 hours of testing, the Caloria HT43 heater at 316C (600F) was discovered to have extensive patches of gummy material that had a bubbly or blistered appearance (Figure 32). However, there was no significant change in thermal resistance due to the deposits. The deposits are believed to have formed around vapor bubbles that nucleated on the heater surface and were not rapidly swept away by the natural convective flow. A larger resistance to heat transfer in the vicinity of the vapor bubble and the slower moving fluid, may have resulted in greater local heating and hence in the formation of surface deposits.

Although more bubbling should occur at the higher wall temperatures of 329C (625F) and 343C (650F), the faster moving natural convective flow near the

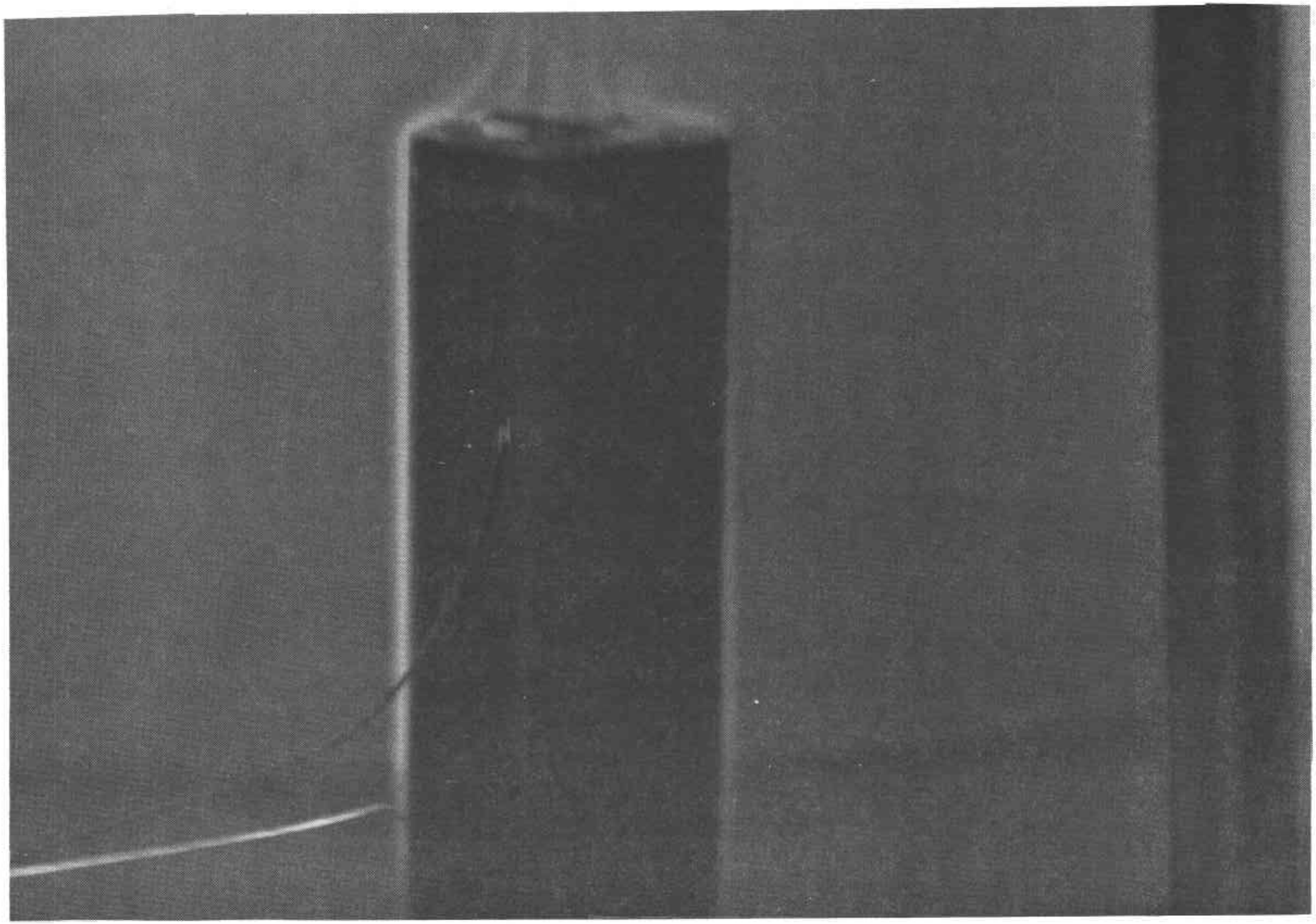

4ES29-12/18/75-C1C*

Figure 30. Heated Surface Fouling Test at 316 C (600 F)
(Note the laminar convective layer)

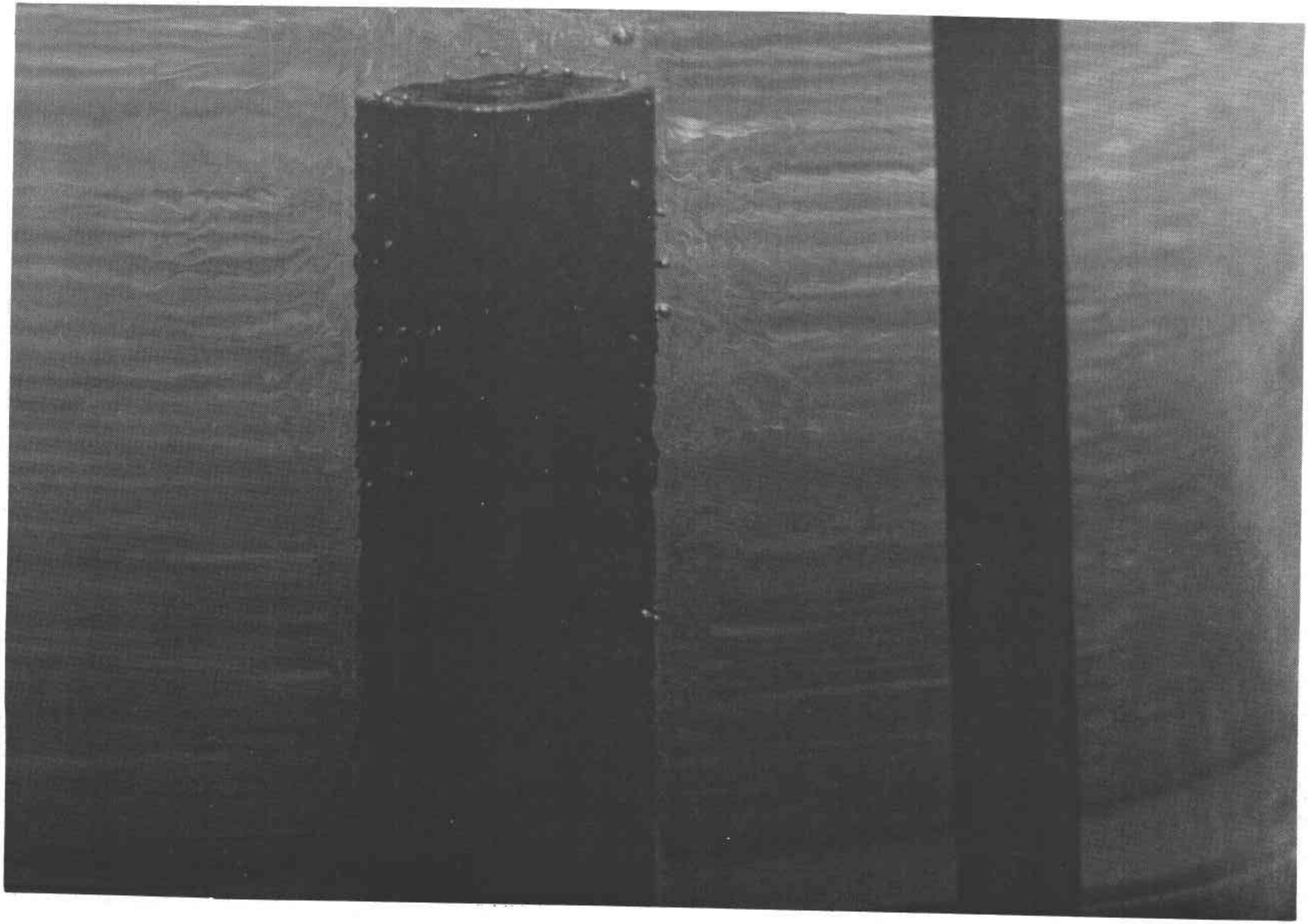

4ES29-12/18/75-C1F*

Figure 31. Heated Surface Fouling Test at 329 C (625 F) (Note the transition from laminar to turbulent flow in the natural convection flow)

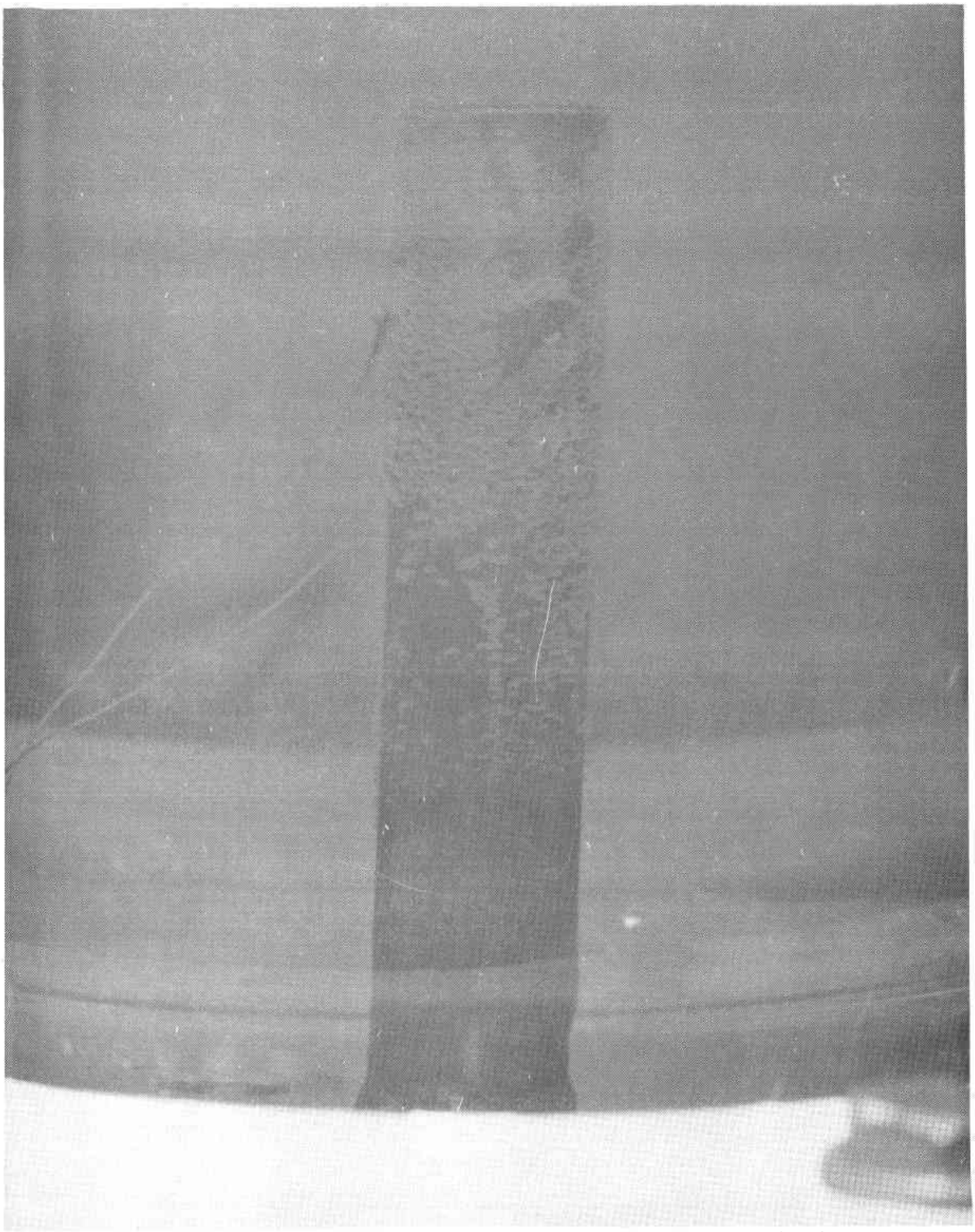

4ES35-6/18/76-C1B*

Figure 32. Heat Exchanger Surface Fouling Test of Caloria HT43 at 316 C (600 F) (Note gummy deposites visible after 200 hours of testing)

heater wall (especially where the flow near the heater wall appeared turbulent) tended to sweep away the bubbles. Hence, very little deposition occurred at the higher wall temperatures. Even for the 316C (600F) Caloria HT43 test, the early surface deposits did not continue to accumulate but steadily decreased to the point where, after about 2000 to 2500 hours, almost no material remained. The fouling test for a heater wall temperature of 316C (600F) was later repeated using fresh Caloria HT43 from a different batch than that used in the initial fouling test. The results were the same. Based upon the results at the two higher temperatures, testing at 316C (600F) was terminated after 7800 hours.

About every 800 hours the Chromel-Alumel thermocouples used to monitor the heater surface temperature for the Caloria HT43 tests would fail at the alumel-heater spot-weld. Similar thermocouple wires used in the Therminol 66 tests were trouble-free. After 2000 to 2500 hours, the Chromel-Alumel thermocouples used in the Caloria HT43 tests were replaced with Iron-Constantan.

When the Caloria HT43 fouling tests were temporarily interrupted, the 316C (600F) heater had accumulated more fouling deposits than the other two heaters. The patchy fouling deposits were confirmed mainly to the lower portion of the heater where the convection velocities were lowest. The top of the heaters was clear of deposits but appeared discolored or stained.

After several thousand hours the heaters immersed in Therminol 66 appeared somewhat discolored. Patchy deposits sometimes observed near the bottom of Caloria HT43 heaters, were not present with Therminol 66. At the end of 3745 hours of testing. the deposit on the 316C (600F) heater immersed in Therminol 66 was scraped from a known area and weighed. The deposit was found to be 0.0015 kg/m^2, which is quite small; however, the effect on heat transfer is not known.

The Therminol 66 used in the tube fouling tests is still light yellow in color after over 20000 hours of heating and is only slightly darker than the fresh fluid. After 14600 and 11500 hours of exposure to wall temperatures of 329C (625F) and 343C (650F), Caloria HT43 had darkened considerably, but appears to be perfectly fine for continued use. Table 6 briefly lists all fouling test conditions and accumulated test time.

TABLE 6. HEAT EXCHANGER SURFACE FOULING.

Tests	Fluid	Wall Temp. °C(°F)	Test Time Hrs (10/1/78)	Comments
1	Caloria HT43	316(600)	7808	Slight deposits near bottom of heater.
2	Caloria HT43	329(625)	14620	No scale on heater, surface is black.
3	Caloria HT43	343(650)	11520	No scale on heater, surface is black.
3A	Caloria HT43	316(600)	360	Gummy deposit formed around bubbles on heater surface
4	Therminol 66	316(600)	3745	No deposits on heater.
5	Therminol 66	329(625)	20300	No deposits on heater.
6	Therminol 66	343(650)	20500	No deposits on heater.
7	Mobiltherm 123	316(600)	4988	Excessive, extensive fouling, terminated 5/15/78.
8	Mobiltherm 123	329(625)	1700	Significant fouling see Fig. 33, terminated 5/15/78.
9	Mobiltherm 123	343(650)	932	Substantial fouling see Fig. 34, terminated 5/15/78.
7A	*Mobiltherm 123	316(600)	1008	Very thin brownish film on heater, terminated 6/29/78
8A	*Mobiltherm 123	329(625)	1008	Brownish film over entire heater surface, terminated 6/29/78.
9A	*Mobiltherm 123	343(650)	1008	Gross fouling, build-up of tarry deposits on heater, terminated 6/29/78.
7B	**Mobiltherm 123	316(600)	2090	Very little scale on heater.
8B	**Mobiltherm 123	329(625)	1590	5 mm thick scale on 3 cm section of heater.
10	Sun Oil 21	316(600)	2090	Slight deposit on heater.
11	Sun Oil 21	329(625)	2090	No deposit on heater.
12	Sun Oil 21	343(650)	2090	No deposits on heater.

---

* Tests No. 7, 8, and 9 were terminated on 5/15/78. Test 7A was begun with fresh Mobiltherm and a clean heater surface (essentially a new test). Tests 8A and 9A were begun with aged Mobiltherm from tests 8 and 9, but with clean heater surface.

** Tests No. 7B and 8B were begun with fresh Mobiltherm and clean heater surfaces (essentially new tests).

Mobiltherm XMTL 123 fouling tests experienced problems with Chromel-Alumel thermocouple failure at the 329C (625F) and 343C (650F) heaters after a few hundred hours. The Chromel-Alumel thermocouples were subsequently replaced with Iron Constantan. After about 1000 hours of additional testing time the Iron Constantan thermocouples also failed. When the test apparatuses were opened for replacement of the dead thermocouples, the heater surfaces maintained at a temperature of 329C (625F) and 343C (650F) were fouled with carbonaceous deposits, or char. Photographs of the deposits are shown in Figures 33 and 34. When disassembled for inspection after 4988 hours, the heater maintained at a surface temperature of 316C(600F) was extensively fouled. After cleaning the heaters and replacing the used fluid with fresh Mobiltherm, the tests were begun anew. Extensive fouling of the 343C (650F) heater after a few hundred hours of testing caused the test to be terminated. At the conclusion of the surface fouling test program the 316C (600F) heater from the Mobiltherm experiment had very slight scale formation while at 329C (625F) a five mm thick scale had built up in about 700 hours. Test data is listed in Table 6.

Samples of the Mobiltherm XMTL 123 batch used in these tests have been forwarded to the Mobil Oil Company for test. The dark color of the fresh fluid in the batch used for these tests is unusual; fresh Mobiltherm XMTL 123 is normally yellowish in color.

In the final months of this program, heater surface fouling tests of Sun Oil 21 were begun at 316C (600F), 329C (625F) and 343C (650F). These tests utilized apparatus from Caloria HT43 and Therminol 66 tests conducted at heater surface temperatures of 316C (600F) and from a Mobiltherm XMTL 123 test conducted at 343C (650F). As shown in Table 6, about 1900 hours have been accumulated on Sun Oil 21. It has been noted that after 1200 hours at 316C (600F) there was a very slight fouling deposit on the heater while at higher heater wall temperatures the surfaces were clean.

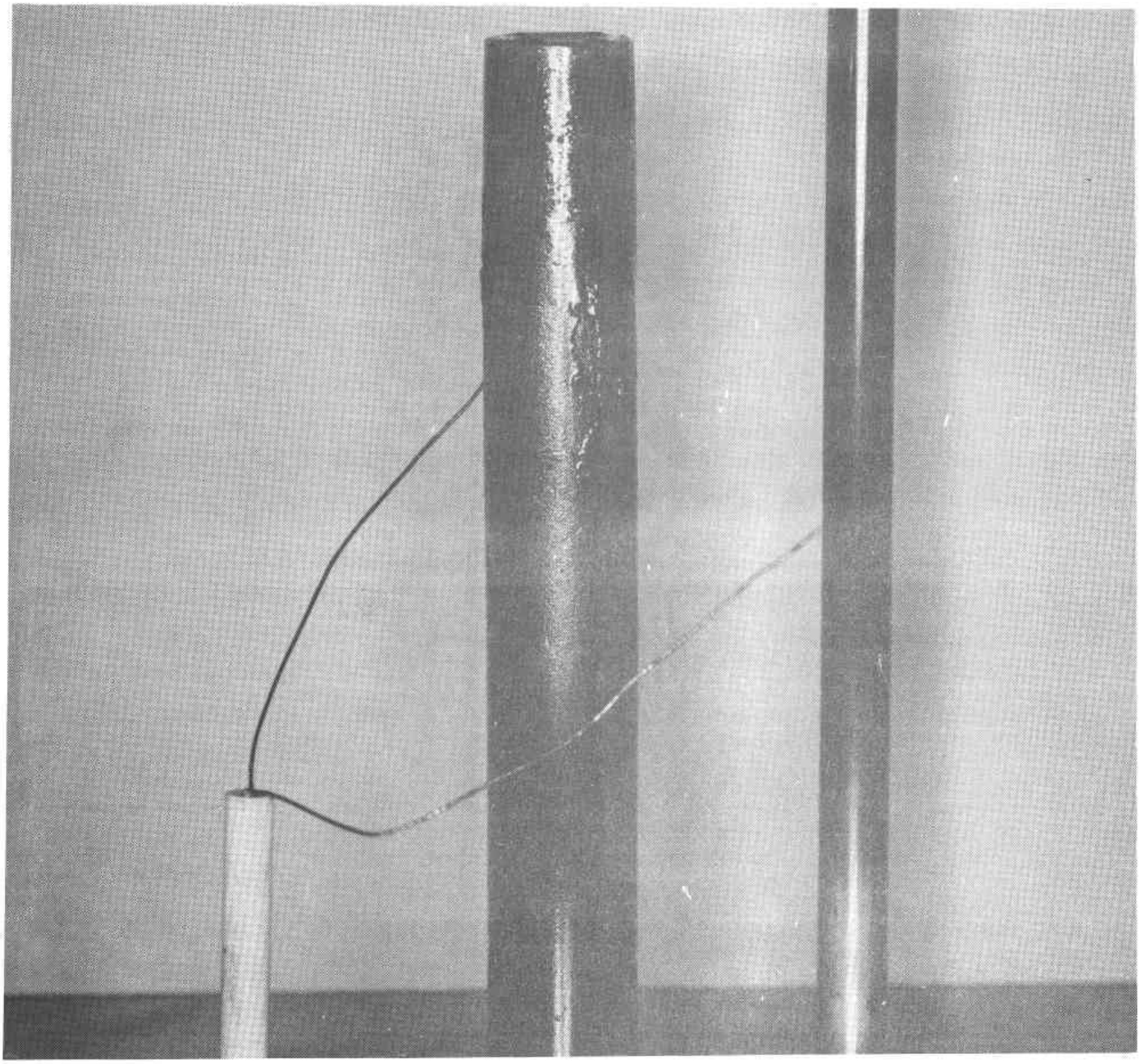

4ES55-5/15/78-C1B*

Figure 33. Surface Fouling Test, Mobiltherm 123 (625F), 1700 Hours

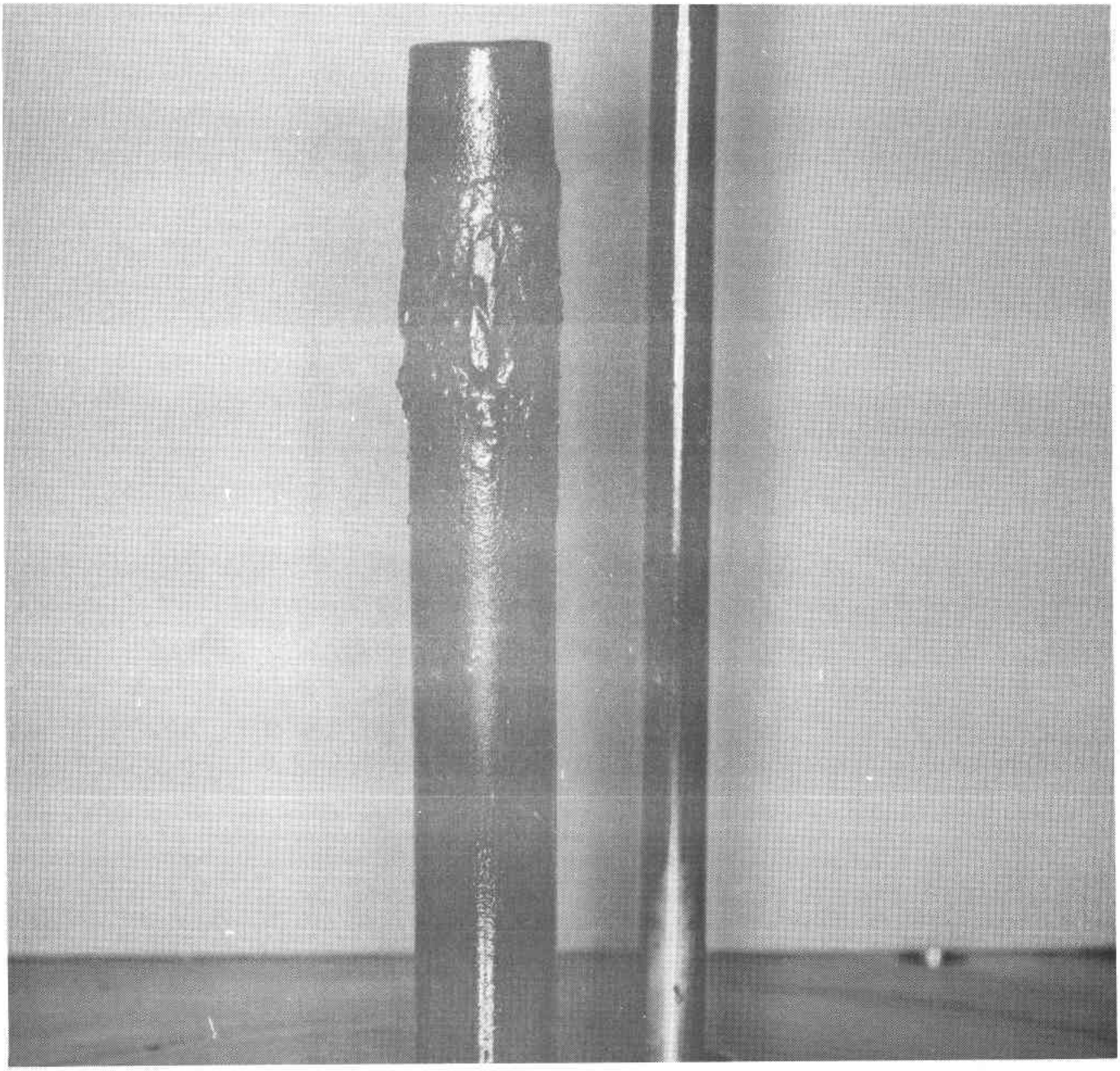

4ES55-5/15/78-C1A*

Figure 34. Surface Fouling Test, Mobiltherm 123 (650F), 932 Hours

MODEL SUBSYSTEM FLOW LOOP

A model subsystem flow loop was constructed and operated to determine the effect of sustained operation on critical operating parameters and fluid characteristics. Of particular interest is the long-term dynamic effects of fluid on sand migration and possible plugging of the thermal storage unit manifolds. Also heat exchanger surface fouling tendencies with forced movement of the fluid across the hot surfaces was not characterized by prior commercial experience or the relatively static conditions of the tests in the previous section. The flow loop would provide insight into the general operating characteristics of the dual medium thermal storage system at a modest cost on a laboratory scale.

The flow loop was not designed to obtain precise quantitative performance information on thermocline characteristics. This type of information was obtained by the 10.5 ft by 43 ft TSU tested at Rocketdyne's field laboratory in 1976 and is reported in Reference 20. The flow loop is intended to provide an operating environment to determine interaction of the principal components with extended duration exposure.

TEST EQUIPMENT AND PROCEDURES

The model subsystem flow loop was assembled by modifying an existing flow loop that was used for initial verification of the thermocline phenomena for thermal energy storage in 1974. The flow loop, Figure 35 schematic and Table 7, contains the principal working elements of a solar thermal energy storage system. Figures 36 and 37 are photographs of the system showing the principal components.

The central energy storage module is the Thermal Storage Unit (TSU) which is filled with gravel and sand of the same size and from the same location that will be used for the Barstow Pilot Plant. Bimodal packing was utilized to achieve a void fraction in the densest region of the rock bed in the TSU of 28 percent.

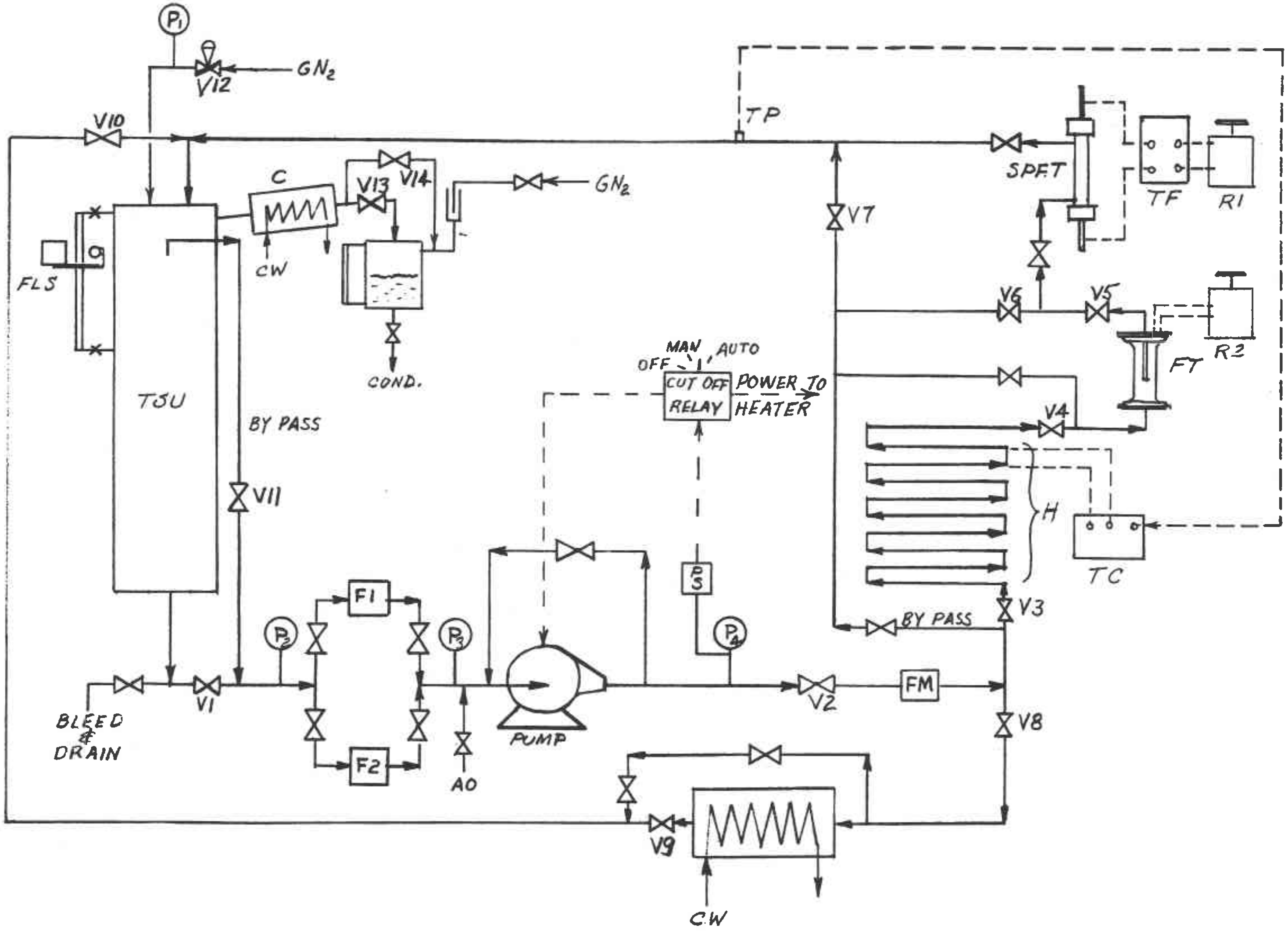

Figure 35. Model Thermal Storage Subsystem Flow Loop

TABLE 7. FLUID FLOW LOOP NOMENCLATURE

AO	Add Oil
C	Condenser
CW	Cooling Water
F1, F2	Fluid Filters
FLS	Fluid Level - Power Relay Switch
FM	Flow Meter
FT	Fouling Test
H	Heaters
P	Pressure Gauge
PS	Pressure - Power Relay Switch
SPFT	Small Probe Fouling Test
TC	Temperature Controller
TF	Transformer
TP	Temperature Probe
TSU	Thermal Storage Unit
R_1, R_2	Variacs
V	Valve

The TSU tank consists of three sections of flanged stainless steel pipe having a combined length of approximately 6 feet, an internal diameter of 7 inches and a wall thickness of 0.125 inch (Figure 38). A $\frac{1}{4}$-inch-thick flow distributor plate containing 54 equally spaced 0.065 inch diameter holes is positioned at the bottom of the tank. The flow distributor plate serves a two-fold purpose: (1) provide uniform fluid distribution throughout the cross section of the tank and (2) support the rock within the tank. In order to simplify construction the model subsystem TSU is fitted with a bottom manifold only. Since the purpose of the flow loop

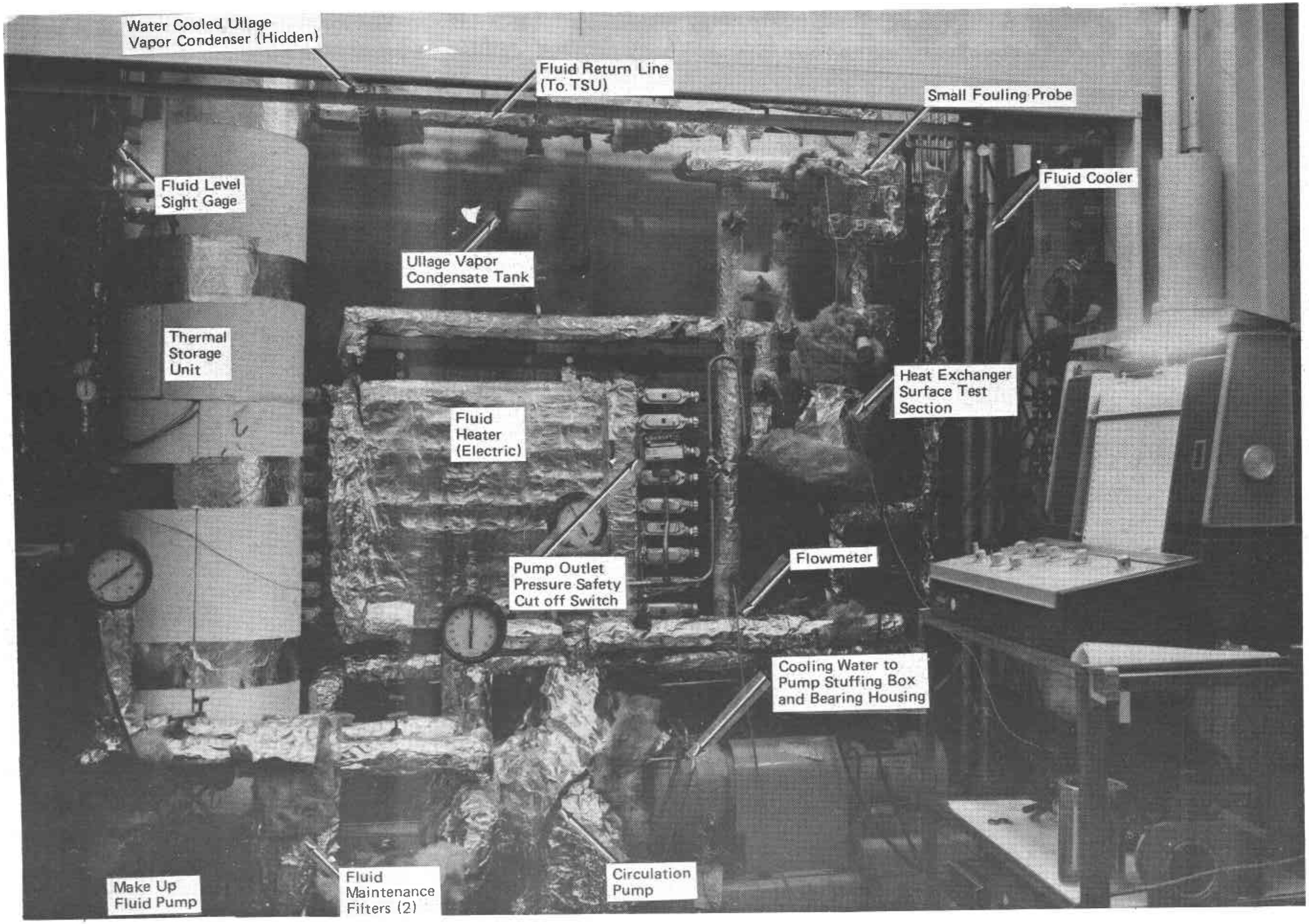

5AJ25-2/17/78-C2C*

Figure 36. Model Subsystem Flow Loop

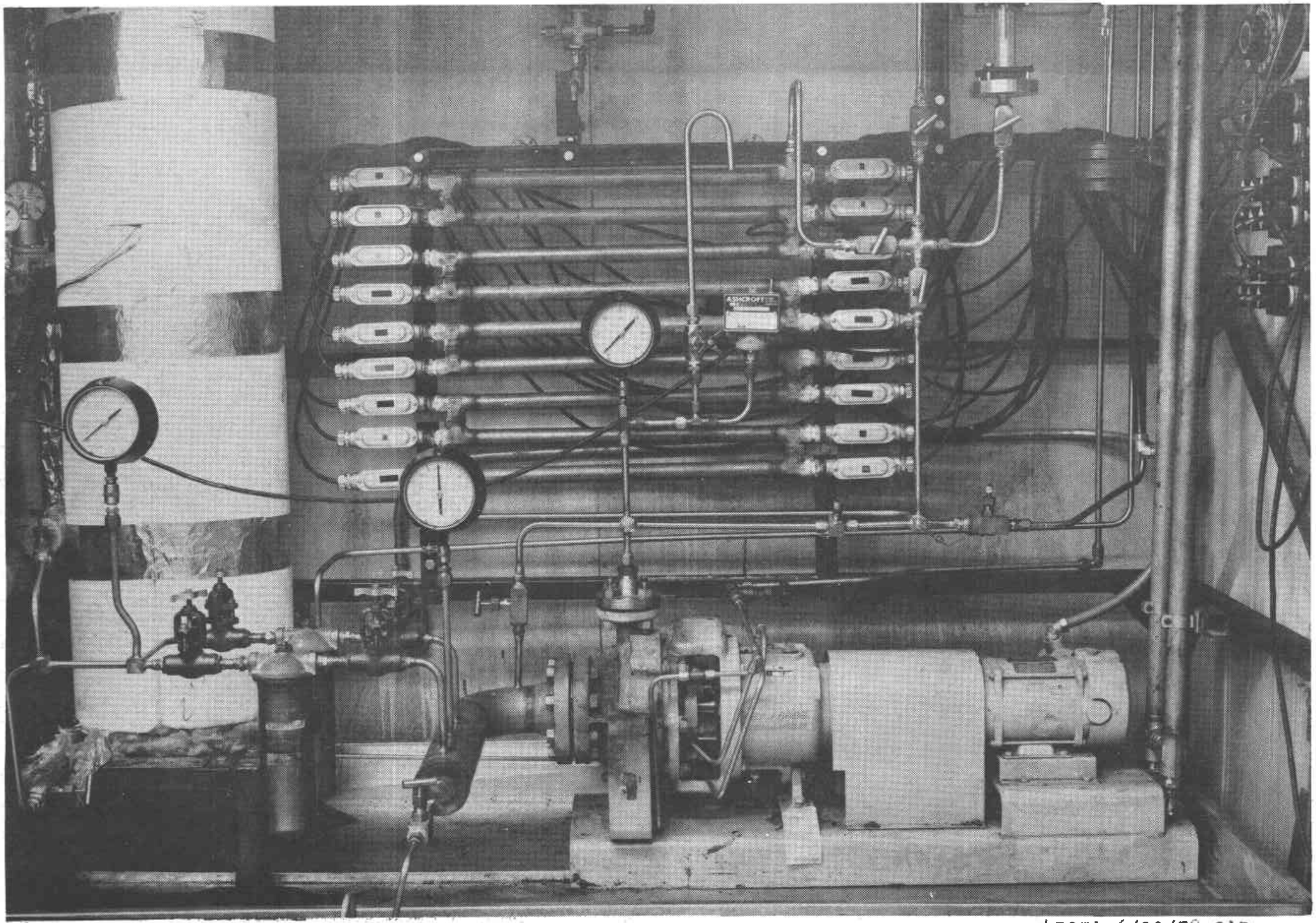

4ES51-6/30/78-C1B

Figure 37. Flow Loop, Insulation Removed (Except for TSU)

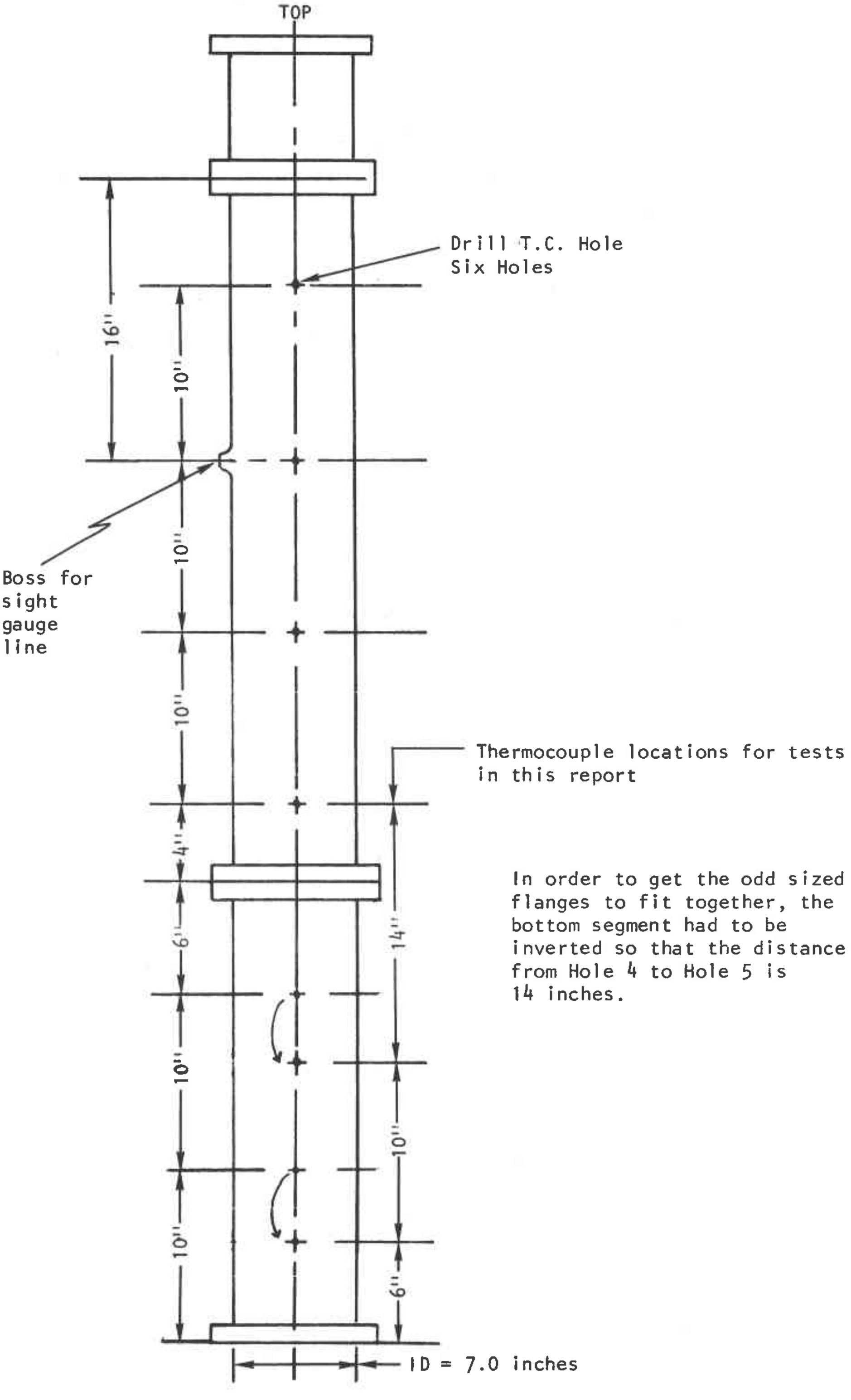

In order to get the odd sized flanges to fit together, the bottom segment had to be inverted so that the distance from Hole 4 to Hole 5 is 14 inches.

Figure 38. Flow Loop TSU Thermocouple Locations

operation was to subject the rock and fluid to long term contact it was not deemed necessary to provide an upper manifold. During heating and cooling fluid flow is downward through the bed. The bottom manifold is considered to be the one most susceptible to build-up of sedimentation, thus providing a conservative test.

The particulate removal portion of fluid maintenance unit, FMU, is performed by the two parallel-mounted 80 mesh filters ahead of the circulation pump. During operation both filters were used to provide a minimum pressure drop between the TSU and the pump inlet.

The circulation pump is a 1 HP 1750 rpm Dean Bros. centrifugal model R434, 1 X 3 X 8½ with a 5½-inch impeller and water cooled stuffing box and bearing housing. The pump was equipped with a mechanical axial contact mechanical seal. The pump type and configuration is identical to that expected to be used in the Pilot and Commercial scale solar power plant.

Fluid heating is accomplished by a bank of 18 600-watt electrical heating elements. Each element can be connected independently to provide 18 power levels of heating. The fluid cooler utilizes tap water in a concentric tube heat exchanger. Cooling rate is controlled by hand valves that adjust heat transfer fluid and water flow.

The heat exchanger fouling section utilizes a standard metal covered electrical heating element in a 2-inch-diameter by 4-inch-long glass observation section (Figures 39 and 40). A thermocouple welded to the surface of the electrical heating element allows the surface temperature to be adjusted to the desired value through a variac supplying power to the heating element.

The small fouling probe test section provides accelerated fouling data and can be used to monitor the fluid to determine sensitivity to fouling as a function of heated surface temperature.

The principal flow sections were plumbed with ½-inch stainless steel tubing using AN fittings where possible. Both AN and threaded connections were

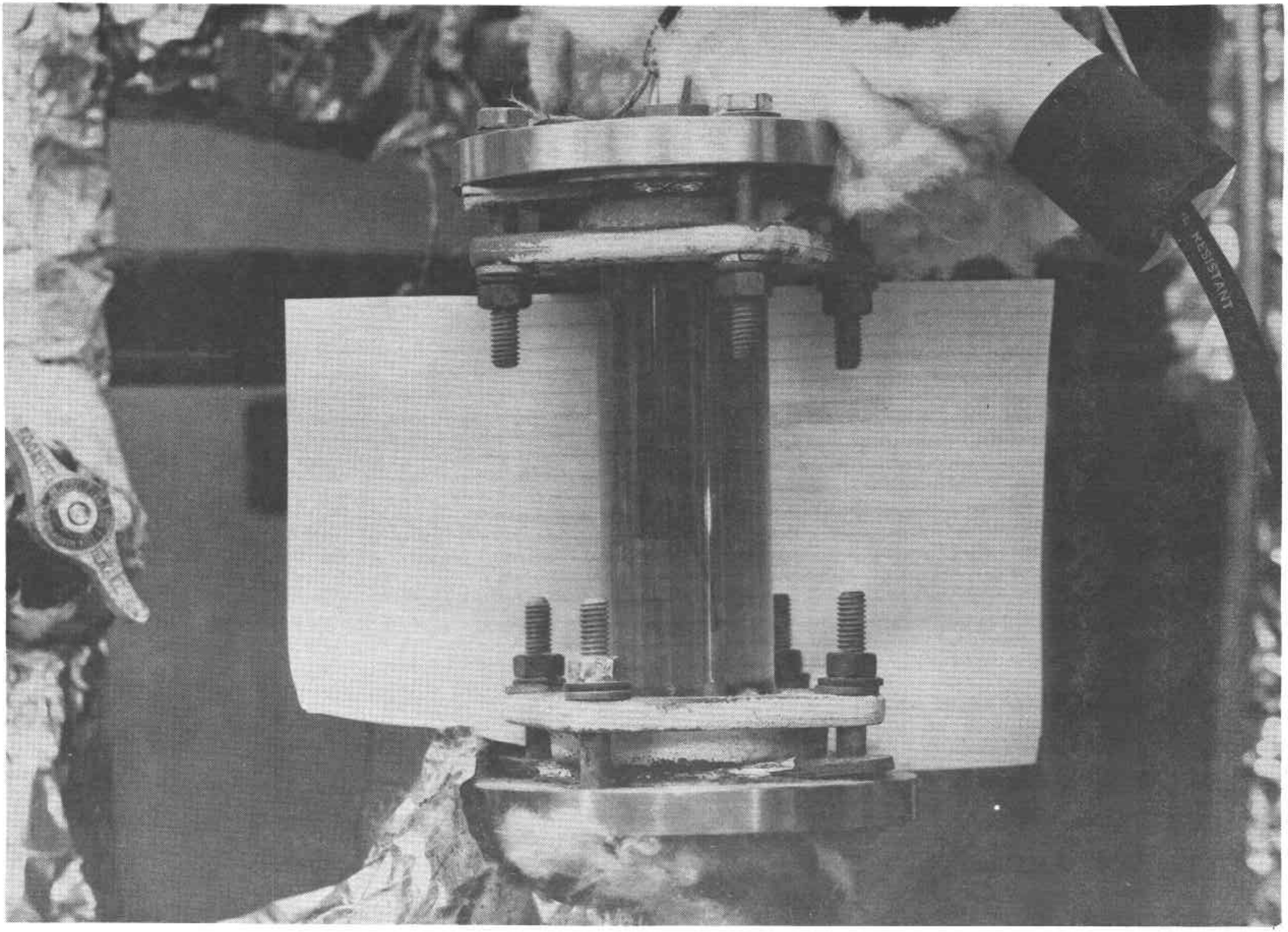

5AJ25-2/17/78-C1A

Figure 39. Flow Loop Heat Exchanger Surface Fouling Test Section, Insulation Removed

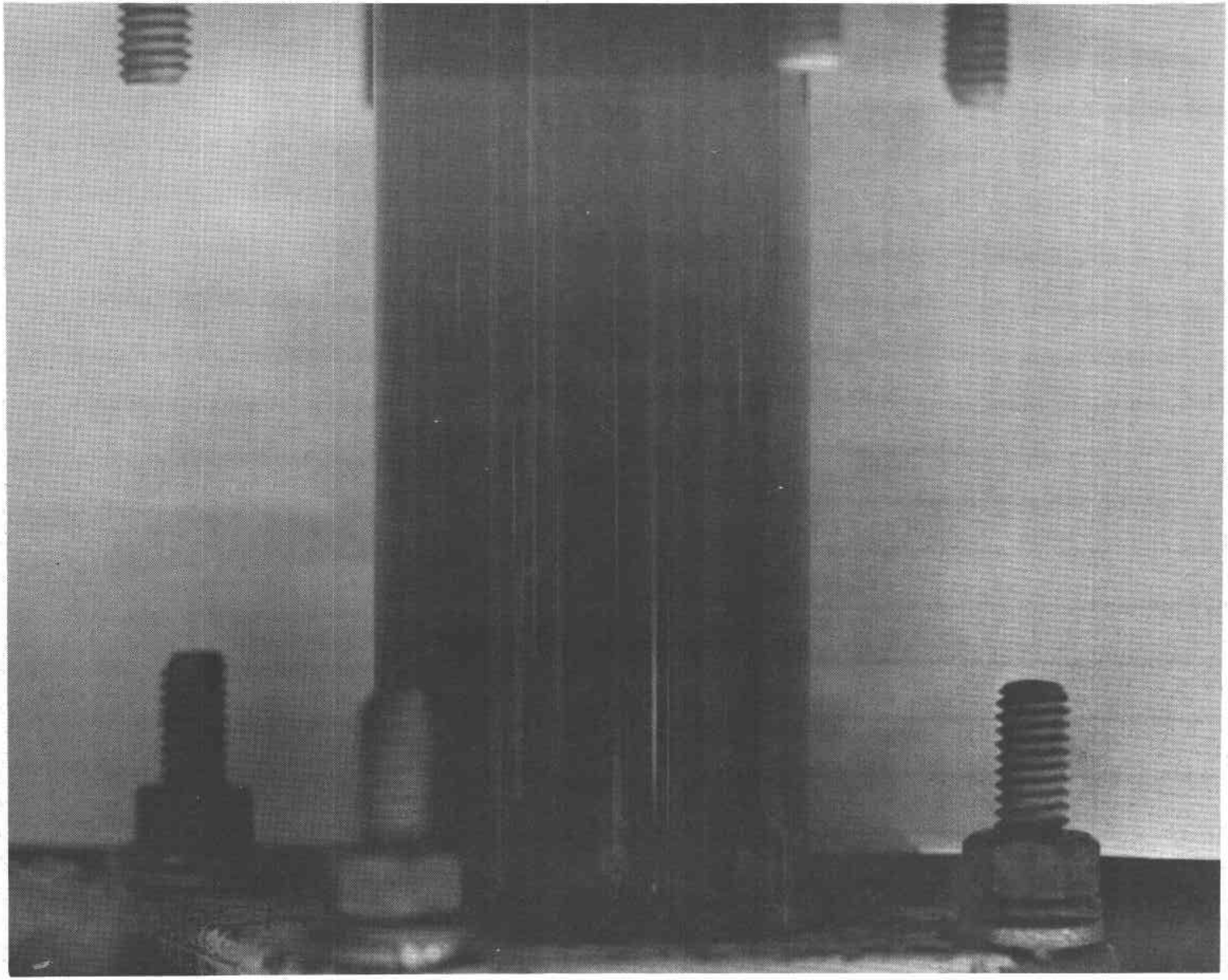

5AJ25-2/17/78-C2B*

Figure 40. Heat Exchanger Surface Fouling Test Section, Close Up, Insulation Removed

welded where possible to provide a minimum of leakage paths while still facilitating disassembly.

Temperature recordings were made on a Doric Digitrend 25 channel data logger. Pressures and flows were visually recorded.

Operation of the flow loop consisted of filling with the heat transfer liquid, activating the circulation pump and heating with full electrical power to the operating temperature level, and setting the temperature controller to the desired level. All tests were run with Caloria HT43 with a nominal TSU control set temperature of 302C (575F).

For a system of this size heat losses are quite large and heater fluid outlet temperature had to be adjusted to 10 to 15C higher in order to retain the TSU bed at 302C (575F). Heating from room temperature to operating temperature took approximately four hours. Once adjusted the fluid heater temperature controller held the TSU temperature within 1 to 2C of the desired temperature.

INSTRUMENTATION

Flow loop instrumentation included six thermocouples mounted axially in the TSU bed (locations in Figure 38) TSU fluid inlet and outlet temperatures, heat exchanger surface test section temperature, ambient temperature, pump inlet and outlet pressure, filter inlet and outlet pressure, small probe fouling test surface temperature, and heat transfer fluid flow rate (at pump outlet). Table 8 lists instrumentation.

Bed temperatures, TSU ullage and outlet, and heat exchanger surface fouling test temperature were recorded on the data logger system (a 20-second sweep multiplexing system). Printout time intervals were adjusted from one minute to 4 hours depending upon the surveillance required. Pressures were recorded visually as required from bourdon tube type dial gages. Flow was recorded visually and measured with a turbine type flowmeter calibrated with water.

TABLE 8. LIST OF INSTRUMENTATION

ID	Recorder	Parameter
	Datalogger	
T_1	001	TSU Ullage Space Temperature, F
T_2	002	TSU Bed Fluid Temperatures, F
through	through	
T_7	007	
T_8	008	TSU Fluid Outlet Temperature, F
-	009	Ambient Temperature (in Hood), F
Ta	010	Ambient Temperature (Room), F
-	011	(Not Connected)
-	012	(Not Connected)
FLS	013	TSU Sight Gage Liquid Level Cutoff Switch, Millivolts
	Strip Chart	
T_{SPFT}		Small Probe Fouling Test Temperature, F
	Sight Gage	
P_1		TSU Ullage Pressure, psig
P_2		TSU Outlet, Filter Inlet Pressure, psig
P_3		Filter Outlet, Pump Inlet Pressure, psig
P_4		Pump Outlet Pressure, psig
FM		Heat Transfer Fluid Flow, gpm

TEST RESULTS AND DISCUSSION

Operation of the loop occurred primarily during two periods. December 1977 through March 1978 accumulated 1650 hours. During August and September another 780 hours was accumulated for a total of 2430 hours.

During the 2430 hours there was no indication of performance degradation resulting from fluid degradation or bed plugging or fouling.

Bed and Manifold Plugging and Fouling

There was no evidence of bed and manifold plugging and fouling during the program. Plugging and fouling was determined by measuring fluid flow and bed pressure drop. Bed pressure drop was computed as the difference between the TSU ullage pressure and filter inlet pressure immediately downstream of the TSU during dynamic (flowing) and static operation. Pressure gage readings were taken after flow stabilized at the desired bed temperature (575F) for several hours (typically overnight). After dynamic readings the pump was shut off and static readings were taken when the TSU sight gage fluid level stabilized (typically 15 to 30 minutes) and before any heat loss. A typical set of readings is shown below. Temperature measured throughout the bed was 575 ±3F.

TSU Characteristics (9/7/78)	Flowing	Static
Flow, gpm	0.7	0
Sight Gage Fluid Level, Inches*	9-3/8	10-1/4
Outlet Pressure, P_2, psig	7.5	8.2
Ullage Pressure, P_1, psig	5.0	5.0
$\Delta P = P_1 - P_2$	-2.5	-3.2
Dynamic Pressure Drop, psid ΔP (flowing) - P (static)	0.7	

A plot of the dynamic pressure drop during the second test period (20 July through 15 September) is shown in Figure 41. Pressure drop values include bed and manifold. Values of pressure drop for the same flow are unchanged from the beginning of the test period to the end. Flow values were not obtained during the first test period because of a faulty flowmeter. The rotating turbine element was jammed from a thin hard caked layer on the flowmeter which blocked the rotating element. Although there is some evidence of air entering during the second test period the system was free of deposits.

---

*Distance above sight gage lower connection.

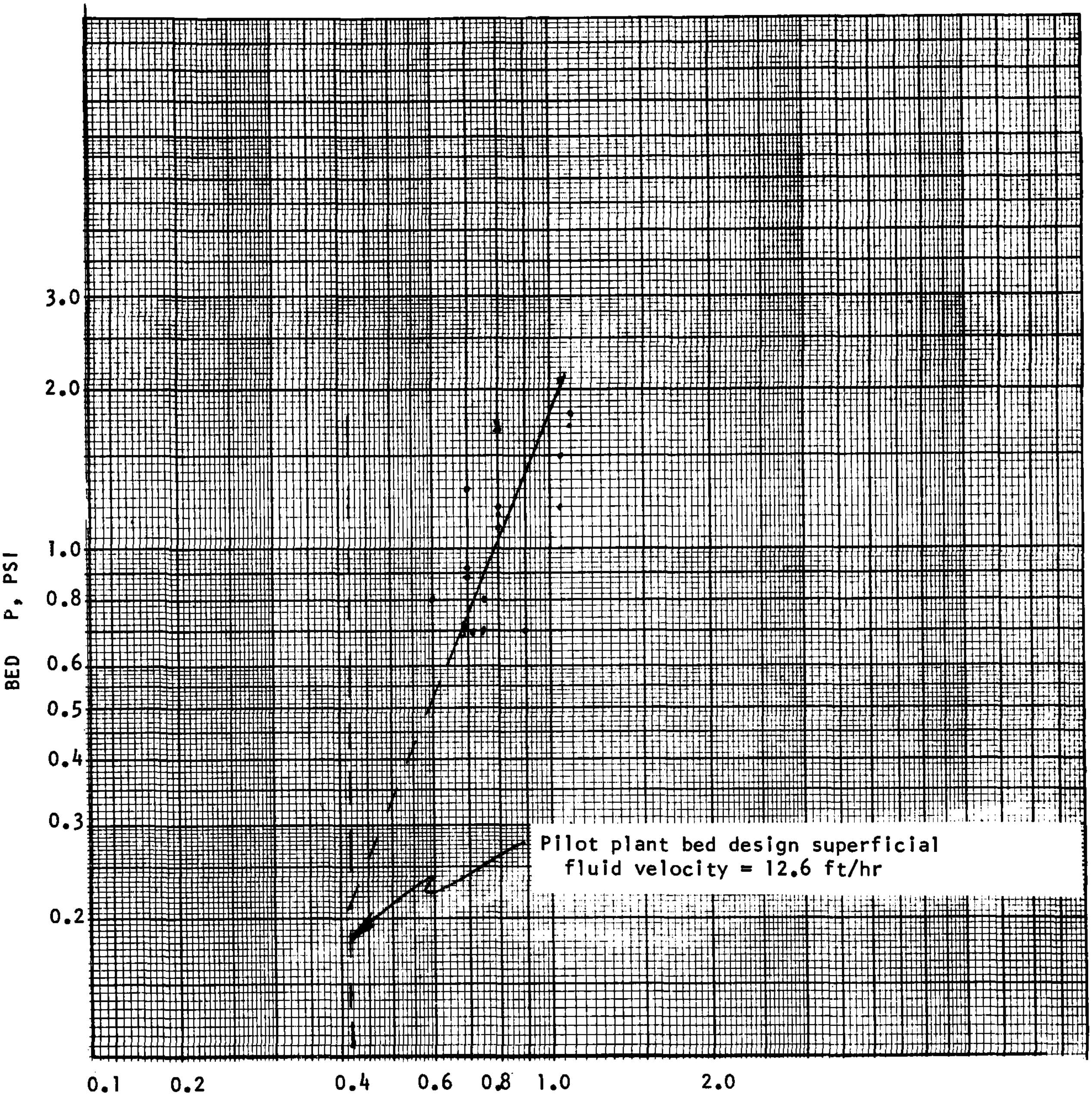

Figure 41. Bed Flow Characteristics (Included Manifold)

The filters were cleaned five times during the 2430 hour test period. Approximately 20 to 30 ml of residue was collected the first cleaning. This was a mix of very fine silt-like material and coarse sand of the size used for packing the bed. Subsequent cleanings produced smaller quantities on the order of 5 ml of primarily sand. These results are similar to that obtained with the 5 MWh_t SRE tests made in 1976. Filtered material is rich in fines during the first few hours of operation and then reduces to a very small quantity. This indicates that fines accompany the rock or are made during filling. Whatever rock movement occurs during subsequent heating and cooling cycles apparently does not produce any appreciable amount of powdering.

Bed Thermocline Performance

The thermocline principle was observed during each of the heating and cooling cycles. Although not a major objective of the program since thermocline operation was characterized with the SRE tests, Reference 20, it serves the purpose of establishing characteristics at this scale level. Figure 42 shows thermocline operation plotted from a cooling test on February 21. Data are listed in Table 9.

Heat Exchanger Surface Fouling

An important consideration in the design of heat exchangers for use with heat transfer fluids is the possibility of the formation of deposits on hot exchanger surfaces resulting from fluid degradation. The surface fouling tests reported in the front section of this report established fluid in a quiescent or static condition. Fluid flow past the tube section was induced only by natural convection resulting from the gradient between the tube and the bulk fluid temperature. Caloria fouling samples characteristically produced a small amount of fouling (which eventually disappeared) in all samples. However those samples at higher wall temperatures produced less fouling which may have resulted from the higher velocities induced by the higher wall temperatures.

In order to provide results for the active portion of the heat exchanger where velocities from forced convection are considerably higher, a transparent test section was provided in the flow loop, Figures 39 and 40.

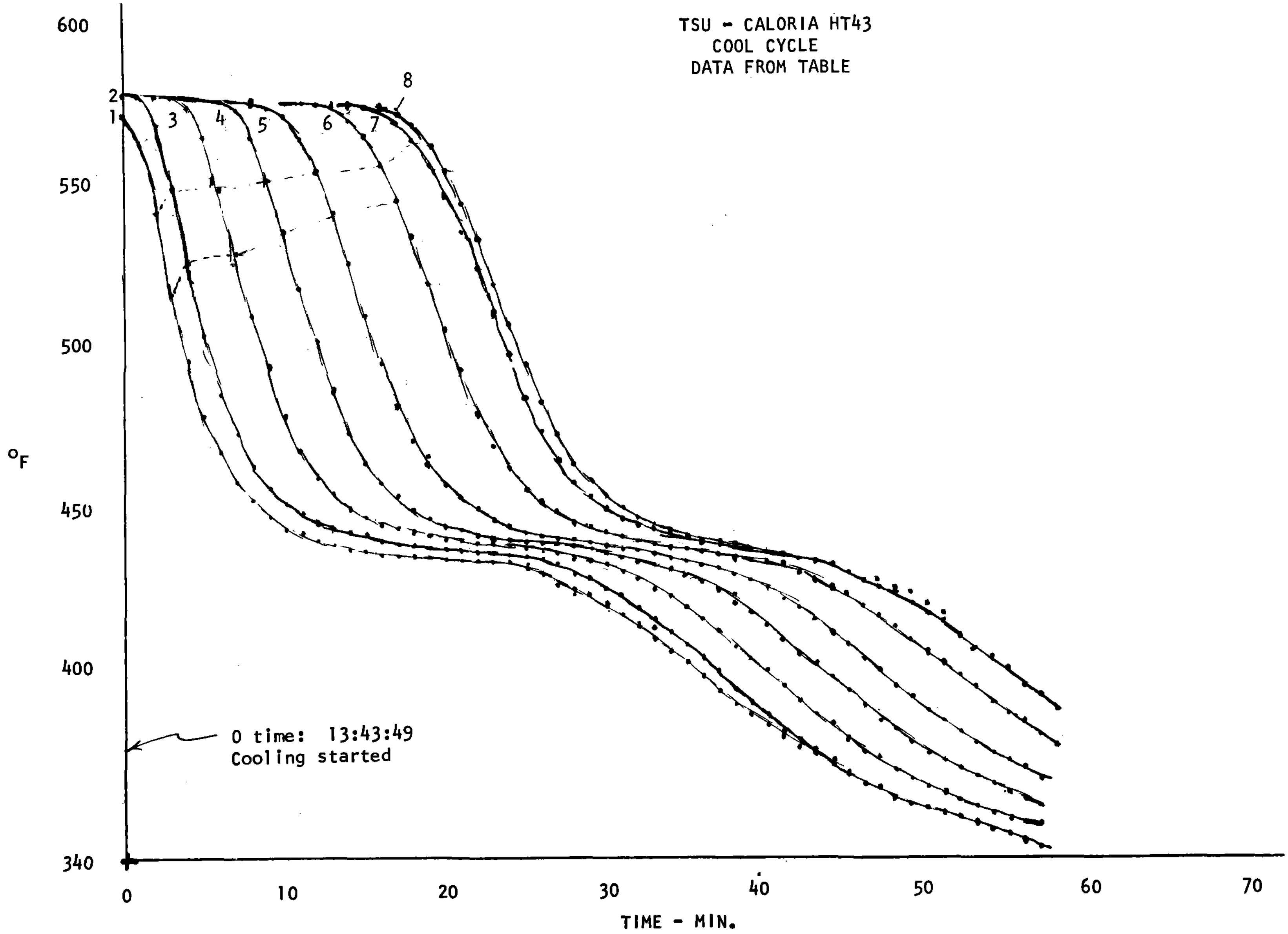

Figure 42. TSU Thermocline During Typical Cooling Cycle

TABLE 9. TEMPERATURES DURING COOLING CYCLE

(Original data sheets)

2-21-78

ALL HEAT OFF.

Time 0. minutes

```
      ? LO
      RUN   DATE
             13:42:53   001 0572.2F   002 0577.5F   003 0576.9F   004 0576.6F
      005 0575.3F   006 0575.4F   007 0574.5F   008 0574.5F   009 0083.7F
      010 0075.5F   011 0624.1F   012 0181.1F   013 00.530V

All (0) RUN   DATE
HEAT         13:43:49   001 0571.9F   002 0577.4F   003 0576.9F   004 0576.6F
"OFF" 005 0575.7F   006 0575.4F   007 0574.5F   008 0574.4F   009 0083.7F
      010 0075.5F   011 0599.4F   012 0179.7F   013 00.529V
minutes
      RUN   DATE
             13:44:49   001 0562.2F   002 0576.9F   003 0577.1F   004 0576.6F
1     005 0575.3F   006 0575.3F   007 0574.6F   008 0574.5F   009 0083.8F
      010 0075.5F   011 0567.4F   012 0134.5F   013 00.529V

      RUN   DATE
2            13:45:49   001 0539.9F   002 0563.4F   003 0577.1F   004 0576.6F   2
      005 0575.7F   006 0575.3F   007 0574.6F   008 0574.4F   009 0083.3F
      010 0075.5F   011 0534.7F   012 0177.3F   013 00.530V

      RUN   DATE
3            13:46:49   001 0515.3F   002 0543.7F   003 0576.6F   004 0576.5F
      005 0575.3F   006 0575.3F   007 0574.6F   008 0574.4F   009 0083.3F
      010 0075.6F   011 0507.5F   012 0172.0F   013 00.532V

      RUN   DATE
4            13:47:49   001 0495.1F   002 0524.9F   003 0573.0F   004 0576.6F   4
      005 0575.7F   006 0575.3F   007 0574.4F   008 0574.4F   009 0083.8F
      010 0075.6F   011 0486.9F   012 0175.9F   013 00.535V

5     RUN   DATE
             13:48:49   001 0473.8F   002 0502.7F   003 0563.3F   004 0576.5F
      005 0575.7F   006 0575.3F   007 0574.4F   008 0574.4F   009 0083.8F
      010 0075.6F   011 0473.0F   012 0175.8F   013 00.534V

6     RUN   DATE
             13:49:49   001 0466.6F   002 0484.7F   003 0547.5F   004 0575.3F
      005 0575.7F   006 0575.3F   007 0574.4F   008 0574.5F   009 0083.8F   6
      010 0075.6F   011 0463.6F   012 0183.2F   013 00.532V

7     RUN   DATE
             13:50:49   001 0457.8F   002 0471.2F   003 0523.4F   004 0571.3F
      005 0575.7F   006 0575.4F   007 0574.4F   008 0574.4F   009 0083.9F
      010 0075.6F   011 0457.3F   012 0179.6F   013 00.533V

8     RUN   DATE
             13:51:49   001 0451.3F   002 0461.3F   003 0509.4F   004 0563.2F   8
      005 0575.3F   006 0575.4F   007 0574.5F   008 0574.4F   009 0083.9F
      010 0075.7F   011 0453.0F   012 0176.5F   013 00.536V

9     RUN   DATE
             13:52:49   001 0446.7F   002 0455.1F   003 0492.1F   004 0553.6F
      005 0573.5F   006 0575.3F   007 0574.4F   008 0574.4F   009 0083.9F
      010 0075.7F   011 0453.2F   012 0134.1F   013 00.536V

10    RUN   DATE
             13:53:49   001 0443.4F   002 0454.3F   003 0473.0F   004 0534.7F   10
      005 0569.7F   006 0575.3F   007 0574.4F   008 0574.4F   009 0083.9F
      010 0075.7F   011 0443.3F   012 0133.6F   013 00.535V
```

July 13, 1978

TABLE 9. (Continued)

```
    RUN    DATE
           13:54:49    001 0441.3F    002 0447.3F    003 0467.1F    004 0517.3F
    005 0563.7F    006 0575.0F    007 0574.5F    008 0574.3F    009 0083.9F
    010 0075.7F    011 0447.0F    012 0179.4F    013 00.535V

12  RUN    DATE
           13:55:49    001 0439.2F    002 0444.7F    003 0459.1F    004 0500.5F    12
    005 0552.9F    006 0574.4F    007 0574.5F    008 0574.3F    009 0083.9F
    010 0075.8F    011 0445.0F    012 0182.3F    013 00.535V

    RUN    DATE
           13:56:49    001 0437.7F    002 0443.0F    003 0453.3F    004 0485.7F
    005 0539.3F    006 0572.7F    007 0574.2F    008 0574.3F    009 0084.0F
    010 0075.3F    011 0445.3F    012 0183.3F    013 00.532V

14  RUN    DATE
           13:57:49    001 0436.3F    002 0441.5F    003 0449.2F    004 0473.7F    14
    005 0525.1F    006 0569.3F    007 0574.0F    008 0574.1F    009 0084.0F
    010 0075.7F    011 0444.7F    012 0177.9F    013 00.534V

    RUN    DATE
           13:58:49    001 0435.9F    002 0440.4F    003 0446.2F    004 0464.3F
    005 0509.4F    006 0563.5F    007 0573.0F    008 0573.6F    009 0084.0F
    010 0075.8F    011 0444.2F    012 0181.6F    013 00.536V

16  RUN    DATE
           13:59:49    001 0435.2F    002 0439.2F    003 0444.0F    004 0457.3F    16
    005 0494.1F    006 0555.3F    007 0571.0F    008 0572.5F    009 0083.9F
    010 0075.3F    011 0443.8F    012 0188.2F    013 00.534V

    RUN    DATE
           14:00:49    001 0434.7F    002 0438.5F    003 0442.3F    004 0452.3F
    005 0480.3F    006 0544.3F    007 0567.6F    008 0570.2F    009 0084.0F
    010 0075.9F    011 0443.6F    012 0180.6F    013 00.539V

18  RUN    DATE
           14:01:49    001 0434.3F    002 0437.9F    003 0441.0F    004 0443.6F    18
    005 0469.9F    006 0532.3F    007 0562.2F    008 0566.2F    009 0084.0F
    010 0075.9F    011 0443.3F    012 0133.9F    013 00.536V

    RUN    DATE
           14:02:49    001 0433.9F    002 0437.5F    003 0439.9F    004 0445.7F
    005 0461.6F    006 0513.7F    007 0554.9F    008 0560.2F    009 0084.0F
    010 0075.8F    011 0443.1F    012 0173.7F    013 00.536V

20  RUN    DATE
           14:03:49    001 0433.3F    002 0436.8F    003 0439.0F    004 0443.6F    20
    005 0455.6F    006 0504.6F    007 0545.5F    008 0552.3F    009 0083.9F
    010 0075.3F    011 0442.7F    012 0132.1F    013 00.536V

    RUN    DATE
           14:04:49    001 0433.0F    002 0436.5F    003 0438.3F    004 0442.1F
    005 0451.1F    006 0493.5F    007 0534.6F    008 0542.5F    009 0084.0F
    010 0075.9F    011 0442.4F    012 0135.5F    013 00.537V

22  RUN    DATE
           14:05:49    001 0432.6F    002 0436.0F    003 0437.7F    004 0440.8F    22
    005 0447.7F    006 0473.7F    007 0522.5F    008 0531.3F    009 0084.0F
    010 0075.9F    011 0441.9F    012 0131.3F    013 00.539V

    RUN    DATE
           14:06:49    001 0431.9F    002 0435.4F    003 0437.1F    004 0439.7F
    005 0445.3F    006 0463.7F    007 0509.6F    008 0519.1F    009 0084.0F
    010 0075.9F    011 0441.1F    012 0131.5F    013 00.535V
```

TABLE 9. (Continued)

```
24  RUN    DATE
           14:07:49   001 0431.2F   002 0434.8F   003 0436.7F   004 0439.0F   24
      005 0443.4F     006 0460.9F   007 0496.1F   008 0506.0F   009 0084.0F
      010 0076.0F     011 0440.1F   012 0180.7F   013 00.536V

    RUN    DATE
           14:08:49   001 0430.0F   002 0433.9F   003 0436.1F   004 0438.3F
      005 0441.8F     006 0454.9F   007 0483.2F   008 0493.0F   009 0084.0F
      010 0075.9F     011 0438.8F   012 0179.0F   013 00.535V

26  RUN    DATE
           14:09:49   001 0428.7F   002 0432.7F   003 0435.5F   004 0437.6F   26
      005 0440.6F     006 0450.4F   007 0472.3F   008 0481.2F   009 0084.0F
      010 0075.9F     011 0436.9F   012 0181.1F   013 00.538V

    RUN    DATE
           14:10:49   001 0426.3F   002 0431.3F   003 0434.9F   004 0436.9F
      005 0439.5F     006 0447.1F   007 0463.7F   008 0471.0F   009 0084.0F
      010 0075.9F     011 0434.5F   012 0180.0F   013 00.533V

28  RUN    DATE
           14:11:49   001 0424.6F   002 0429.4F   003 0433.9F   004 0436.5F   28
      005 0438.9F     006 0444.6F   007 0457.2F   008 0462.9F   009 0084.0F
      010 0076.0F     011 0431.7F   012 0137.3F   013 00.536V

    RUN    DATE
           14:12:49   001 0422.0F   002 0427.0F   003 0432.9F   004 0435.9F
      005 0438.1F     006 0442.3F   007 0452.3F   008 0456.7F   009 0084.0F
      010 0076.0F     011 0428.5F   012 0176.4F   013 00.536V

30  RUN    DATE
           14:13:49   001 0419.0F   002 0424.3F   003 0431.3F   004 0435.2F   30
      005 0437.5F     006 0441.2F   007 0448.6F   008 0451.9F   009 0084.0F
      010 0076.0F     011 0424.9F   012 0171.6F   013 00.537V

    RUN    DATE
           14:14:49   001 0415.7F   002 0421.3F   003 0429.5F   004 0434.3F
      005 0436.7F     006 0440.0F   007 0445.8F   008 0448.3F   009 0084.1F
      010 0076.0F     011 0421.1F   012 0184.1F   013 00.532V

32  RUN    DATE
           14:15:49   001 0412.3F   002 0417.7F   003 0427.3F   004 0433.2F   32
      005 0436.2F     006 0439.1F   007 0443.6F   008 0445.6F   009 0084.1F
      010 0076.0F     011 0416.9F   012 0179.0F   013 00.534V

    RUN    DATE
           14:16:49   001 0408.4F   002 0413.8F   003 0424.7F   004 0431.8F
      005 0435.5F     006 0438.3F   007 0441.9F   008 0443.4F   009 0084.1F
      010 0076.1F     011 0412.5F   012 0182.0F   013 00.535V

34  RUN    DATE
           14:17:49   001 0404.4F   002 0409.6F   003 0421.6F   004 0430.2F   34
      005 0434.6F     006 0437.5F   007 0440.6F   008 0441.8F   009 0084.0F
      010 0076.1F     011 0408.2F   012 0177.8F   013 00.536V

    RUN    DATE
           14:18:49   001 0400.6F   002 0405.4F   003 0418.2F   004 0428.1F
      005 0433.5F     006 0436.3F   007 0439.4F   008 0440.5F   009 0084.1F
      010 0076.1F     011 0403.7F   012 0177.9F   013 00.536V

36  RUN    DATE
           14:19:49   001 0396.5F   002 0401.0F   003 0414.5F   004 0425.6F   36
      005 0432.1F     006 0436.1F   007 0438.4F   008 0439.4F   009 0084.0F
      010 0076.1F     011 0399.4F   012 0177.6F   013 00.533V
```

TABLE 9. (Continued)

```
     RUN   DATE
           14:20:49   001 0392.5F   002 0396.6F   003 0410.5F   004 0422.6F
     005 0430.6F   006 0435.3F   007 0437.6F   008 0438.6F   009 0084.1F
     010 0076.1F   011 0395.2F   012 0173.5F   013 00.533V

38   RUN   DATE
           14:21:49   001 0383.8F   002 0392.0F   003 0406.4F   004 0419.5F   38
     005 0428.6F   006 0434.5F   007 0436.9F   008 0437.8F   009 0084.1F
     010 0076.1F   011 0391.3F   012 0175.1F   013 00.536V

     RUN   DATE
           14:22:49   001 0385.0F   002 0387.7F   003 0402.1F   004 0416.0F
     005 0426.2F   006 0433.5F   007 0436.1F   008 0437.0F   009 0084.1F
     010 0076.1F   011 0387.5F   012 0182.3F   013 00.535V

40   RUN   DATE
           14:23:49   001 0381.5F   002 0383.6F   003 0397.7F   004 0412.2F   40
     005 0423.4F   006 0432.3F   007 0435.4F   008 0436.2F   009 0084.1F
     010 0076.1F   011 0383.9F   012 0172.4F   013 00.531V

     RUN   DATE
           14:24:49   001 0378.2F   002 0379.8F   003 0393.4F   004 0408.2F
     005 0420.4F   006 0430.8F   007 0434.5F   008 0435.5F   009 0084.1F
     010 0076.1F   011 0380.7F   012 0170.6F   013 00.546V

42   RUN   DATE
           14:25:49   001 0375.0F   002 0376.1F   003 0389.1F   004 0404.1F   42
     005 0417.1F   006 0429.1F   007 0433.5F   008 0434.5F   009 0084.1F
     010 0076.1F   011 0377.6F   012 0166.9F   013 00.565V

     RUN   DATE
           14:26:49   001 0372.0F   002 0372.9F   003 0385.0F   004 0399.9F
     005 0413.6F   006 0427.3F   007 0432.2F   008 0433.5F   009 0084.0F
     010 0076.2F   011 0374.7F   012 0171.8F   013 00.575V

44   RUN   DATE
           14:27:49   001 0369.3F   002 0369.6F   003 0381.2F   004 0395.7F   44
     005 0409.8F   006 0424.5F   007 0430.7F   008 0432.2F   009 0084.1F
     010 0076.2F   011 0372.0F   012 0167.4F   013 00.587V

     RUN   DATE
           14:28:49   001 0366.8F   002 0366.7F   003 0377.6F   004 0391.6F
     005 0405.9F   006 0421.8F   007 0429.1F   008 0430.6F   009 0084.1F
     010 0076.2F   011 0369.5F   012 0166.4F   013 00.598V

46   RUN   DATE
–          14:29:49   001 0364.3F   002 0364.0F   003 0374.2F   004 0387.6F   46
     005 0401.3F   006 0418.7F   007 0426.9F   008 0428.8F   009 0084.1F
     010 0076.2F   011 0367.2F   012 0165.6F   013 00.593V

     RUN   DATE
           14:30:49   001 0362.1F   002 0361.7F   003 0371.1F   004 0383.7F
47 min diff
     005 0397.9F   006 0415.4F   007 0424.5F   008 0426.8F   009 0084.1F
     010 0076.2F   011 0365.0F   012 0166.0F   013 00.603V

48   RUN   DATE
           14:31:49   001 0359.9F   002 0359.5F   003 0368.2F   004 0380.2F   48
     005 0393.9F   006 0411.8F   007 0421.9F   008 0424.4F   009 0084.0F
     010 0076.2F   011 0363.0F   012 0161.1F   013 00.629V

     RUN   DATE
           14:32:49   001 0357.9F   002 0357.8F   003 0365.5F   004 0376.6F
     005 0390.1F   006 0403.2F   007 0419.0F   008 0421.8F   009 0084.1F
     010 0076.2F   011 0360.9F   012 0159.9F   013 00.679V
```

TABLE 9. (Concluded)

```
50  RUN    DATE
           14:33:49    001 0356.1F    002 0355.9F    003 0363.0F    004 0373.4F   50
    005 0386.3F    006 0404.4F    007 0415.9F    008 0418.8F    009 0084.0F
    010 0076.2F    011 0359.1F    012 0163.0F    013 00.685V

    RUN    DATE
           14:34:49    001 0354.2F    002 0353.9F    003 0360.7F    004 0370.5F
    005 0382.8F    006 0400.5F    007 0412.5F    008 0415.6F    009 0084.0F
    010 0076.2F    011 0357.3F    012 0169.0F    013 00.687V

52  RUN    DATE
           14:35:49    001 0352.4F    002 0352.2F    003 0358.6F    004 0367.7F   52
    005 0379.5F    006 0396.7F    007 0409.0F    008 0412.2F    009 0084.0F
    010 0076.2F    011 0355.6F    012 0170.5F    013 00.697V

    RUN    DATE
           14:36:49    001 0350.7F    002 0350.6F    003 0356.7F    004 0365.1F
    005 0376.3F    006 0392.8F    007 0405.4F    008 0408.7F    009 0084.1F
    010 0076.3F    011 0353.8F    012 0165.1F    013 00.698V

54  RUN    DATE
           14:37:49    001 0349.0F    002 0348.8F    003 0354.8F    004 0362.8F   54
    005 0373.3F    006 0389.1F    007 0401.5F    008 0405.1F    009 0084.1F
    010 0076.2F    011 0352.1F    012 0167.5F    013 00.731V

55  RUN    DATE
           14:38:49    001 0347.3F    002 0347.1F    003 0352.9F    004 0360.5F
55 min # 005 0370.5F    006 0385.4F    007 0397.8F    008 0401.3F    009 0084.0F
    010 0076.2F    011 0350.4F    012 0164.4F    013 00.702V

Oil DOWN
-" in Column
    RUN    DATE
           14:39:49    001 0345.7F    002 0345.5F    003 0351.1F    004 0358.4F   56
    005 0367.9F    006 0382.0F    007 0394.1F    008 0397.7F    009 0084.1F
HEAT 010 0076.3F    011 0348.6F    012 0159.3F    013 00.712V
ON →                                           FLUID DOWN 8" HEAT ON
                                               IN COLUM.
    RUN    DATE
           14:40:49    001 0344.0F    002 0343.8F    003 0349.3F    004 0356.4F
    005 0365.4F    006 0378.6F    007 0390.5F    008 0394.0F    009 0084.1F
    010 0076.3F    011 0377.9F    012 0165.0F    013 00.728V

    RUN    DATE
           14:41:49    001 0352.2F    002 0344.7F    003 0347.4F    004 0354.5F
    005 0363.2F    006 0375.5F    007 0386.8F    008 0390.3F    009 0084.0F
    010 0076.3F    011 0414.2F    012 0164.5F    013 00.739V

    RUN    DATE
           14:42:49    001 0374.7F    002 0363.8F    003 0345.7F    004 0352.7F
    005 0361.0F    006 0372.5F    007 0383.3F    008 0386.6F    009 0084.1F
    010 0076.3F    011 0447.6F    012 0159.5F    013 00.724V

    RUN    DATE
           14:43:49    001 0400.2F    002 0393.6F    003 0346.3F    004 0350.8F
    005 0358.9F    006 0369.7F    007 0379.9F    008 0383.0F    009 0084.0F
    010 0076.3F    011 0475.5F    012 0159.1F    013 00.655V

    RUN    DATE
           14:44:49    001 0422.7F    002 0421.2F    003 0354.3F    004 0349.0F
    005 0356.9F    006 0367.1F    007 0376.7F    008 0379.3F    009 0084.1F
    010 0076.3F    011 0497.0F    012 0152.2F    013 00.629V

    RUN    DATE
           14:45:49    001 0443.3F    002 0443.4F    003 0373.1F    004 0347.8F
    005 0354.9F    006 0364.6F    007 0373.5F    008 0376.5F    009 0084.1F
    010 0076.3F    011 0511.5F    012 0159.2F    013 00.536V
```

During operation the simulated heat exchanger surface was heated to 625F measured by a thermocouple welded directly to the surface. During the 2430 hours of testing the thermocouple surface remained free of fouling deposits. The forced fluid velocity apparently preventing the fouling observed with the static fouling setups.

Small Probe Fouling Test (SPFT)

Atomic Energy of Canada Limited SPFT Experience. Fouling of heat transfer surfaces in organic heat transfer systems may be caused by any one of, or a combination of, several impurities. Determination of the coolant fouling potential based on a chemical analysis for any one recognized impurity has met with only limited success. It was necessary to develop a fouling indicator which integrates all chemical variables. The most successful indicator is the SPFT which has evolved from the early work of Bancroft. Detailed descriptions of the equipment and operating procedures are available in a number of AECL publications, References 1, and 6 through 15.

A small flow from the primary organic coolant system is passed over an electrically heated stainless steel probe for ~24 hours. At the end of this period, the probe is washed and the film is scraped from a fixed length of the hottest region. The weight loss on scraping is a measure of the coolant fouling potential and is expressed as $mg/m^2 \cdot h$. Typical operating conditions are shown in the following table.

AECL SPFT OPERATING CONDITIONS

Surface Temperature (°C)	480
Heat Flux (kW/m^2)	650 - 850
N_{Re} (approximate)	2×10^4
Coolant Velocity (m/S)	2.5
Coolant Flow Rate (g/s)	60
Coolant Pressure (MPa)	1.4 - 1.7
Coolant Temperature (C)	350 - 375
(F)	662 - 707

The SPFT is strictly an empirical tool and the operating variables are fixed arbitrarily. These variables are not matched completely to those of the reactor fuel so the fouling potential determined is not quantitatively related to the rate of deposition of fouling film on the fuel. The SPFT fouling rate is much greater than that of the fuel so that measurable deposit can form in a short test. Trends of increasing fouling potential can therefore be established and corrective action taken before the fuel surfaces are fouled.

By correlating the daily measured values of the coolant fouling potential with the results of the irradiated fuel examination at the end of each reactor operating cycle, a semi-quantitative relationship is being developed. The data obtained so far indicate that if the coolant fouling potential is consistently maintained below 5 $mg/m^2 \cdot h$, fuel irradiated to over 144 MWh/kgU (average coolant velocity over 7.5 m/s, maximum sheath temperature over 485C [905F]) comes out of the reactor with a fouling film thinner than 10 µm. It has been demonstrated that WR-1 can be operated over long periods with a coolant fouling potential of <5 $mg/m^2 \cdot h$ and the thin fouling films observed on the fuel have no detrimental effects.

When the coolant fouling potential is between 10 and 100 $mg/m^2 \cdot h$ over a long period, fuels have thicker fouling films, particulate type fouling films grow around wire wraps and closed gap regions, and some subchannels are blocked. Some fuels will fail and therefore such conditions are not acceptable in a power reactor.

When the coolant fouling potential is over 1 $g/m^2 \cdot h$, any fuel operating with a miximum sheath temperature exceeding 480C (896F) develops massive deposits of film in a day or two. Most of these fuels fail. Fuels operating at or below a maximum sheath temperature of 450C (842F) develop less severe fouling deposits, and normally do not fail.

Based on these observations, the following detailed specifications for reactor operation based on SPFT fouling potential can be made.

Fouling Potential <5 $mg/m^2 \cdot h$ - no fouling problem. This should be the goal for long-term reactor operation.

Fouling Potential 5 - 20 $mg/m^2 \cdot h$ - warning. There will be a slow film buildup but the increase in a few days will be negligible. For long-term operation, there will be progressively thicker films.

Fouling Potential 20 - 200 $mg/m^2 \cdot h$ - severe warning. There will be a more rapid film buildup and significant amounts may be deposited in a few days. Immediate corrective action must be taken.

Fouling Potential >200 $mg/m^2 \cdot h$ - serious fouling problem. Significant amounts of film will be deposited in a very short time. Reactor power and/or coolant temperature should be lowered to reduce film buildup while corrective action is being taken.

It takes one day to obtain a fouling measurement with the SPFT, but this has been found to be fast enough to detect loss of coolant chemistry control in time to take corrective action. If the fouling potential is high (say, >100 $mg/m^2 \cdot h$), it can be estimated during the run by monitoring the probe temperature. Since the probe runs at a fixed power, the buildup of a film on the surface reduces the heat transfer to the coolant and increases the probe temperature. For low fouling coolants, there is not a significant increase in temperature in 24 hours. A six-hour test has been developed and is normally used during periods of high fouling. Since corrective action is being taken to reduce the fouling, a shortened test is required to monitor the corrective operations.

The SPFT is the only reliable indicator of the coolant fouling potential, so an extremely high reliability and availability must be designed into this facility in any organic coolant system.

Rocketdyne SPFT Experience. Operation of the SPFT in the model subsystem flow loop indicated that a considerable safety margin exists when operating the Caloria HT43 between 302C (575F) and 316C (600F). Operation of the SPFT at a wall temperature of 399C (750F) for a period of 24 hours produced no perceptible fouling. The tests confirm that Caloria HT43 has a low propensity to fouling and is a good choice for the Pilot and Commercial Plants based on fouling characteristics. However, these tests were limited and should be more extensive to provide data for long duration exposure.

FLUID MONITORING PROCEDURES

The fourth task conducted on the program is the recommendation of tests to be conducted for monitoring fluid quality when solar thermal plants are on stream. Because heat transfer fluids like Caloria HT43 and Sun Oil 21 are a mix of many compounds, no single test can provide a measure of the suitability of that fluid for its intended purpose. Contact with the fluid manufacturers indicate that fluid quality relies heavily on following established production methods with a particular type of crude stock. Quality control is accomplished primarily with measurement of physical properties such as density and viscosity, and in some cases distillation. Commercial customers traditionally do not apply acceptance test procedures. The fluid is simply purchased and used until it is no longer useable. Different users have different criteria. These differ from the manufacturers criteria. One large manufacturer recommends that the fluid be replaced if the viscosity has doubled. However, a large user is still operating his systems very satisfactorily with fluid at twice the original viscosity. This type of uncertainty must be resolved for the coming generation of solar thermal electrical power generation plants.

Laboratory analytical tests considered to date include kinematic viscosity, gel permeation chromatography and infrared spectroscopy measurements. In addition to the lab tests, the small probe fouling test (SPFT) can be used to assess the tendency of the fluid to foul high thermal flux heat transfer surfaces.

Kinematic viscosity is the easiest and most direct measurement that can be performed and is an important operating parameter. The fluid viscosity directly influences heat transfer as well as pumping losses. Viscosity is also a good indicator of general fluid condition. The value of fluid viscosity decreases when thermal cracking occurs creating lower molecular weight constituents. Viscosity will increase with the formation of polymerized species or the further cracking and subsequent vaporization of low molecular weight compounds. Viscosity can be measured within an hour or two of drawing a sample with a Saybolt viscometer, a readily available, easily operable, and low cost piece of equipment.

Although fluid constituents cannot easily be measured directly, standard laboratory procedures using gel permeation chromatograph and infrared spectroscopy can provide a measure of molecular size distribution and group type identification. These tests can be used to determine the relative change of the fluid makeup with time.

The SPFT is an empirical tool. The heat flux initial surface temperature, fluid flow rate, Reynolds number, etc., can be set so that the SPFT fouling rate is much greater than the fouling rate in the plant heat exchanger. Thus, conditions can be arranged so as to obtain a measurable deposit in a short duration test (e.g., 8 to 24 hours). Increases in fouling potential with fluid age and concomitant thermal degradation, can be related to the mass/area of the fouling film formed during a standard SPFT and/or operating limit established. Because of the speed of the SPFT corrective action can be taken before heat exchanger fouling can occur.

CONCLUSIONS

The use of commercial heat transfer fluids with low cost rock in a dual medium thermal storage system is an economic and practical method for storing thermal energy in the 302C (575F) to 316C (600F) range. For the Barstow Pilot Plant conditions, 302C (575F), Exxon's Caloria HT43 in combination with rock has been demonstrated to be the most cost effective of the five commercial fluids tested for periods up to five years for a typical commercial solar thermal plant duty cycle.

The combined fluid loss rate of 7 percent per year plus low initial and replacement cost result in a yearly replenishment cost of 0.0138 percent of initial capital cost for a 100 MWe solar thermal plant (1977 values), Fig. 43.

Fluid heater surface temperatures may as a minimum operate at 329C (625F) and possibly 14C (25F) higher. The higher value should be confirmed by tests with exposure similar to that in the model subsystem flow loop.

Design of a plant using heat transfer fluids should include fluid testing methods to provide continuous monitoring of fluid condition. Monitoring should include periodic viscosity, laboratory analytical methods, and use of the AECL Small Probe Fouling Test. Fluid properties should be correlated with changes in heat transfer and pumping performance during operation of the Pilot Plant to establish limits and costs for operation of larger commercial size plants.

The use of these fluids and knowledge of characteristics for long term maintenance-free operation is in the embryo state. Although these fluids have been available and used for commercial application for many years, there is very little quantitative information on loss rates, fluid degradation products, and heat exchanger surface fouling available for solar thermal plant design. These tests, and tests conducted at Sandia-Livermore by

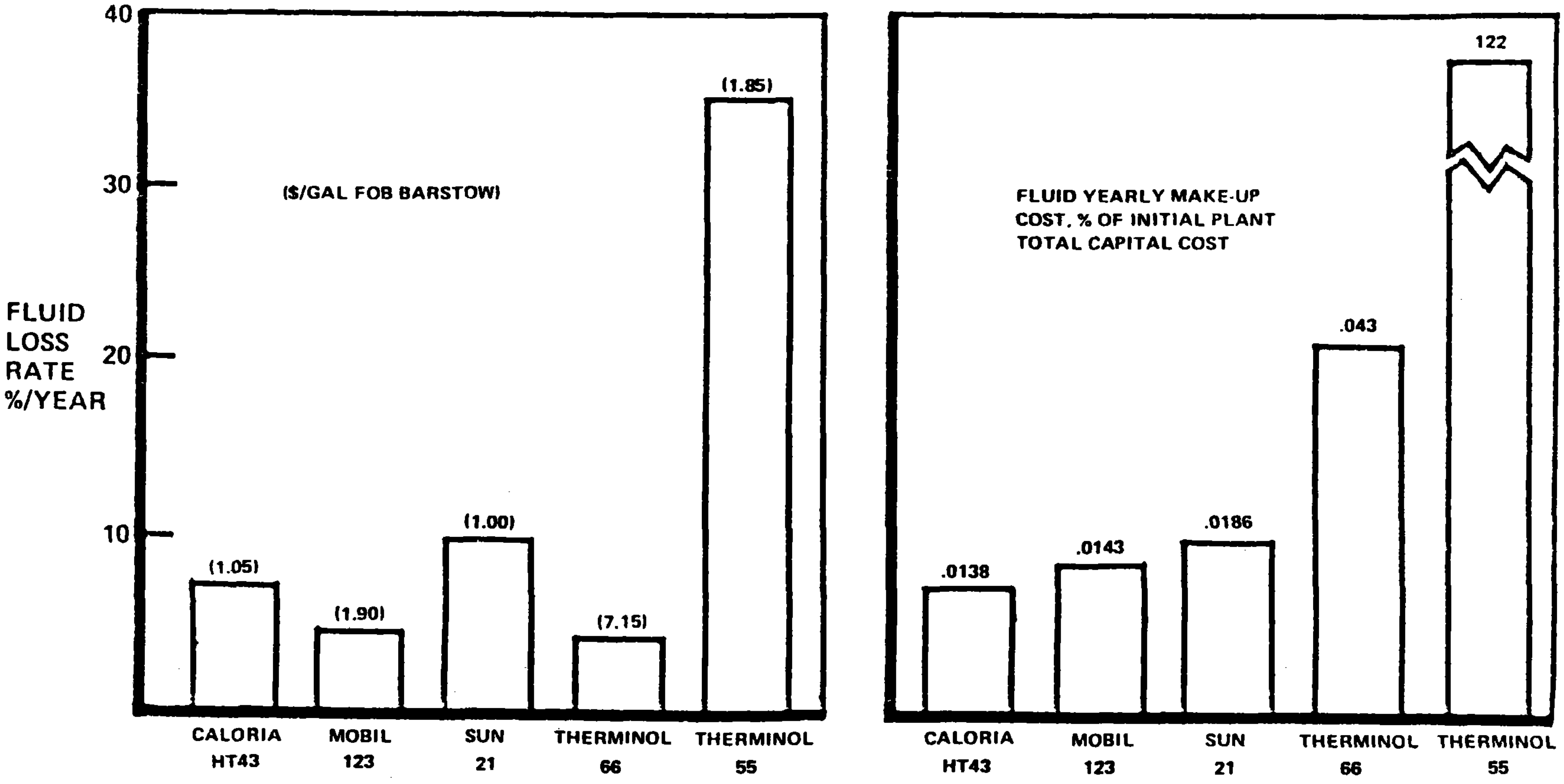

Figure 43. Comparative Costs of Thermal Storage Heat Transfer Fluids for Pilot Plant Conditions, (302 C), (575 F) Dual Medium Environment

V. P. Burolla, are the only tests to date on the dual medium concept. Both fall far short of characterizing the fluids for 30-year life required for solar thermal plant operation.

Further, there are still some unresolved critical issues. Questions as to effect of rock surface area to fluid volume ratio, size of rock, and the availability of new and lower cost fluids should be resolved by further testing.

Testing with the model subsystem flow loop is a useful and economical method of testing critical components of the thermal storage subsystem. The flow loop extended results of the heat exchanger surface fouling into the dynamic regime. An important result of the flow loop operation was that blockage of the lower manifold in the TSU did not occur after 2000 hours of both steady as well as intermittent operation. Cyclic thermal operation did not result in any measurable amount of particulate formation that entered the system (as measured by full flow line filters). However, these tests should be continued to provide operational data closer to the required plant life of 30 years.

RECOMMENDATIONS

Based on the tests conducted in this program, it is recommended that:

(1) The dual medium (solids/liquid) concept be used for storage of thermal energy where the use of commercial low vapor pressure heat transfer fluids is economically attractive.

(2) Caloria HT43 plus rock be used for the transport and storage medium up to 302C (575F).

(3) The central receiver 10 MWe solar thermal pilot plant to be built at the Southern California Edison Daggett site utilize Caloria HT43 plus Barstow gravel with Sand City sand as the thermal storage system storage medium. Purchase specifications and verification procedures should be established for construction programs.

(4) The fluid monitoring and subsystem flow loop tests described herein should be continued and expanded to include the effect of rock surface area to fluid volume ratio and as to clarify the anomalies that exist. These tests would explore and define cost savings associated with using solids with a lower surface area to liquid volume ratio. Correlations and a detailed technical basis would be established for the pilot plant and for plants (solar and non-solar) to be built in the future.

(5) The heat transfer fluid and condensed vaporized decomposition products be monitored during operation of the pilot plant. Both physical and chemical properties as well as coking and fouling tests with the SPFT should be conducted. Results should be compared with the tests from this report as well as other investigators.

REFERENCES

1. Smee, J. L., V. R. Puttagunta, R. F. S. Robertson and S. R. Hatcher, Organic Coolant Summary Report, AECL-4922, Atomic Energy of Canada, Limited, Whiteshell Nuclear Research Establishment, Pinawa, Manitoba, ROE 1LO, August 1975.

2. Caloria HT43, Exxon Corporation product bulletin, 1 July 1973.

3. Weiss, R. W., Fluid Life Evaluation Test, Monsanto Industrial Chemicals Company, St. Louis, Missouri, not dated, c. 1969.

4. Smith, R. S., "Offshore Production Utilities - 1," Oil and Gas Journal, 53 (11 August 1975).

5. Lipscomb, T. G. II, Marketing Technical Services, Exxon Corporation, USA, Personal Communications, August 1975 and March 1976.

6. Smee, J. L. and W. E. Krajcarski, Some Physical Properties of HB-40 Based Coolant, Edition II, Report WNRE-105, Atomic Energy of Canada, Limited, Whiteshell Nuclear Research Establishment, Pinawa, Manitoba, ROE 1LO, August 1972.

7. Stewart, R. B., Organic Reactor Coolant Analysis: Canadian Practice, 1970, AECL-3672, Atomic Energy of Canada, Limited, Whiteshell Nuclear Research Establishment, Pinawa, Manitoba, March 1971.

8. Stewart, R. B., and J. L. Smee, Methods for Analysis of Organic Coolants, AECL-2643, Atomic Energy of Canada, Limited, Whiteshell Nuclear Research Establishment, Pinawa, Manitoba, May 1966.

9. Smee, J. L. and W. E. Krajcarski, Decomposition Rates of Irradiated Hydrogenated Terphenyls in Reactor Systems, II: High Temperature Operation, Report WNRE-79, Atomic Energy of Canada, Limited, Whiteshell Nuclear Research Establishment, Pinawa, Manitoba, ROE 1LO, February 1972.

10. Smee, J. L. and M. Tomlinson, Decomposition Rates of Irradiated Hydrogenated Terphenyls in Reaction Systems, Report WD1-115, Atomic Energy of Canada, Limited, Whiteshell Nuclear Research Establishment, Pinawa, Manitoba, September 1968.

11. Tomlinson, M., A. W. Boyd and S. R. Hatcher, The Radiation and Thermal Decomposition of Terphenyls and Hydroterphenols, AECL-2641, Atomic Energy of Canada, Limited, Whiteshell Nuclear Research Establishment, Pinawa, Manitoba, May 1966.

12. Hollies, R. E., D. E. Minns, V. R. Puttagunta and B. A. Finlay, Fouling Performance of Organic Coolants for WR-1, Data for Period Startup to Semptember 1970, WNRE-38, Atomic Energy of Canada, Limited, Whiteshell Nuclear Research Establishment, Pinaw, Manitoba, ROE 1LO, October 1973.

13. Hatcher, S. R., B. A. Finlay and J. L. Smee, Heat Transfer, Impurities and Fouling in Organic Coolants, AECL-2642, Atomic Energy of Canada, Limited, Whiteshell Nuclear Research Establishment, Pinawa, Manitoba, ROE 1LO, May 1966.

14. Bancroft, A. R., D. H. Charlesworth and J. H. Duerksen, Impurity Effects in the Fouling of Heat Transfer Surfaces by Organic Coolants, CRCE-1189 AECL-1913, Atomic Energy of Canada, Limited, Chalk River, Ontario, May 1965.

15. Charlesworth, D. H., Fouling in Organic Cooled Systems, CRCE-1096, AECL-1761, Atomic Energy of Canada, Limited, Chalk River, Ontario, April 1963.

16. Burolla, V. P., Analysis of Thermally Degraded Sensible Heat Storage Hydrocarbon, Sandia Laboratories, Energy Report SAND 77-8264, December 1977.

17. Burnett, G. M., Mechanism of Polymer Reactions, Interscience Publ. Inc., New York/London, 1954.

18. Semenov, N. N., Some Problems in Chemical Kinetics and Reactivity, Vol. I., p. 125, Princeton University Press, Princeton, NJ, 1958.

19. Hughes, G., "Oxidation Reactions Induced by Ionizing Radiation," p. 47 in Oxidation and Combusion Reviews Vol. I., C. F. H. Tipper, Edit., Elsevier Publ. Co., New York, NY, 1965.

20. Hallet, R. W. and R. L. Gervais, "Central Power Receiver Solar Thermal Power System Phase 1," CDRL Item 2, Pilot Plant Preliminary Design Report, Vol. V, Thermal Storage Subsystem MDAC Co., October 1977.

21. Frost, A. A. and R. G. Pearson, Kinetics and Mechanisms, 2nd Vol., p. 241, John Wiley & Sons, Inc., New York, London, 1961.

☆U.S. GOVERNMENT PRINTING OFFICE: 1980-740-146/1083